

Testing Homogeneity with Galaxy Star Formation Histories



**BH, Rita Tojeiro, Raul Jimenez,
Alan Heavens, Chris Clarkson,
Roy Maartens ApJ, 762, L9 2012
([arXiv:1209.6181](https://arxiv.org/abs/1209.6181))**



OPINAS Garching 15 Jan 2013

LCDM

The concordance cosmological model is built upon the well tested theory of gravity G.R. (binary pulsars, Kramer 2012) and the FLRW metric.

LCDM

The concordance cosmological model is built upon the well tested theory of gravity G.R. (binary pulsars, Kramer 2012) and the FLRW metric.

Based on a few parameters

$$\Omega_b, \Omega_m, \Omega_\Lambda, w, \sigma_8, n_s, ..$$

LCDM

The concordance cosmological model is built upon the well tested theory of gravity G.R. (binary pulsars, Kramer 2012) and the FLRW metric.

Based on a few parameters

$$\Omega_b, \Omega_m, \Omega_\Lambda, w, \sigma_8, n_s, ..$$

Based on a few assumptions

Isotropy

-- All directions (at fixed redshift) look the same

+ Copernican Principle

-- No special location

= Homogeneity

-- All redshift block (slice & direction) look the same, once evolution corrections have been applied.

G.R

LCDM

The concordance cosmological model is built upon the well tested theory of gravity G.R. (binary pulsars, Kramer 2012) and the FLRW metric.

Based on a few parameters

$$\Omega_b, \Omega_m, \Omega_\Lambda, w, \sigma_8, n_s, ..$$

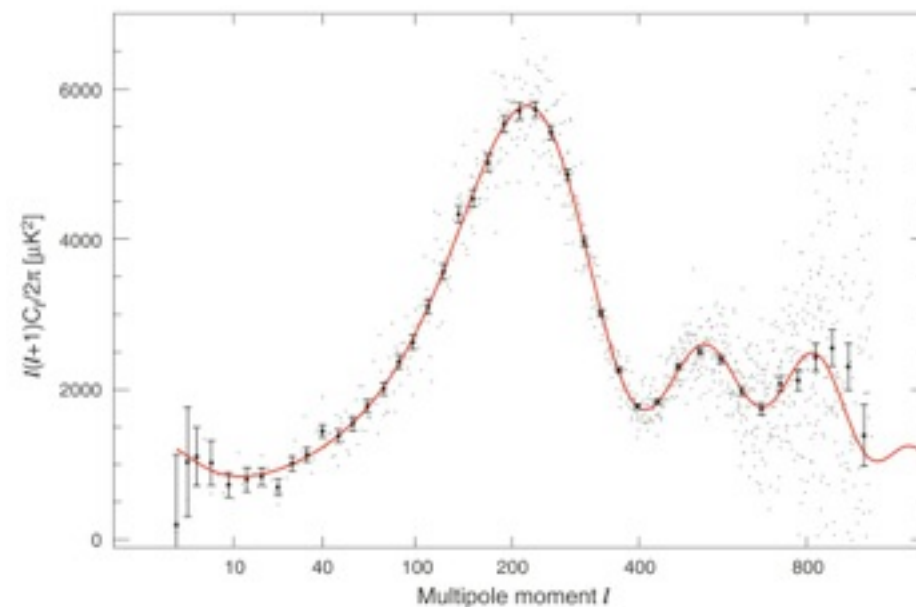
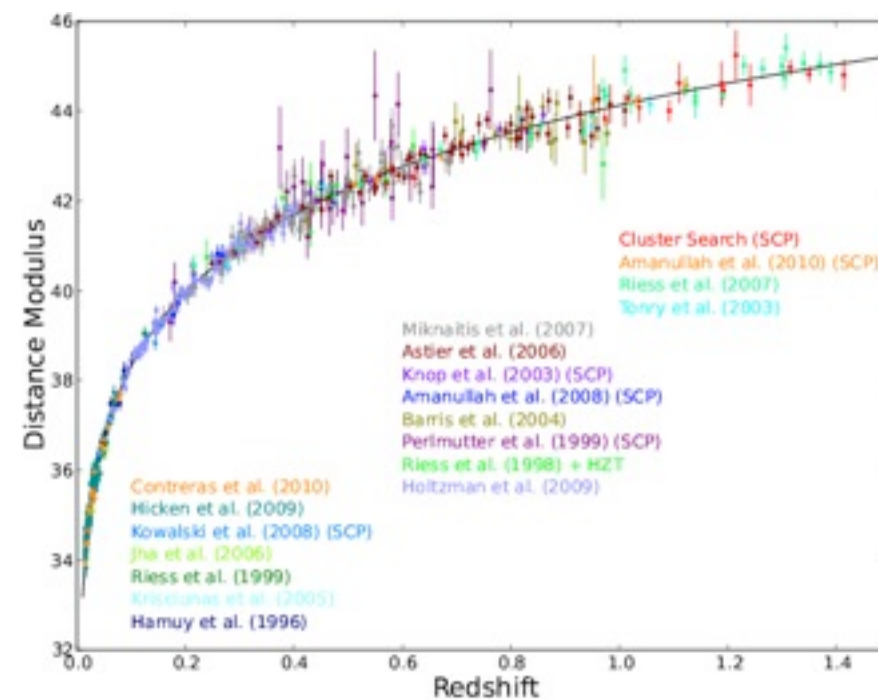
Based on a few assumptions

Isotropy

+ Copernican Principle

= Homogeneity

G.R



LCDM

The concordance cosmological model is built upon the well tested theory of gravity G.R. (binary pulsars, Kramer 2012) and the FLRW metric.

Based on a few parameters

$$\Omega_b, \Omega_m, \Omega_\Lambda, w, \sigma_8, n_s, ..$$

Based on a few assumptions

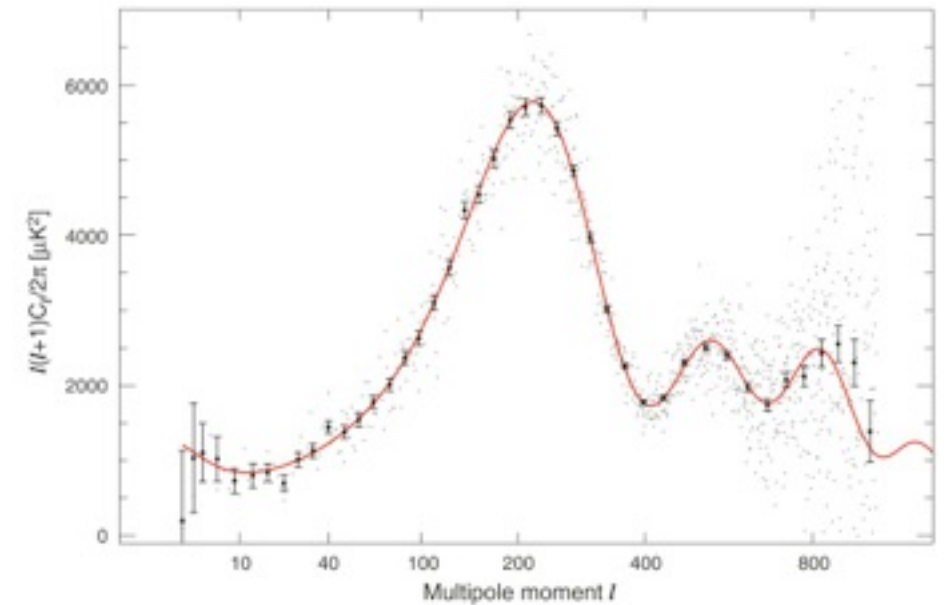
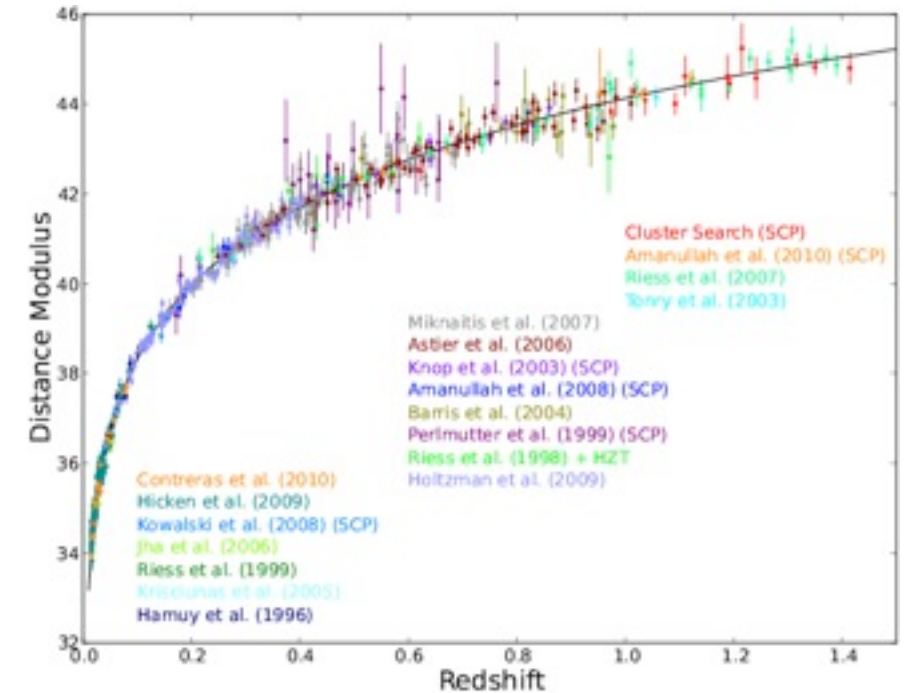
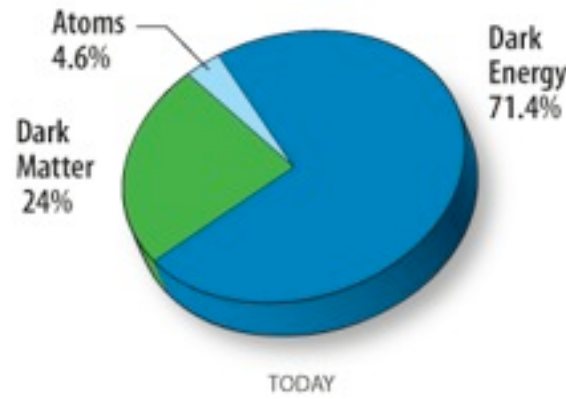
Isotropy

+ Copernican Principle

= Homogeneity

G.R

LCDM has excellent predictive power and is in agreement with (\sim) all current observations



LCDM

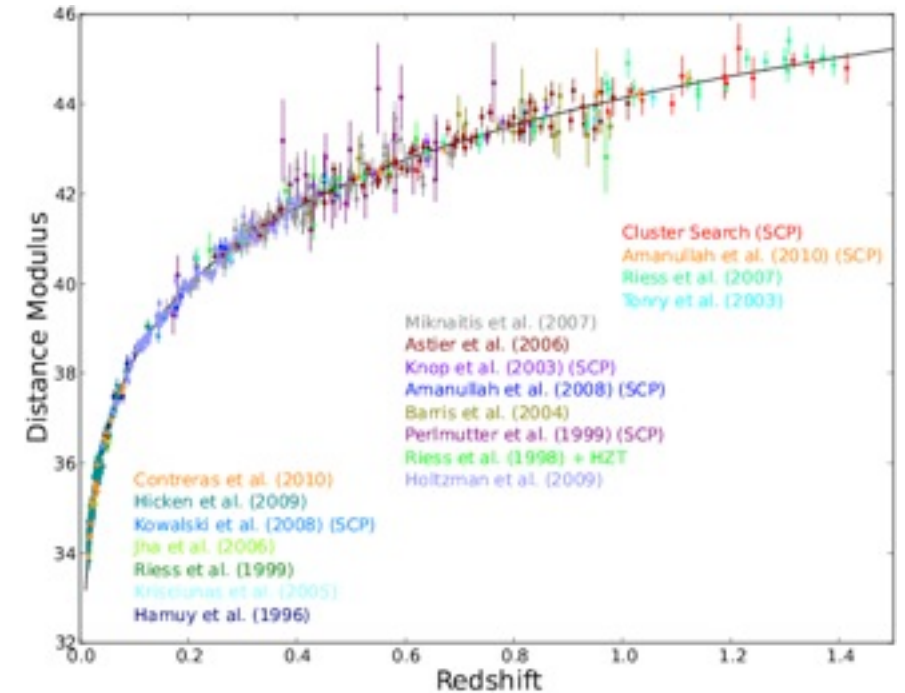
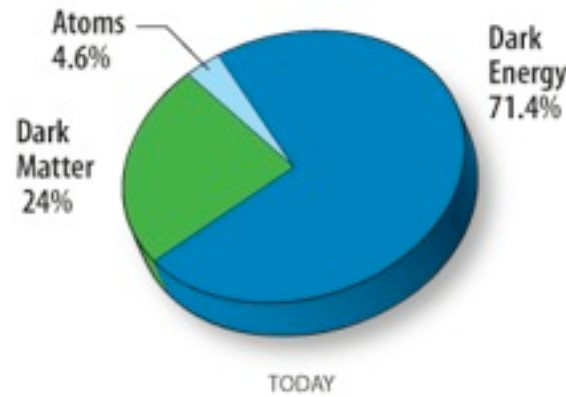
The concordance cosmological model is built upon the well tested theory of gravity G.R. (binary pulsars, Kramer 2012) and the FLRW metric.

Based on a few parameters

$$\Omega_b, \Omega_m, \Omega_\Lambda, w, \sigma_8, n_s, ..$$

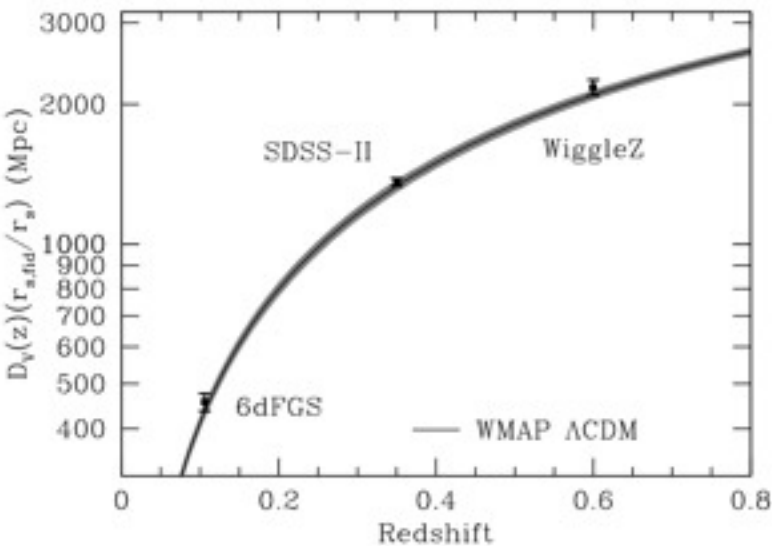
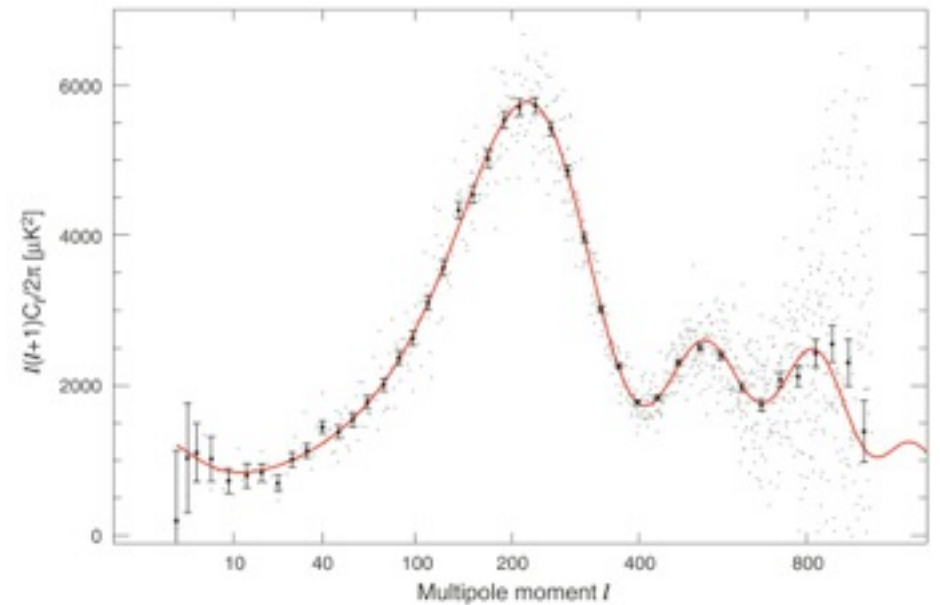
Based on a few assumptions

Isotropy
 + Copernican Principle
 = Homogeneity
 G.R



LCDM has excellent predictive power and is in agreement with (~) all current observations

It predicts the pos. of the BAO peak, as measured from the galaxy correlation functions of SDSS, WiggleZ, 6dFGS



LCDM

The concordance cosmological model is built upon the well tested theory of gravity G.R. (binary pulsars, Kramer 2012) and the FLRW metric.

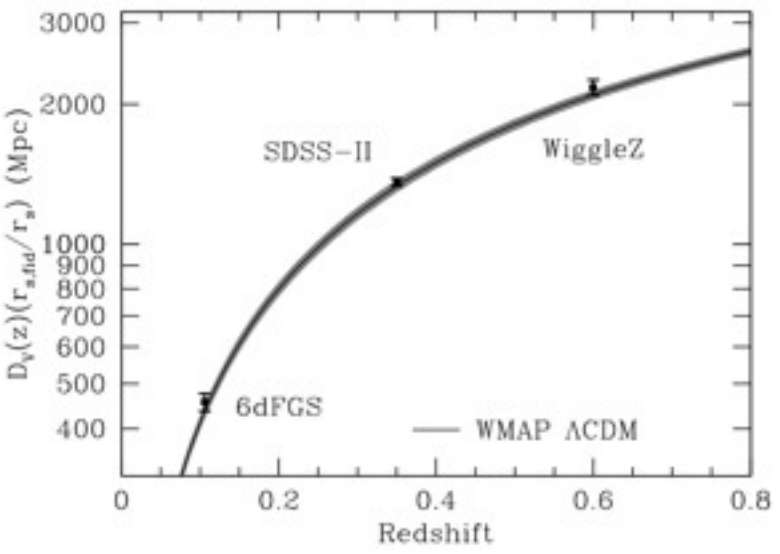
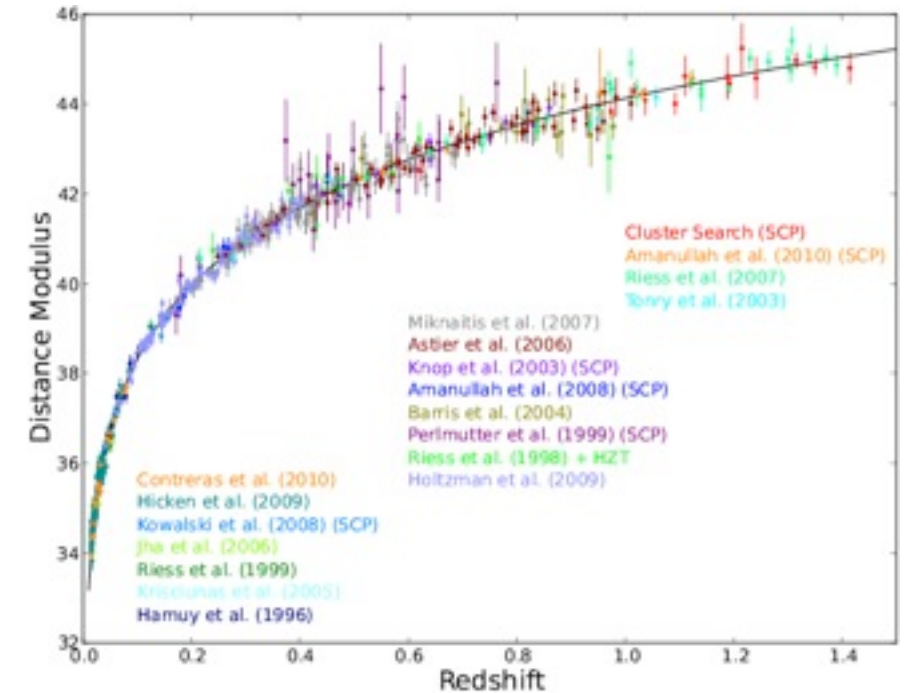
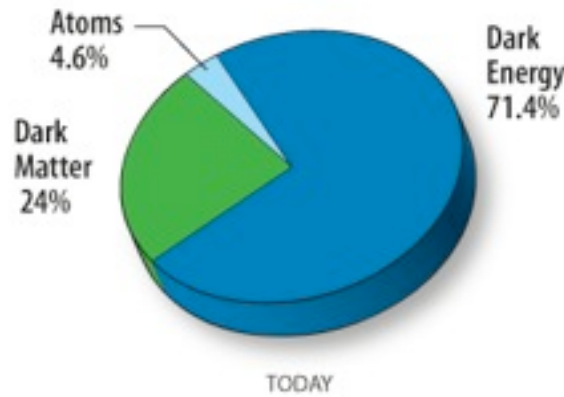
Based on a few parameters

$$\Omega_b, \Omega_m, \Omega_\Lambda, w, \sigma_8, n_s, ..$$

Based on a few assumptions

- Isotropy
- + Copernican Principle
- = Homogeneity
- G.R

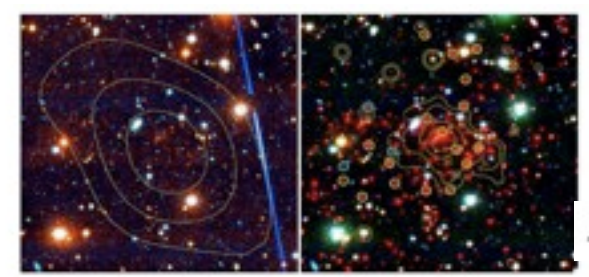
LCDM has excellent predictive power and is in agreement with (~) all current observations



K. Mehta et al.

It predicts the pos. of the BAO peak, as measured from the galaxy correlation functions of SDSS, WiggleZ, 6dFGS

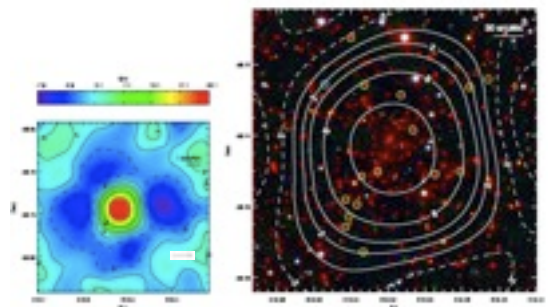
It predicts the existence of massive high redshift galaxy clusters (BH et al 2011, JCAP), once thought to cause tension with LCDM + $f_{\text{nl}} \neq 0$ (e.g. B.H et al 2011, PRD)



SPT CL J0546-5345
Brodwin et al 2010

$$M_{200} = 1.27 \times 10^{15} h^{-1} M_\odot$$

Fig. 1. Left: Optical r' -band image (μm) of SPT-CL J0546-5345, with SDSS magnitude contours overlaid ($\Delta m = 2.4, 0.4$, and 0.4). Right: False color optical (g' -band) image of SPT-CL J0546-5345, with Chandra X-ray contours overlaid ($0.2, 0.4, 0.8$, and 1.6 counts per $2'' \times 2''$ pixel) on the $0.5-2$ keV band. North is up, east is to the left. Due to the high angular resolution, Chandra is able to resolve substructure in the SW, which may be evidence of a possible merger. These images highlight the importance of BAO mapping in tracking the galaxies in high redshift, optically thin clusters. Spectroscopic redshift-type (blue-type) members are indicated with yellow (open) circles. Green squares show the spectroscopic non-members.



SPT-CL J2106-5844

Foley et al 2011

$$M_{200} \sim 10^{15} M_\odot$$

LCDM

The concordance cosmological model is built upon the well tested theory of gravity G.R. (binary pulsars, Kramer 2012) and the FLRW metric.

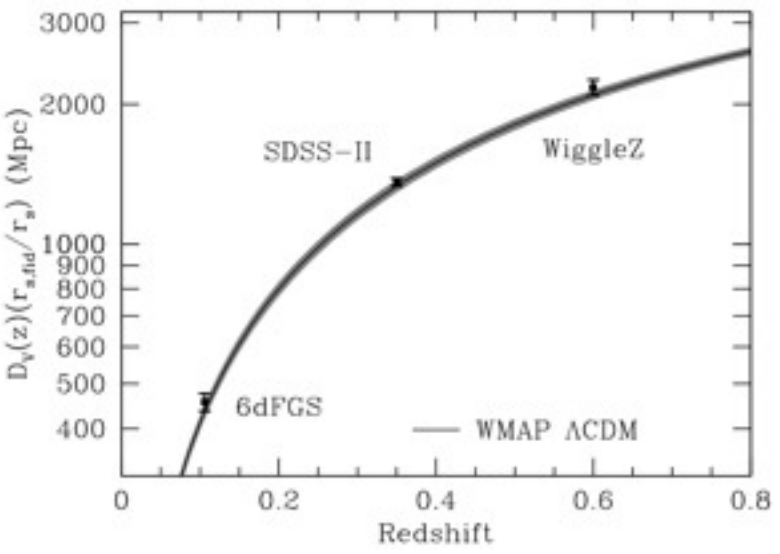
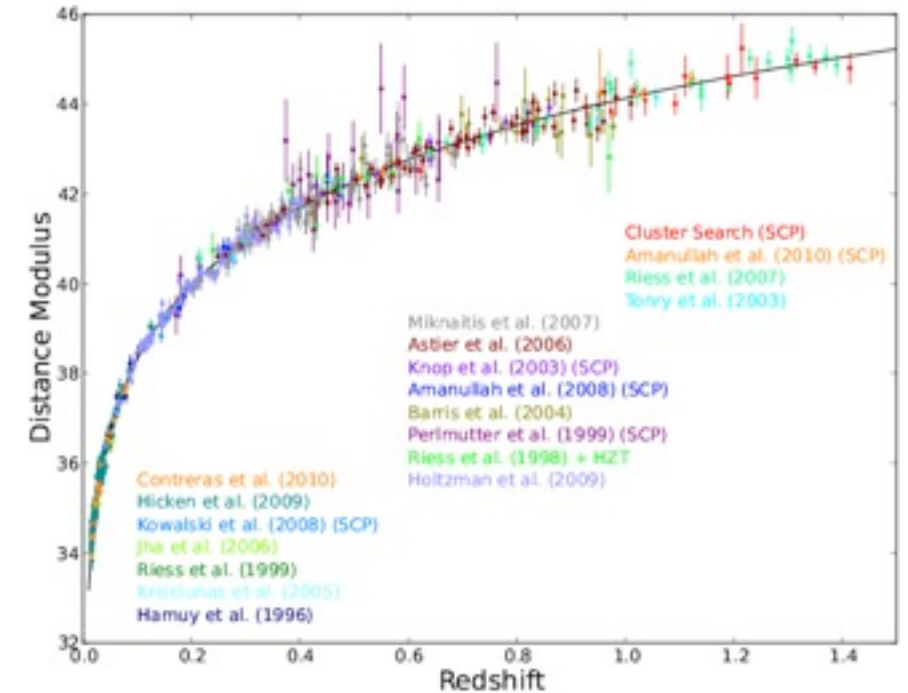
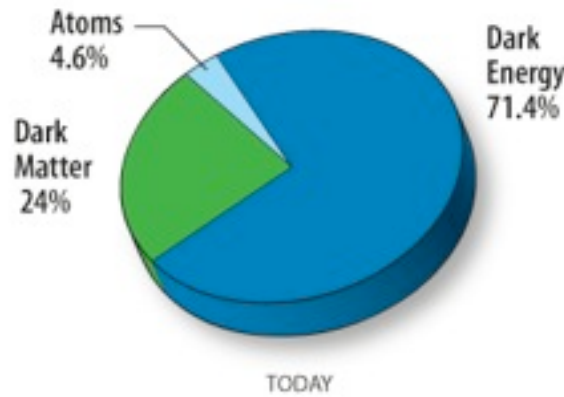
Based on a few parameters

$$\Omega_b, \Omega_m, \Omega_\Lambda, w, \sigma_8, n_s, \dots$$

Based on a few assumptions

- Isotropy
- + Copernican Principle
- = Homogeneity
- G.R

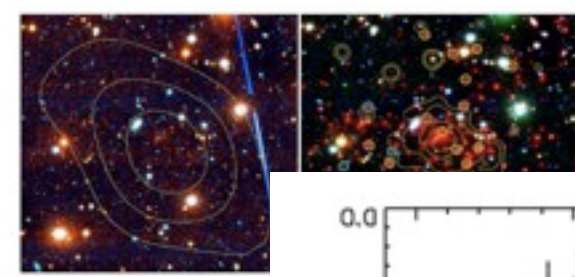
LCDM has excellent predictive power and is in agreement with (~) all current observations



K. Mehta et al.

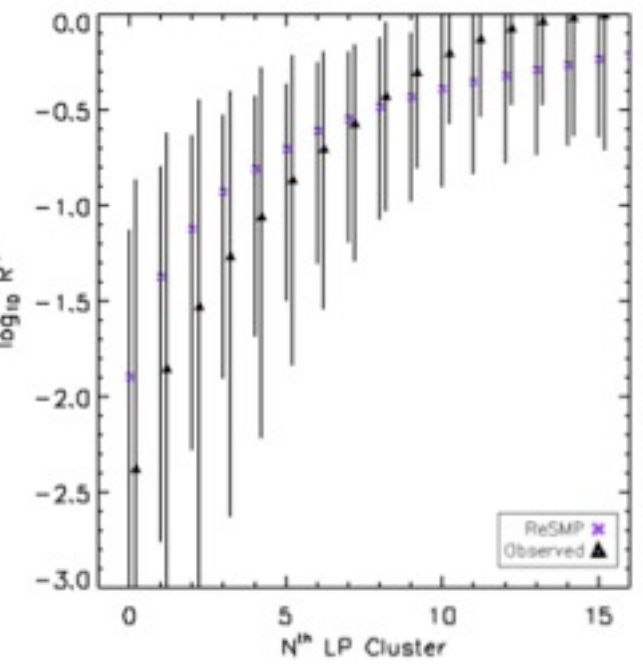
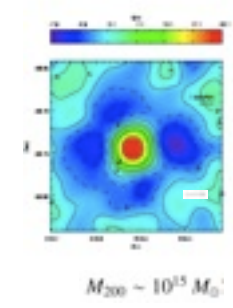
It predicts the pos. of the BAO peak, as measured from the galaxy correlation functions of SDSS, WiggleZ, 6dFGS

It predicts the existence of massive high redshift galaxy clusters (BH et al 2011, JCAP), once thought to cause tension with LCDM + $f_{nl} \neq 0$ (e.g. B.H et al 2011, PRD)



SPT CL J0546-5345
Brodwin et al 2010

Fig. 1. Left: Optical r' - i' color image (ps) of SPT-CL J0546-5345. Right: False color optical (ps) + IRAC (3.6 μ m) image of SPT-CL J0546-5345. The image is able to resolve substructure in the SW, which may be useful in searching for galaxies in high redshift, especially those (other (ps)) clusters. Green squares show the spectroscopic redshift.



LCDM

The concordance cosmological model is built upon the well tested theory of gravity G.R. (binary pulsars, Kramer 2012) and the FLRW metric.

Based on a few parameters

$$\Omega_b, \Omega_m, \Omega_\Lambda, w, \sigma_8, n_s, ..$$

Based on a few assumptions

Isotropy

+ Copernican Principle

= Homogeneity

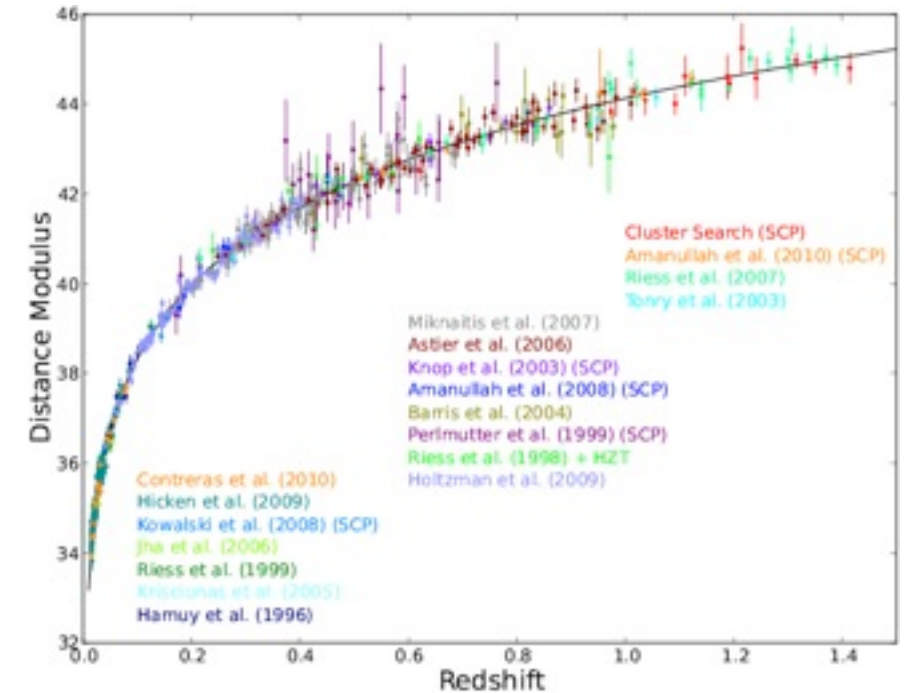
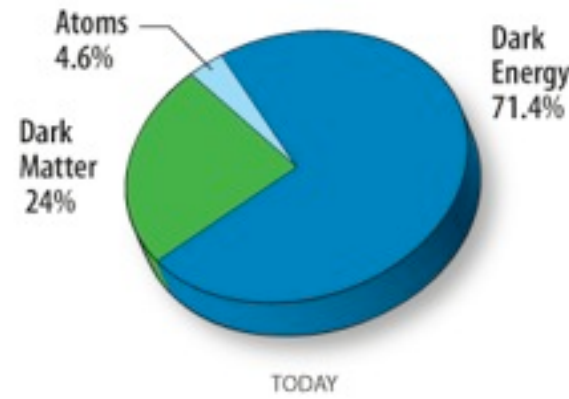
G.R

LCDM has excellent predictive power and is in agreement with (\sim) all current observations

But, what is the nature of dark energy?

We have no theoretical motivation for it

The predicted value of vacuum energy from particle physics is way off



LCDM

The concordance cosmological model is built upon the well tested theory of gravity G.R. (binary pulsars, Kramer 2012) and the FLRW metric.

Based on a few parameters

$$\Omega_b, \Omega_m, \Omega_\Lambda, w, \sigma_8, n_s, ..$$

Based on a few assumptions

Isotropy

+ Copernican Principle

= Homogeneity

G.R

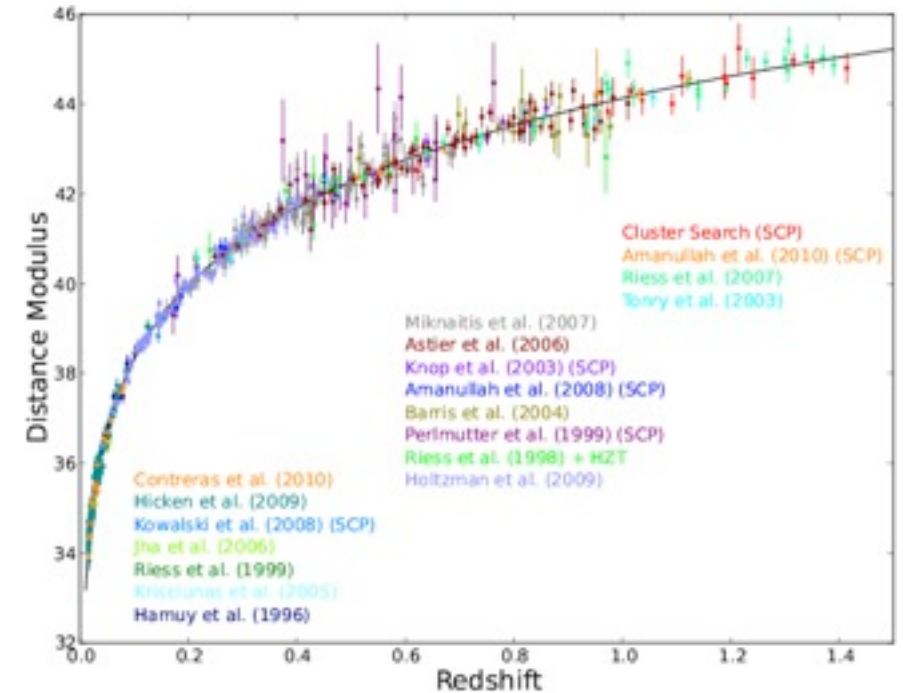
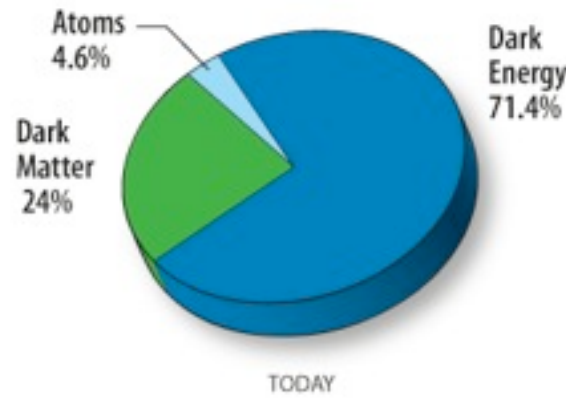
LCDM has excellent predictive power and is in agreement with (\sim) all current observations

But, what is the nature of dark energy?

We have no theoretical motivation for it

The predicted value of vacuum energy from particle physics is way off

Perhaps it can be safely removed, if we relax some of our underlying assumptions about the Universe.



LCDM

The concordance cosmological model is built upon the well tested theory of gravity G.R. (binary pulsars, Kramer 2012) and the FLRW metric.

Based on a few parameters

$$\Omega_b, \Omega_m, \cancel{\Omega_\Lambda}, \cancel{w}, \sigma_8, n_s, ..$$

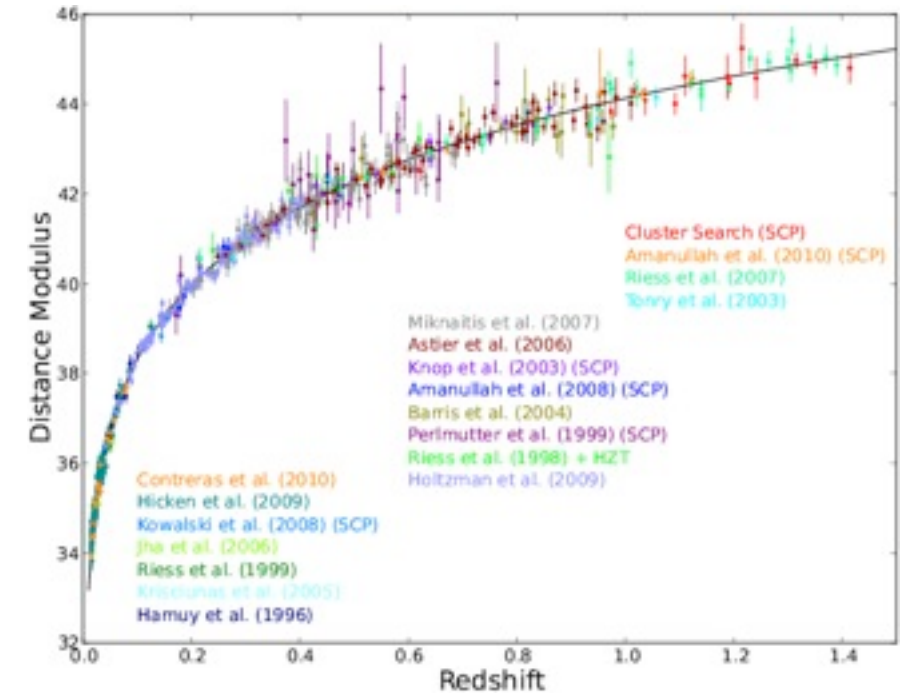
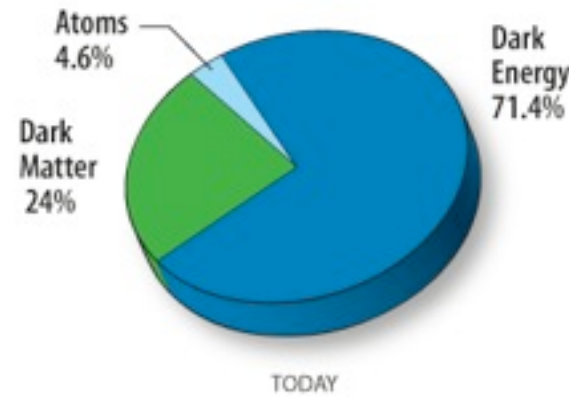
Based on a few assumptions

Isotropy ?

~~+ Copernican Principle~~

~~= Homogeneity~~

G.R. ?



LCDM has excellent predictive power and is in agreement with (\sim) all current observations

But, what is the nature of dark energy?

We have no theoretical motivation for it

The predicted value of vacuum energy from particle physics is way off

Perhaps it can be safely removed, if we relax some of our underlying assumptions about the Universe.

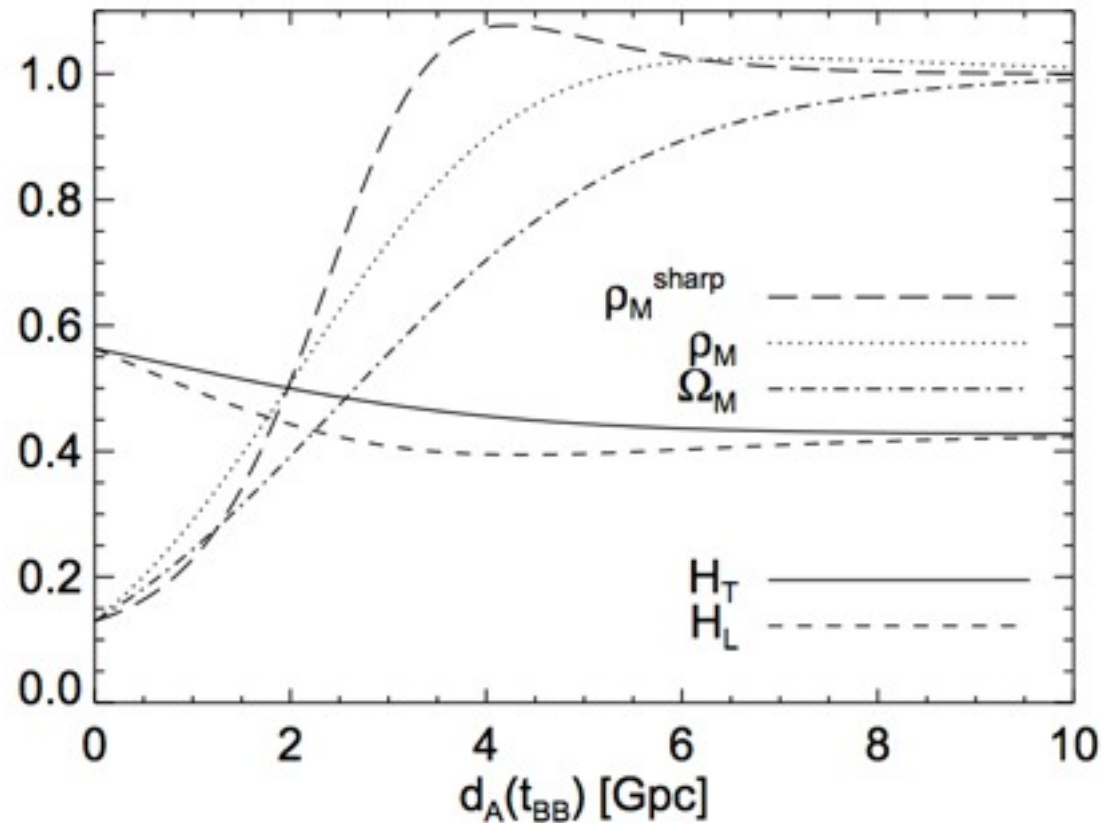
Void models LTB

Popular inhomogeneous models are the Lemaitre-Tolman- Bondi (LTB), which are spherically symmetric but inhomogeneous (see e.g., Enqvist 2008). Spatial variation in matter density and Hubble rate can have the same effect on redshift as acceleration in a perfectly homogeneous universe.

Void models LTB

Popular inhomogeneous models are the Lemaitre-Tolman- Bondi (LTB), which are spherically symmetric but inhomogeneous (see e.g., Envquist 2008). Spatial variation in matter density and Hubble rate can have the same effect on redshift as acceleration in a perfectly homogeneous universe.

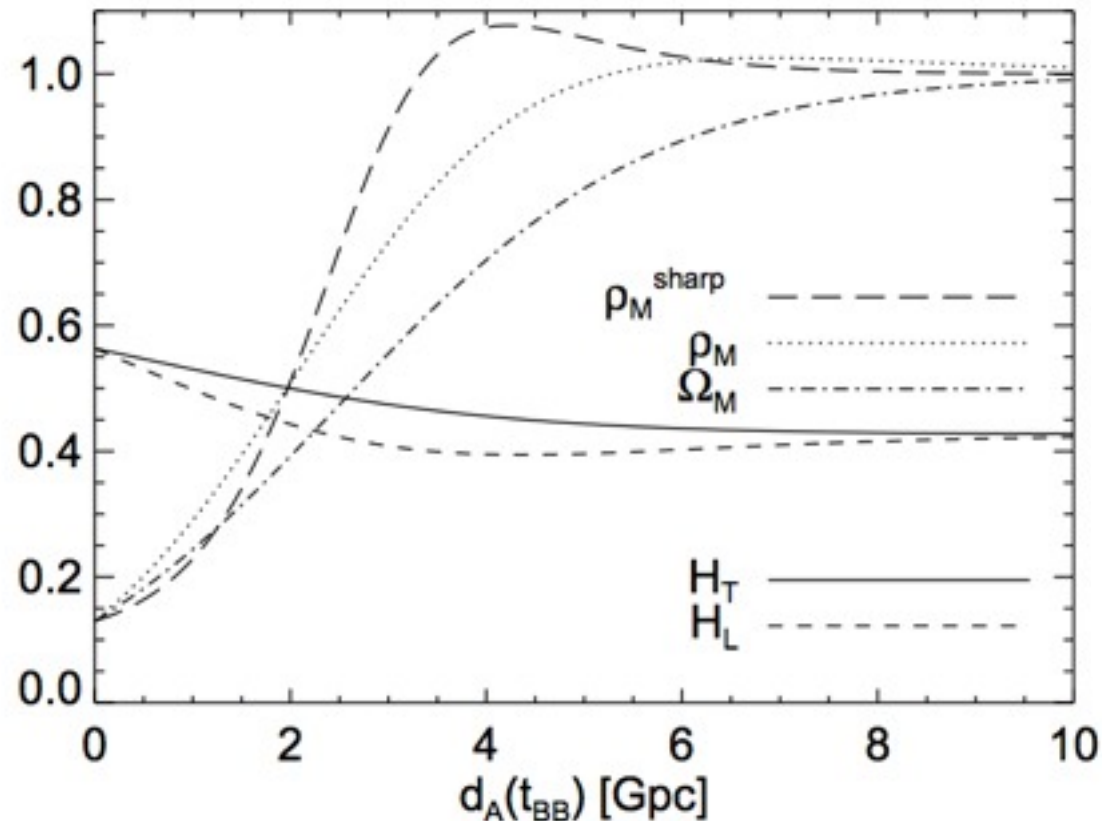
Bellido & Haugbølle 2008



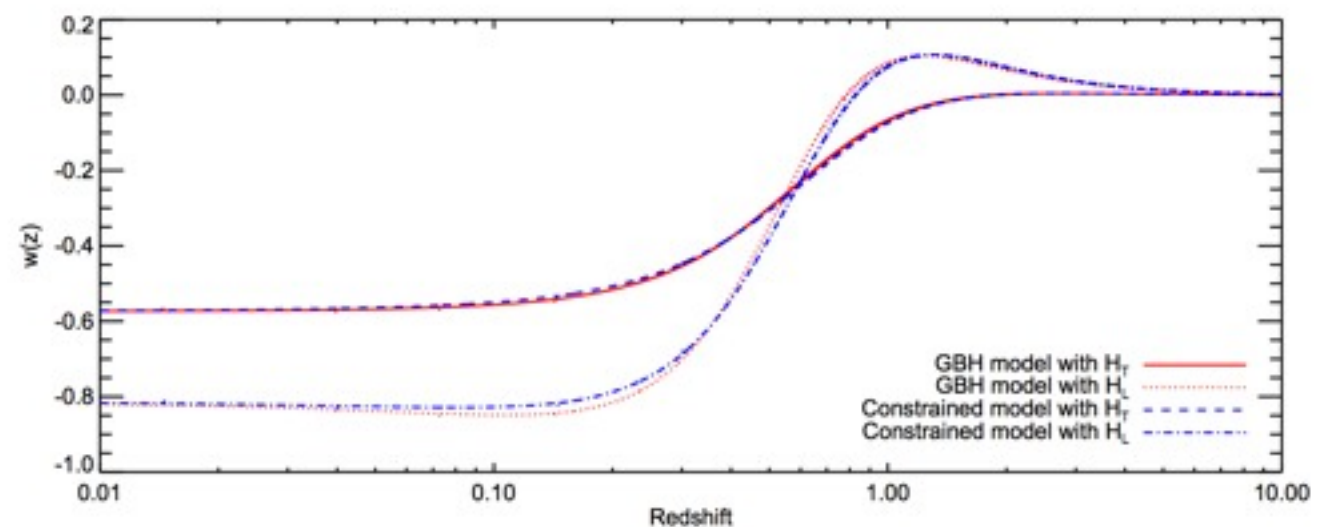
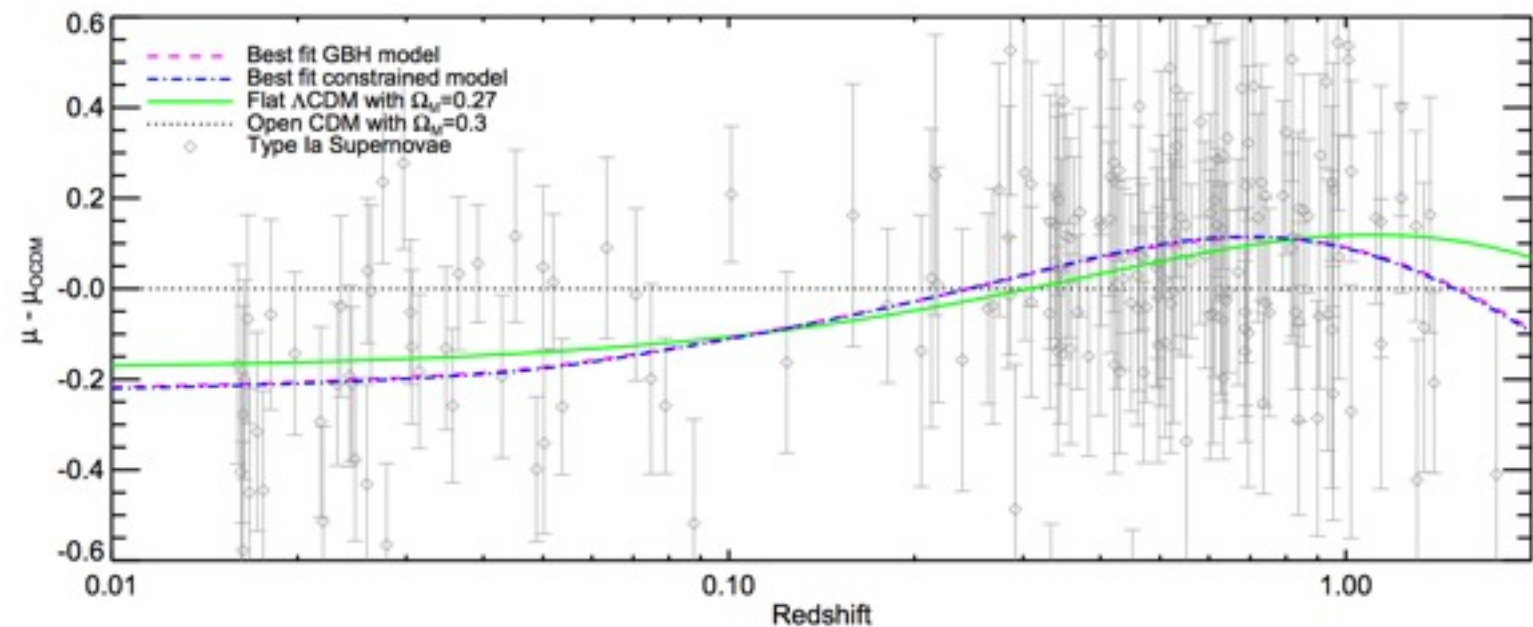
Void models LTB

Popular inhomogeneous models are the Lemaitre-Tolman- Bondi (LTB), which are spherically symmetric but inhomogeneous (see e.g., Envquist 2008). Spatial variation in matter density and Hubble rate can have the same effect on redshift as acceleration in a perfectly homogeneous universe.

Bellido & Haugbølle 2008



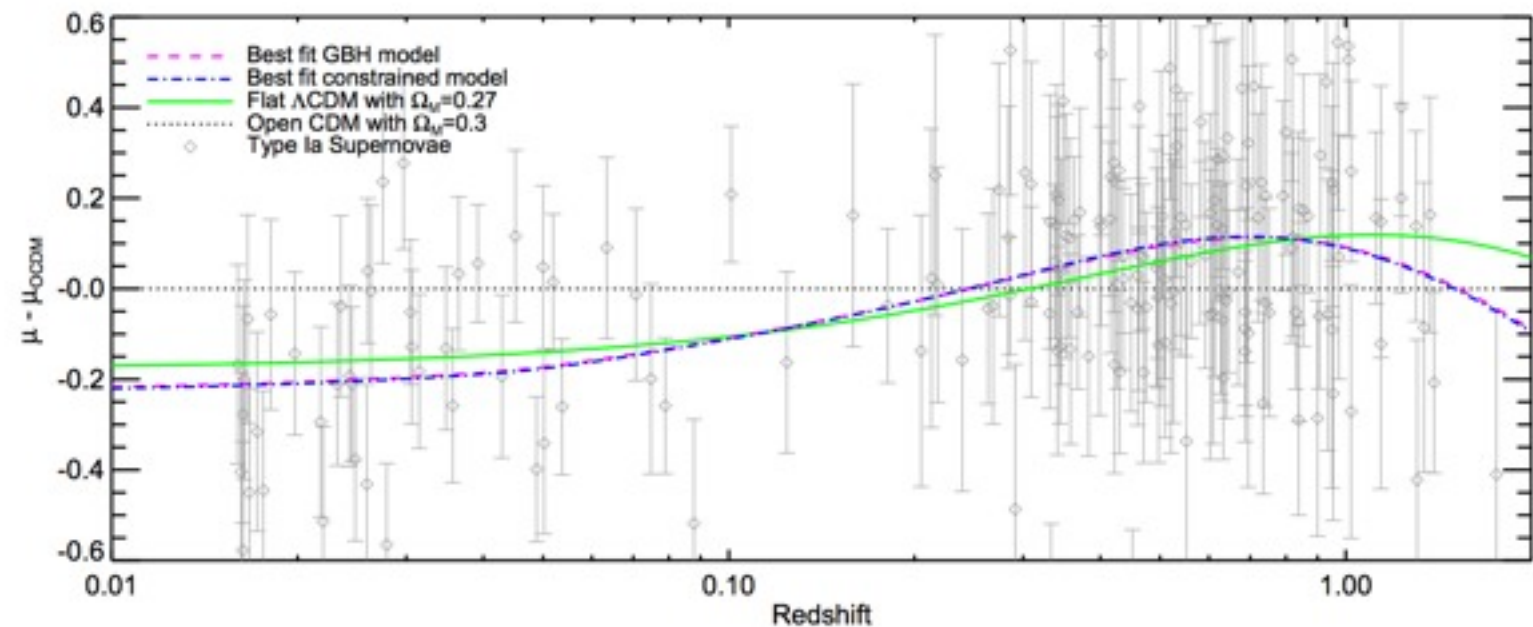
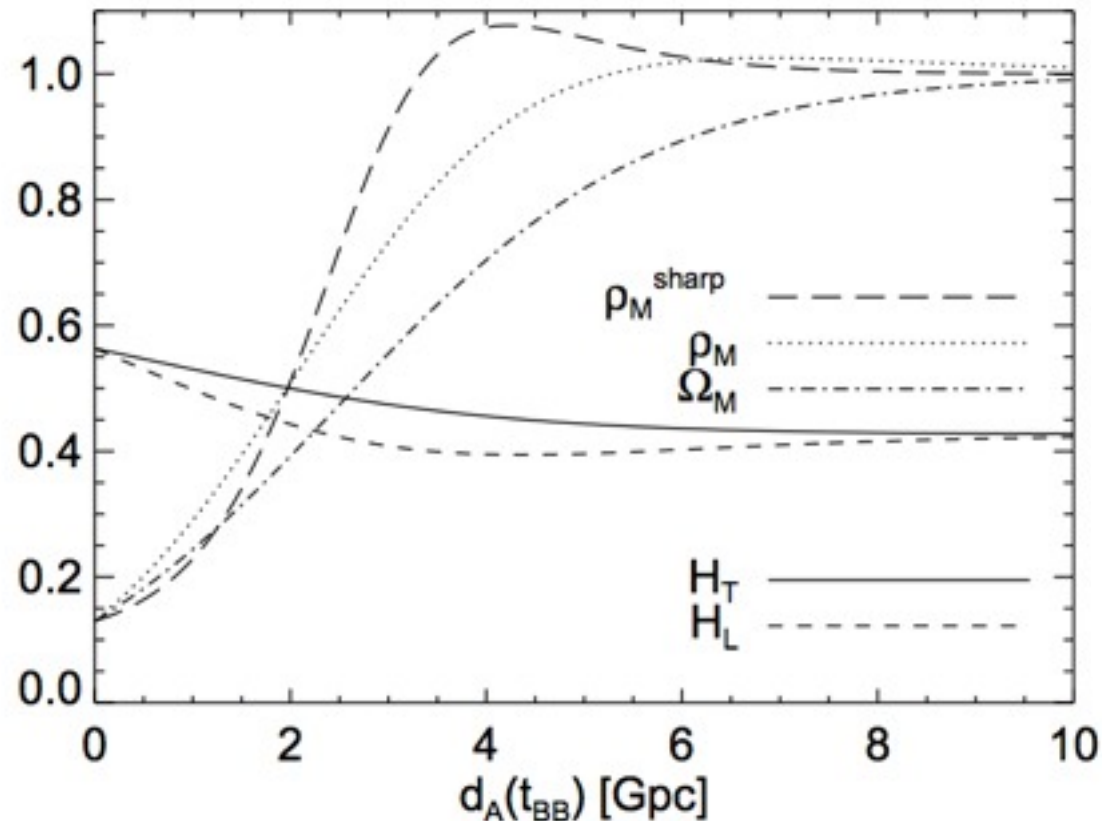
Results: Dark Energy appears as a local effect, due to the low matter density void. Outside of the void $w=0$, dark energy = 0, dark matter = 1



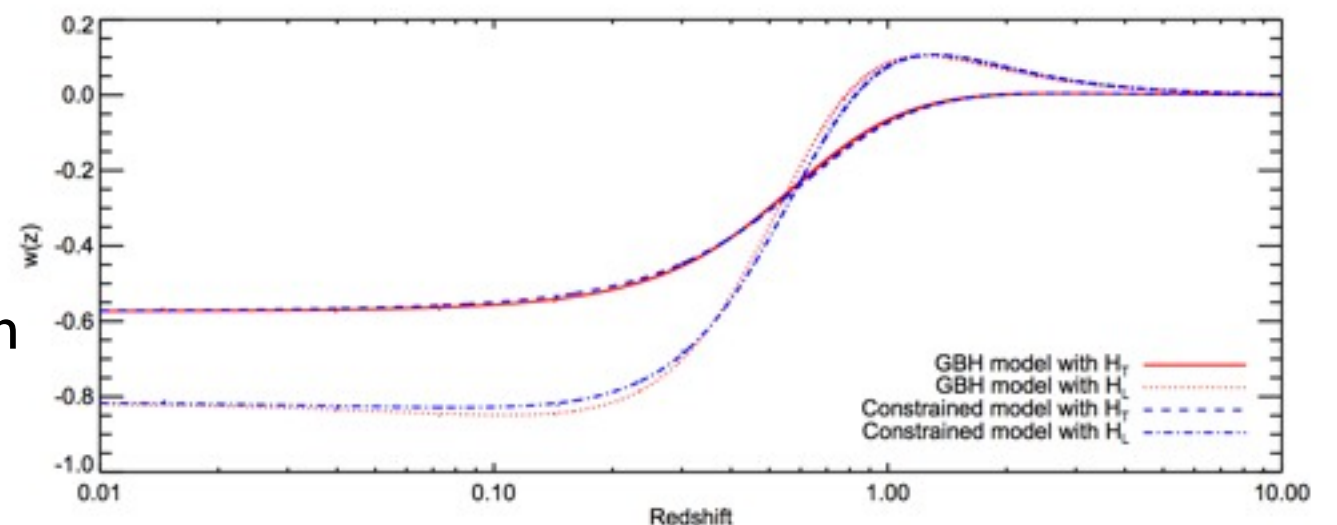
Void models LTB

Popular inhomogeneous models are the Lemaitre-Tolman- Bondi (LTB), which are spherically symmetric but inhomogeneous (see e.g., Envquist 2008). Spatial variation in matter density and Hubble rate can have the same effect on redshift as acceleration in a perfectly homogeneous universe.

Bellido & Haugbølle 2008



Fine tuning: For this to be consistent with the CMB, we must abandon the copernican principle and live near centre of void, or within a ~ 100 kpc otherwise we would measure a much larger CMB dipole.



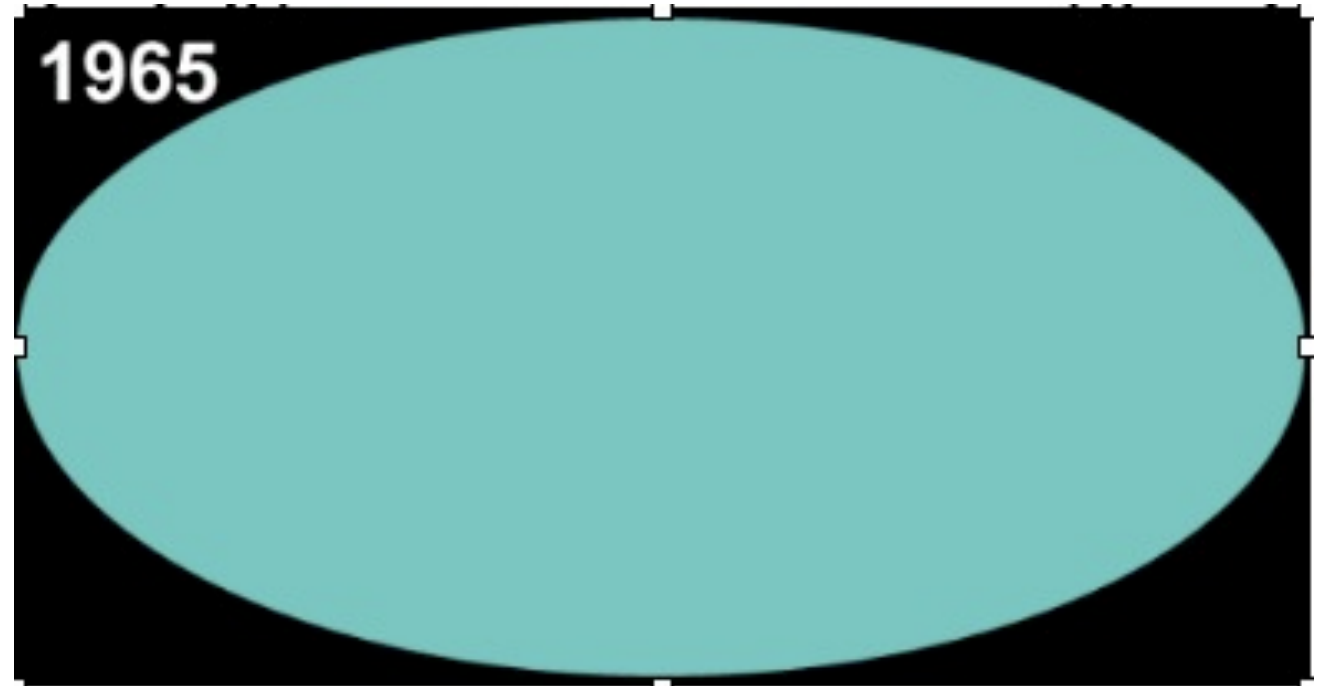
However, these models are now also disfavoured by current cluster kinetic SZ data e.g., Bull et al 2012

Isotropy

To test isotropy we compare different positions on the sky at the same redshift.

CMB $z \approx 1100$

The CMB looks the same in all directions (COBE).



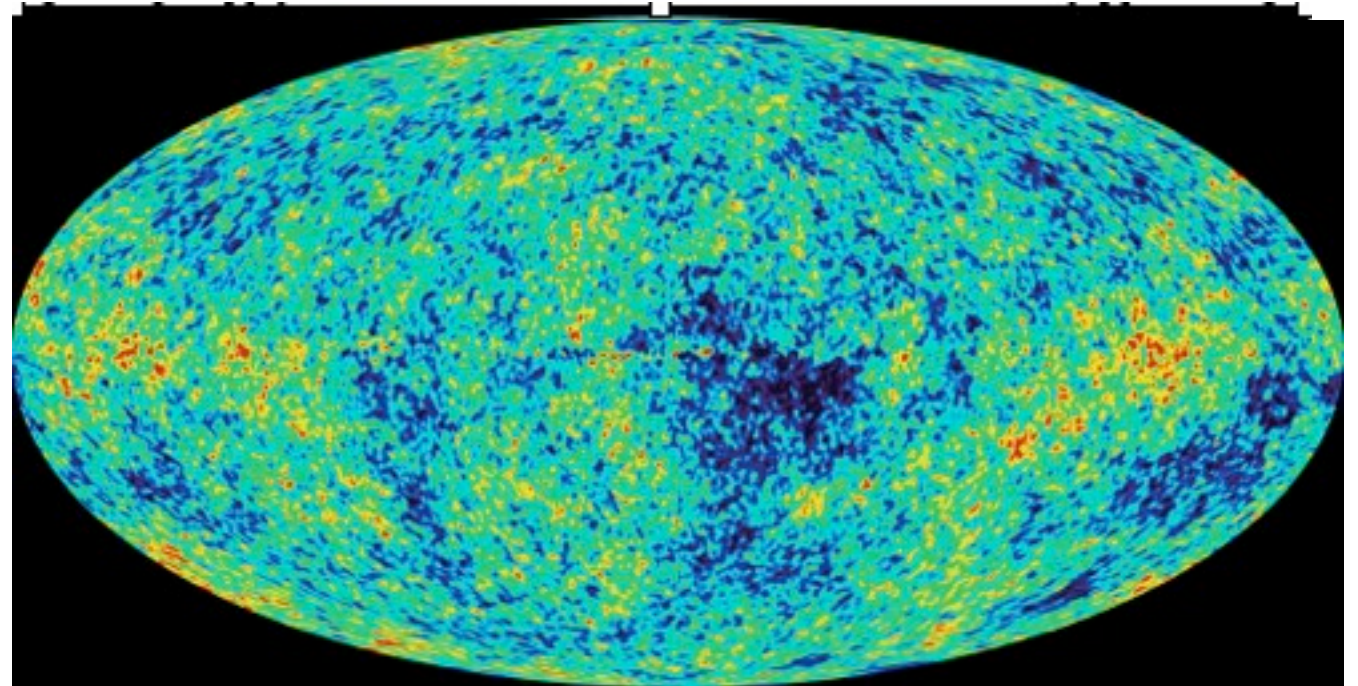
Isotropy

To test isotropy we compare different positions on the sky at the same redshift.

CMB $z \approx 1100$

The CMB looks the same in all directions (COBE).

The actual variations in the temperature of the CMB are tiny.



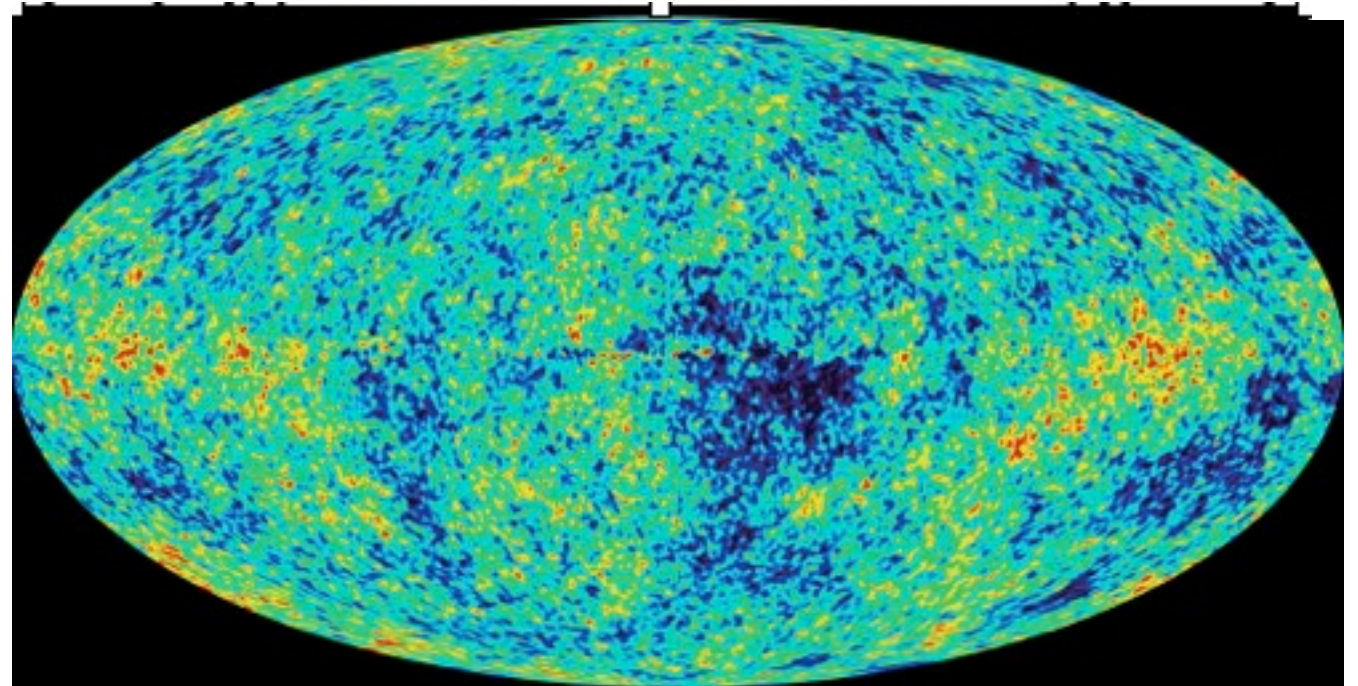
Isotropy

To test isotropy we compare different positions on the sky at the same redshift.

CMB $z \approx 1100$

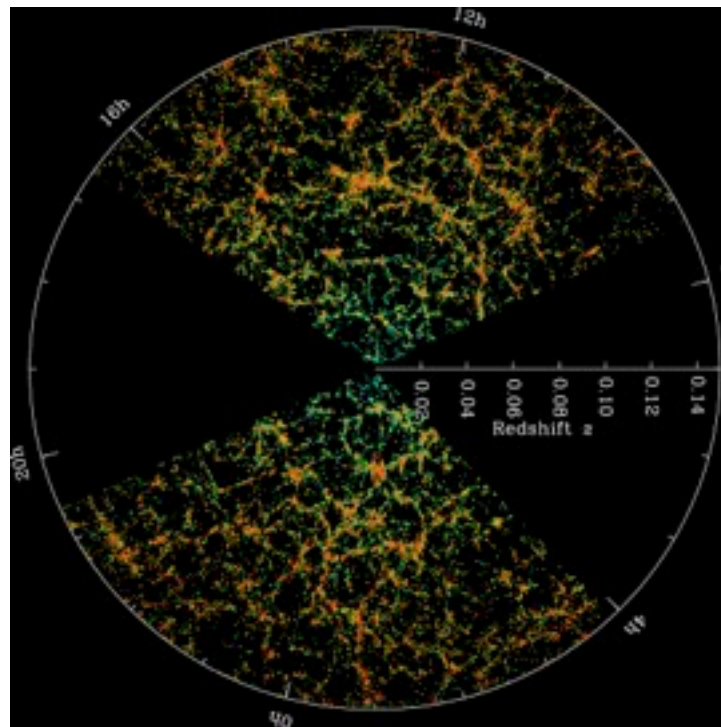
The CMB looks the same in all directions (COBE).

The actual variations in the temperature of the CMB are tiny.



LSS $z \lesssim 0.5$

The distribution of large scale structure, smoothed on large scaled look isotropic, as measured by the SDSS.



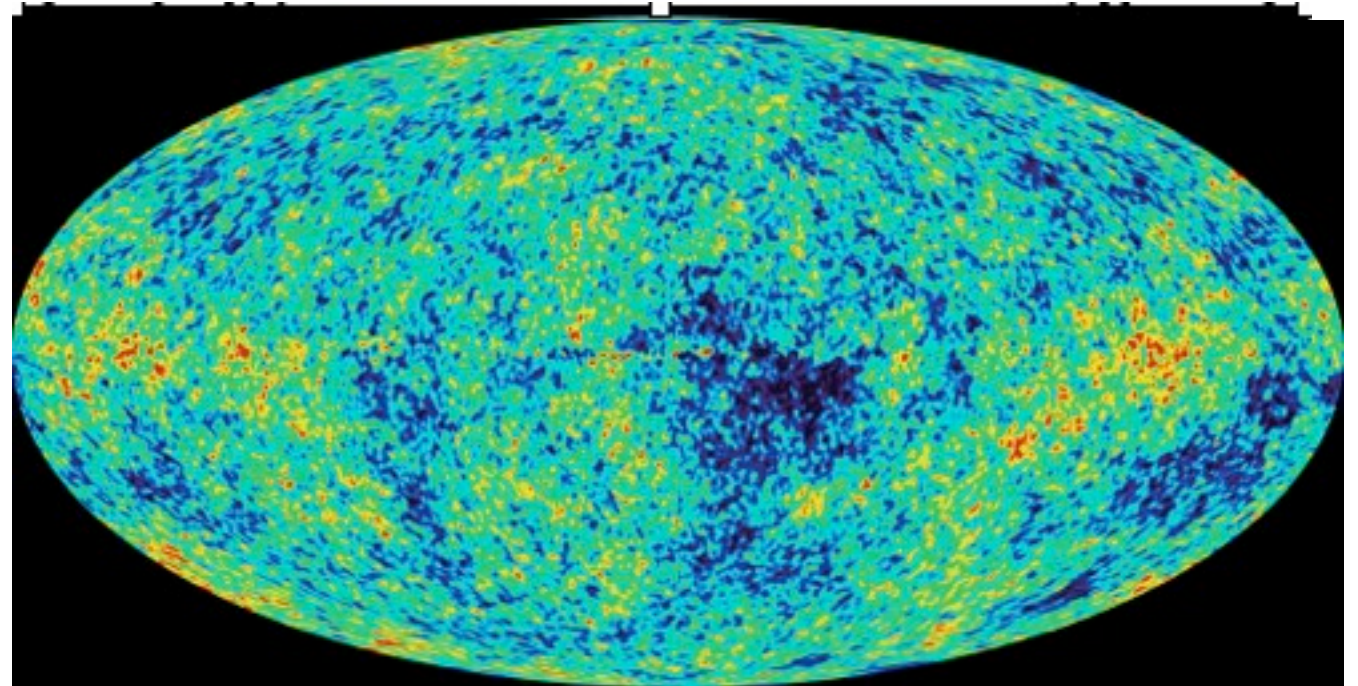
Isotropy

To test isotropy we compare different positions on the sky at the same redshift.

CMB $z \approx 1100$

The CMB looks the same in all directions (COBE).

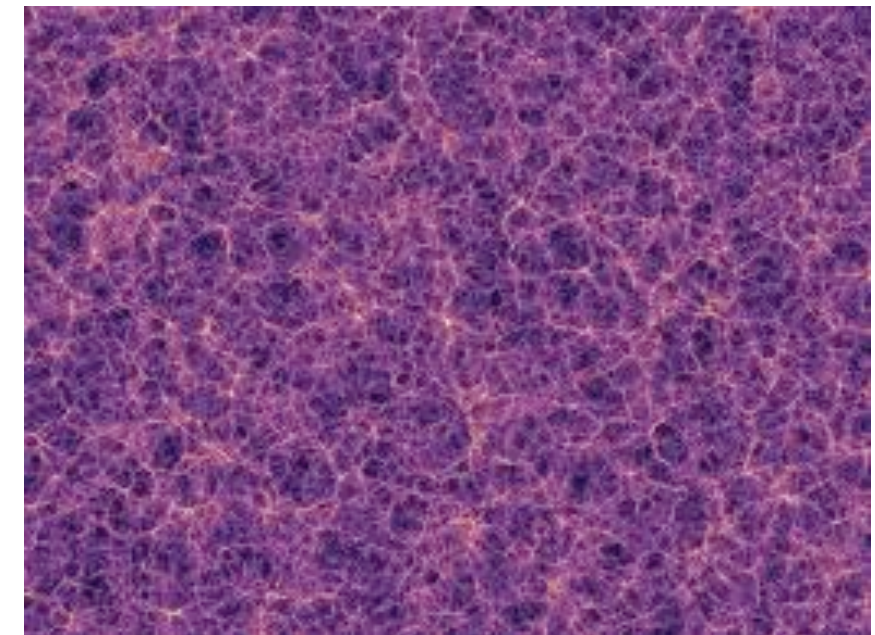
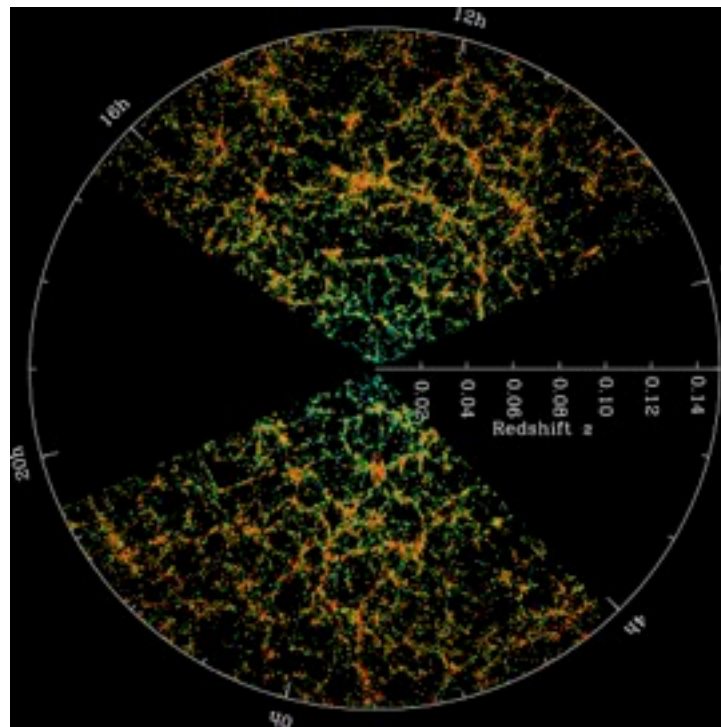
The actual variations in the temperature of the CMB are tiny.



LSS $z \lesssim 0.5$

The distribution of large scale structure, smoothed on large scaled look isotropic, as measured by the SDSS.

On smaller scales, at fixed redshift there is lots of structure, which are in good agreement with the Millennium Simulation (performed assuming homogeneity/isotropy).



Homogeneity

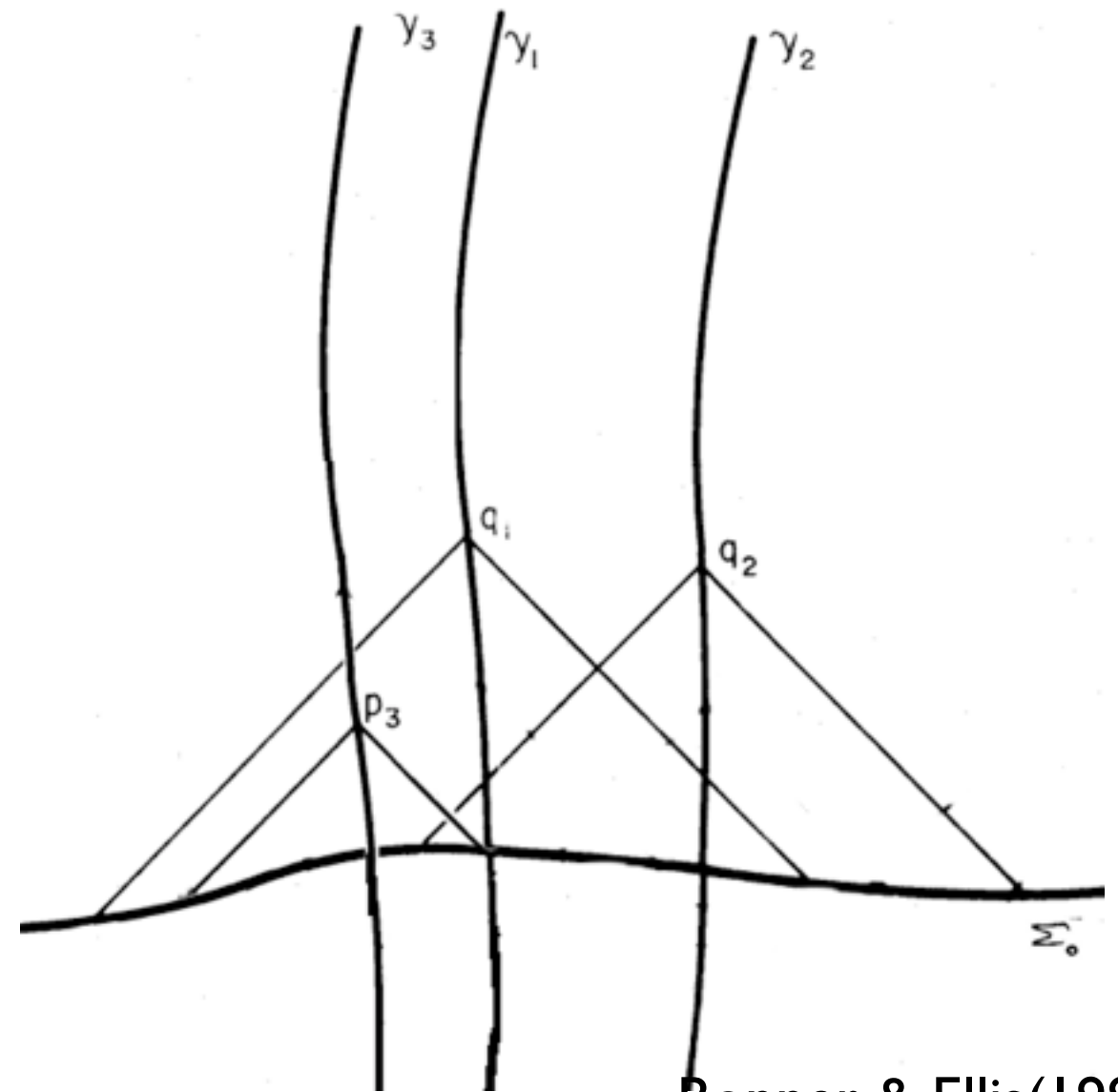
To test homogeneity we must compare 2 or more (different) locations in the sky with different redshifts, and reconstruct some property of theirs to a common redshift (or hyper-surface).

Homogeneity

To test homogeneity we must compare 2 or more (different) locations in the sky with different redshifts, and reconstruct some property of theirs to a common redshift (or hyper-surface).

Space-time diagrams: Recall vertical lines represent world lines (observers at rest), x-direction denote spatial coordinates (hyper surfaces). Signals (e.g light from CMB) follow 45 deg. trajectories.

We make direct measurements along our past light cone.



Bonner & Ellis (1986)

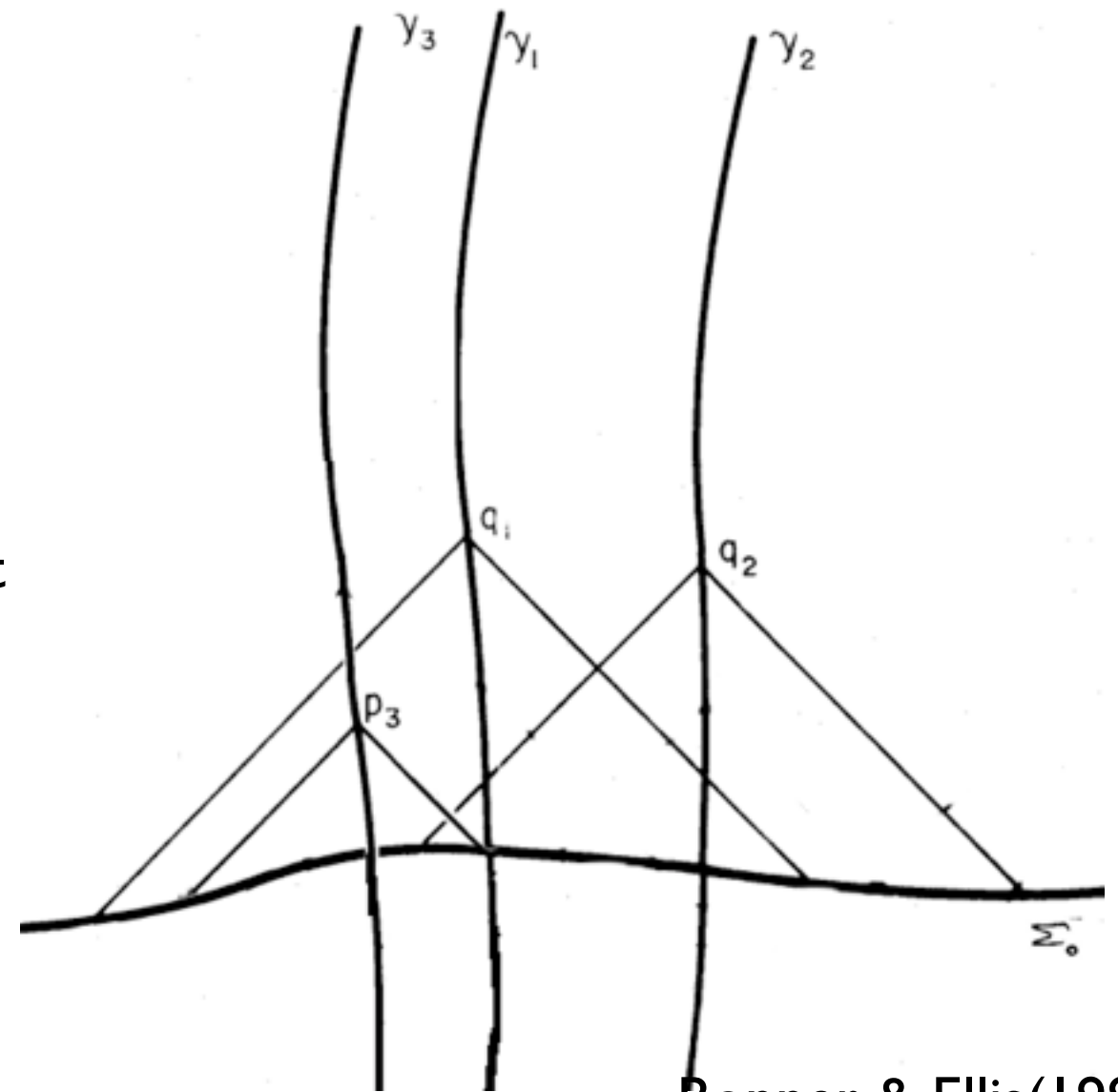
Homogeneity

To test homogeneity we must compare 2 or more (different) locations in the sky with different redshifts, and reconstruct some property of theirs to a common redshift (or hyper-surface).

Space-time diagrams: Recall vertical lines represent world lines (observers at rest), x-direction denote spatial coordinates (hyper-surfaces). Signals (e.g light from CMB) follow 45 deg. trajectories.

We make direct measurements along our past light cone.

Measurements: To measure properties at different locations on the hyper-surface, we would need observers separated in space (not in causal contact).



Bonner & Ellis (1986)

Homogeneity

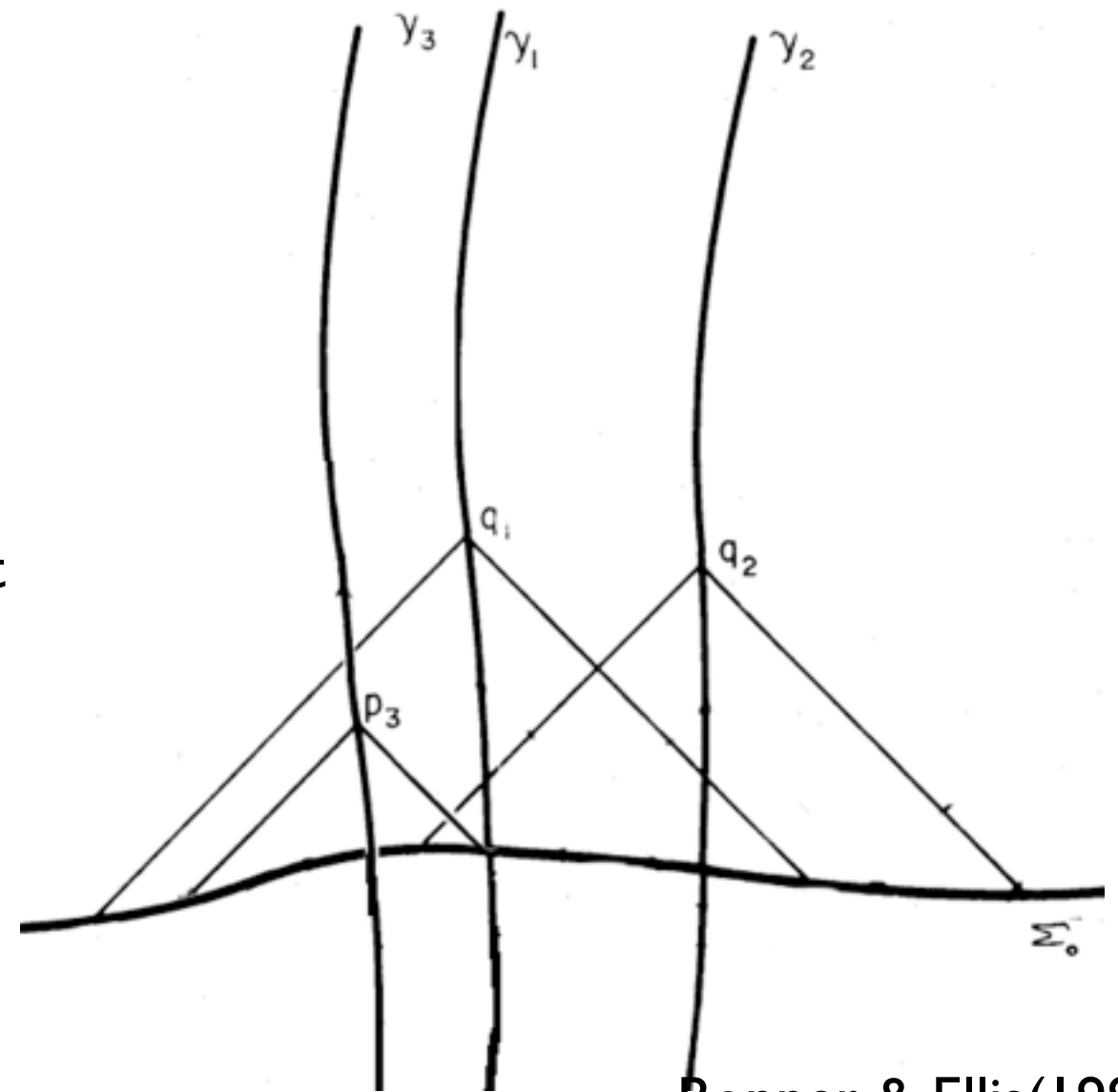
To test homogeneity we must compare 2 or more (different) locations in the sky with different redshifts, and reconstruct some property of theirs to a common redshift (or hyper-surface).

Space-time diagrams: Recall vertical lines represent world lines (observers at rest), x-direction denote spatial coordinates (hyper-surfaces). Signals (e.g light from CMB) follow 45 deg. trajectories.

We make direct measurements along our past light cone.

Measurements: To measure properties at different locations on the hyper-surface, we would need observers separated in space (not in causal contact).

Testing Homogeneity: We need to reconstruct some quantity measured on the past light cone, to some earlier time within the past light cone. The reconstructed quantity probes different hyper-surface coordinates

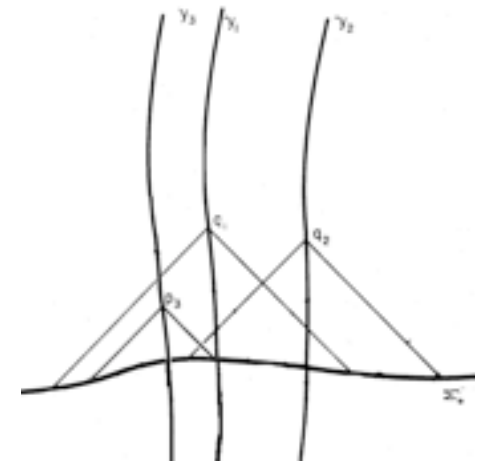


Bonner & Ellis (1986)

Homogeneity

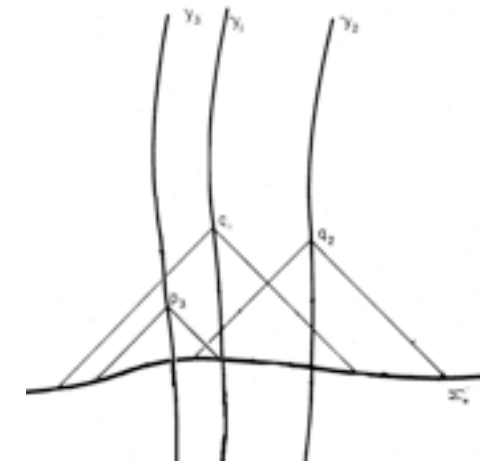
To test homogeneity we must compare 2 or more (different) locations in the sky with different redshifts, and reconstruct some property of theirs to a common redshift (or hyper-surface).

Kinetic SZ: Galaxy clusters contain an hot diffuse ICM which interacts with the CMB (SZ effect). We can reconstruct the CMB temperature, as seen from a nearby Galaxy Cluster, in particular paying attention to the CMB photons which are bounced off the ICM, and can be distinguished from CMB photons coming directly toward us. This analysis is shows full consistency with homogeneity, e.g., Bull et al (2012).



Homogeneity

To test homogeneity we must compare 2 or more (different) locations in the sky with different redshifts, and reconstruct some property of theirs to a common redshift (or hyper-surface).

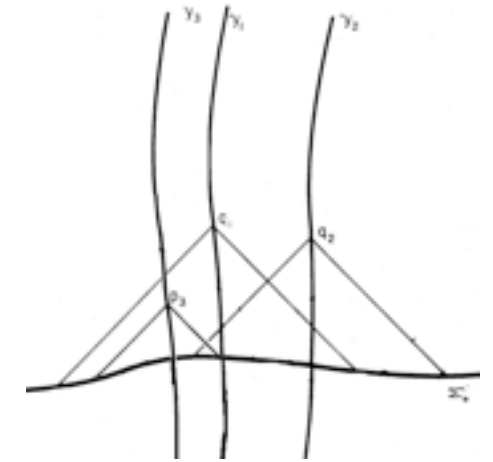


Kinetic SZ: Galaxy clusters contain an hot diffuse ICM which interacts with the CMB (SZ effect). We can reconstruct the CMB temperature, as seen from a nearby Galaxy Cluster, in particular paying attention to the CMB photons which are bounced off the ICM, and can be distinguished from CMB photons coming directly toward us. This analysis is shows full consistency with homogeneity, e.g., Bull et al (2012).

Thermal histories: Bonnor & Ellis (1986) suggested comparing local stars with those in distant galaxies. Similar stars would suggest similar thermal histories in widely separated regions of the Universe.

Homogeneity

To test homogeneity we must compare 2 or more (different) locations in the sky with different redshifts, and reconstruct some property of theirs to a common redshift (or hyper-surface).



Kinetic SZ: Galaxy clusters contain an hot diffuse ICM which interacts with the CMB (SZ effect). We can reconstruct the CMB temperature, as seen from a nearby Galaxy Cluster, in particular paying attention to the CMB photons which are bounced off the ICM, and can be distinguished from CMB photons coming directly toward us. This analysis is shows full consistency with homogeneity, e.g., Bull et al (2012).

Thermal histories: Bonnor & Ellis (1986) suggested comparing local stars with those in distant galaxies. Similar stars would suggest similar thermal histories in widely separated regions of the Universe.

SFRH: Comparing the Star Formation Rate Histories across cosmic time, reconstructed from galaxy spectra, for widely separated galaxies, at different redshift can also probe homogeneity

“Testing homogeneity with the fossil record of galaxies”
Heavens, Jimenez, Martens 2011

Overview

- Concordance cosmology & homogeneity.
- Extracting Star Formation Histories (SFH) from galaxy spectra using VESPA.
- VESPA and voids.
- Using VESPA to test for homogeneity.
- Modeling assumptions.
- The student t-distribution as outliers.
- The full probability distribution.
- Homogeneity $< 5.8\%$
- Conclusions.

Extracting SP with VESPA I

- VErsatile SPectral Analysis (VESPA) Tojeiro et al 2007, Tojeiro et al 2009
- Uses all available absorption lines and the continuum shape to interpret the galaxy in terms of its star formation history, using the latest synthetic and empirical stellar population models for both the SDSS Luminous Red Galaxies, LRG and Main Sample Galaxies MGS samples.
- Improvement over previous software packages (MOPED, STARLIGHT etc) because it uses adaptive binning to determine the best number of recovered parameters without over parameterising.
- Recovered quantities: Mass(look-back time), Star formation rates (look-back time), Metallicity(look-back time)

Extracting SP with VESPA I

- VErsatile SPectral Analysis (VESPA) Tojeiro et al 2007, Tojeiro et al 2009
- Uses all available absorption lines to interpret the galaxy in terms of the latest synthetic and empirical SDSS Luminous Red Galaxy samples.
- Improvement over previous (MOPED, STARLIGHT etc) in determining the best number of components for parameterising.
- Recovered quantities: Mass (look-back time), Metallicity

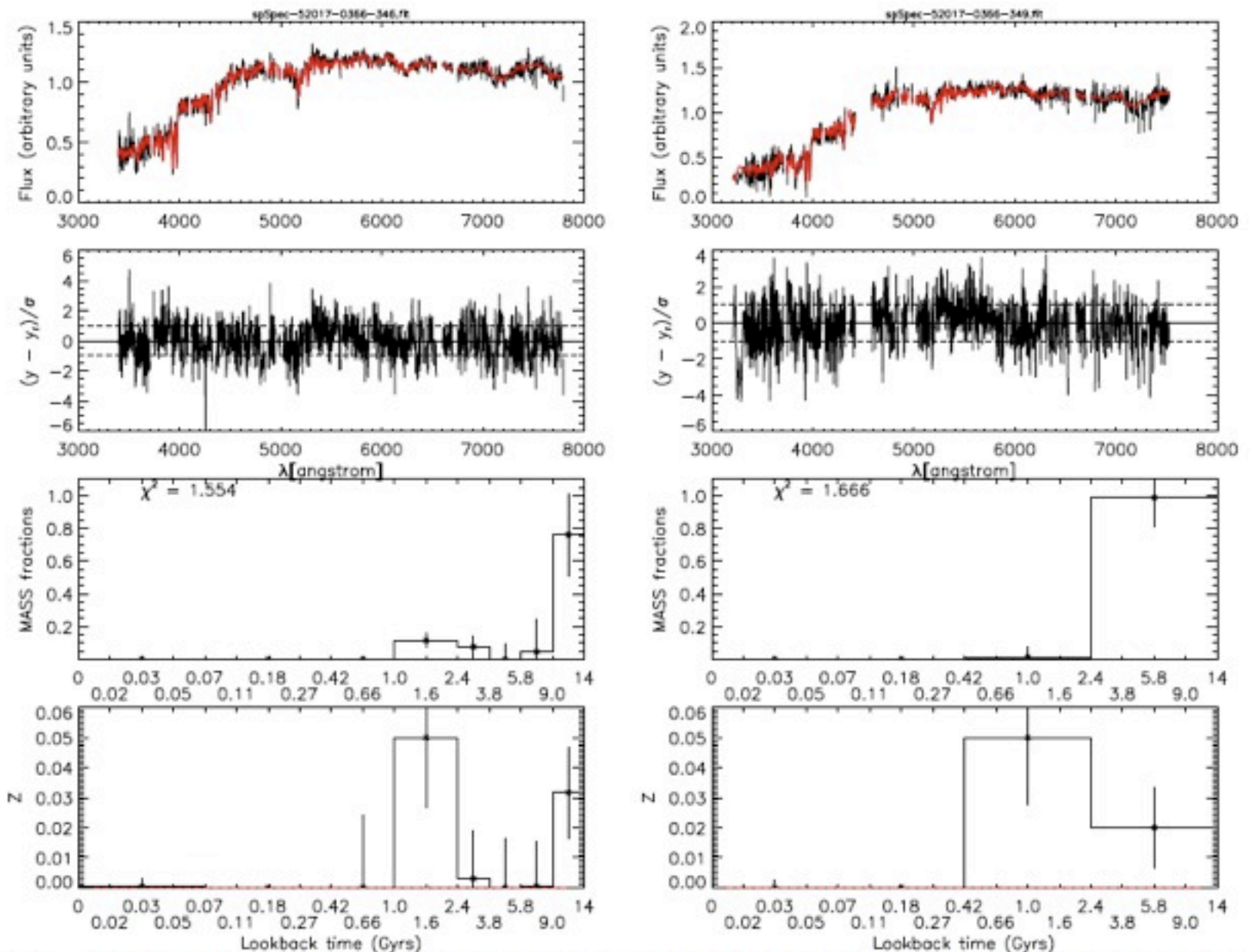


FIG. 2.— Two SDSS galaxies analysed with VESPA. In each case the top panels show the observed and fit spectrum (black and red respectively; only the fitted regions are shown), the second panel the residuals, the third panel the recovered star formation mass fractions and in the bottom panel we show the recovered metallicity in each age bin. The example on the right shows a galaxy from which little information could safely be recovered which is translated into large age bins. The interpretation should be that the majority of this galaxy's mass was formed 11-14 Gyrs ago in the rest-frame, but we cannot tell more precisely when, within that interval, this happened. The example on the left shows a galaxy with a history which is better resolved.

Extracting SP with VESPA II

VESPA iteratively compares the observed spectra flux F_λ , as a function of wavelength, with a model spectral flux \hat{F}_λ , obtained from sets of simple stellar populations $S_\lambda(t, Z)$, with various star formation rates $\psi(t)$.

Tojeiro et al 2009

$$\chi^2 = \frac{\sum_\lambda (F_\lambda - \hat{F}_\lambda)^2}{\sigma_\lambda^2}.$$

$$\hat{F}_\lambda(t_0) = \int_0^{t_0} f_{dust}(\tau_\lambda, t) \psi(t) S_\lambda(t, Z) dt,$$

With a two component dust model of Charlot & Fall (2000).

Extracting SP with VESPA II

VESPA iteratively compares the observed spectra flux F_λ , as a function of wavelength, with a model spectral flux \hat{F}_λ , obtained from sets of simple stellar populations $S_\lambda(t, Z)$, with various star formation rates $\psi(t)$.

Tojeiro et al 2009

$$\chi^2 = \frac{\sum_\lambda (F_\lambda - \hat{F}_\lambda)^2}{\sigma_\lambda^2}.$$

$$\hat{F}_\lambda(t_0) = \int_0^{t_0} f_{dust}(\tau_\lambda, t) \psi(t) S_\lambda(t, Z) dt,$$

With a two component dust model of Charlot & Fall (2000).

BinID	T_{B+} Bin Start [Gyrs]	T_{B+} Bin End [Gyrs]
0	0.002	0.074
1	0.074	0.177
2	0.177	0.275
3	0.275	0.425
4	0.425	0.657
5	0.657	1.020
6	1.020	1.570
7	1.570	2.440
8	2.440	3.780
9	3.780	5.840
10	5.840	7.440
11	7.440	8.239
12	8.239	9.040
13	9.040	10.28
14	10.28	11.52
15	11.52	13.50

Extracting SP with VESPA II

VESPA iteratively compares the observed spectra flux F_λ , as a function of wavelength, with a model spectral flux \hat{F}_λ , obtained from sets of simple stellar populations $S_\lambda(t, Z)$, with various star formation rates $\psi(t)$.

Tojeiro et al 2009

$$\chi^2 = \frac{\sum_\lambda (F_\lambda - \hat{F}_\lambda)^2}{\sigma_\lambda^2}$$

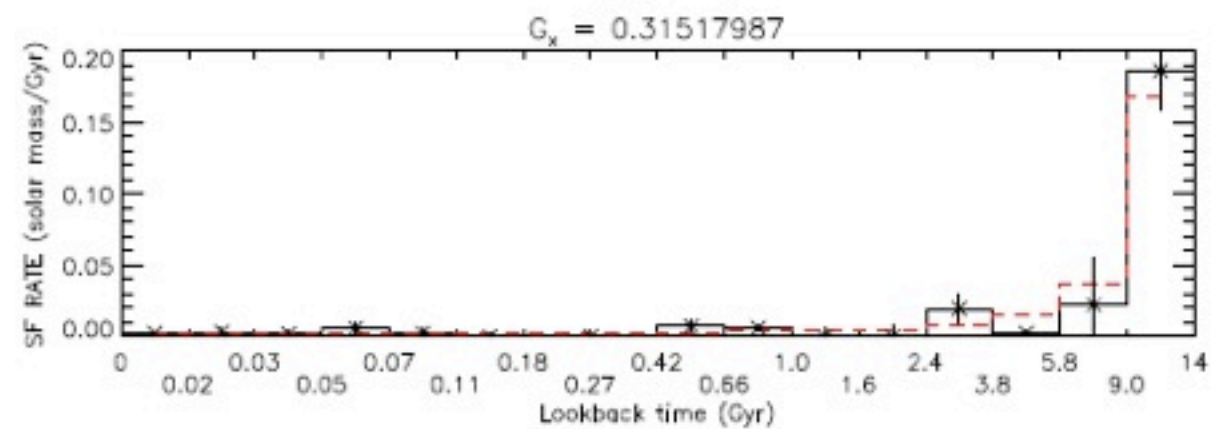
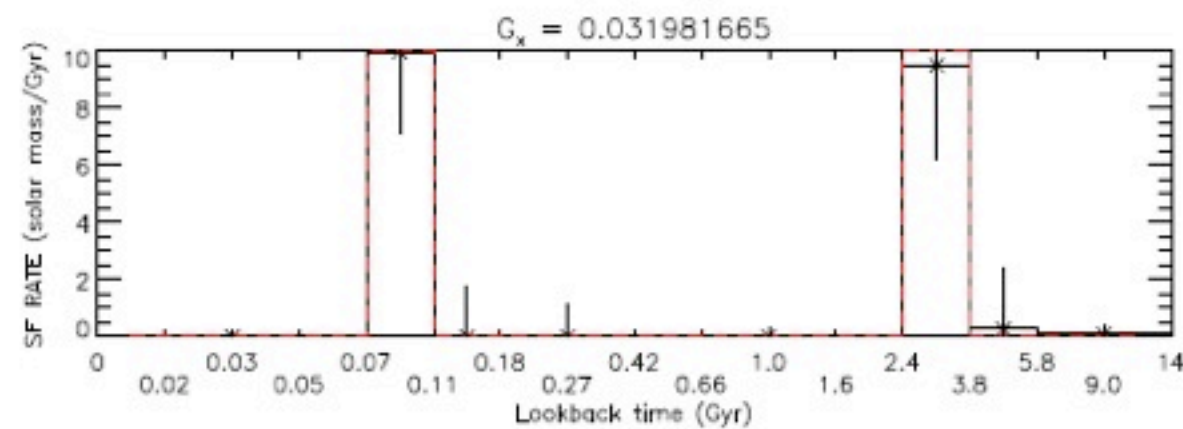
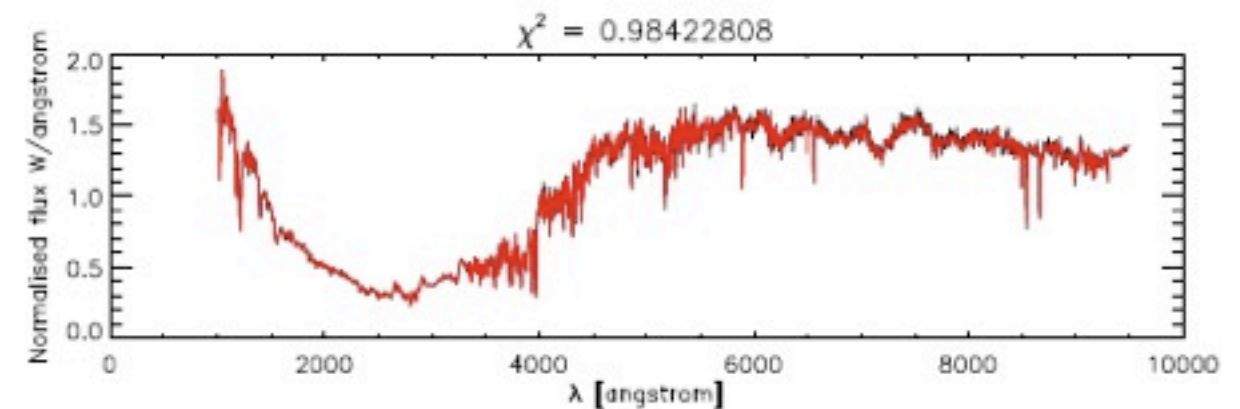
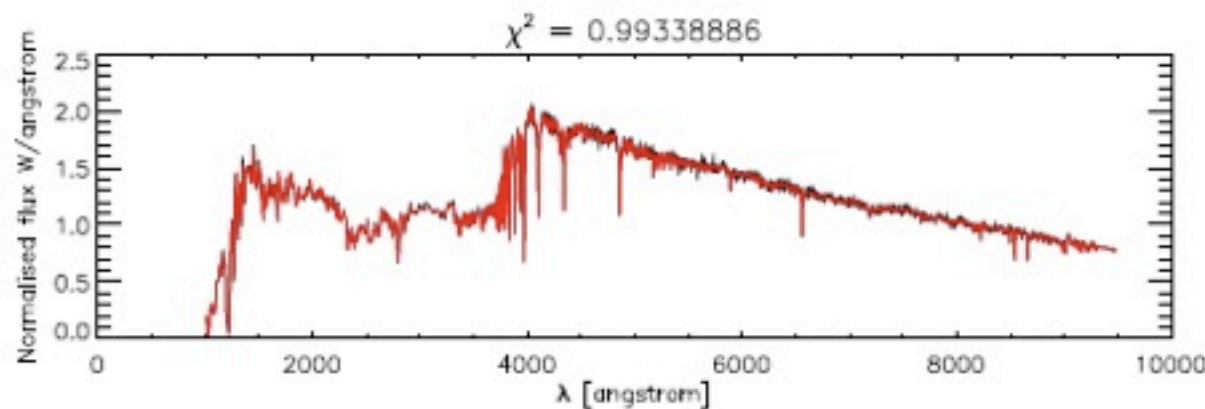
$$\hat{F}_\lambda(t_0) = \int_0^{t_0} f_{dust}(\tau_\lambda, t) \psi(t) S_\lambda(t, Z) dt,$$

BinID	T_{B+} Bin Start [Gyrs]	T_{B+} Bin End [Gyrs]
0	0.002	0.074
1	0.074	0.177
2	0.177	0.275
3	0.275	0.425
4	0.425	0.657
5	0.657	1.020
6	1.020	1.570
7	1.570	2.440
8	2.440	3.780
9	3.780	5.840
10	5.840	7.440
11	7.440	8.239
12	8.239	9.040
13	9.040	10.28
14	10.28	11.52
15	11.52	13.50

With a two component dust model of Charlot & Fall (2000).

VESPA has been tested on synthetic spectra, and retrieves good agreement for high signal-to-noise galaxies.

Recovering galaxy histories using VESPA 9



Extracting SP with VESPA II

VESPA iteratively compares the observed spectra flux F_λ , as a function of wavelength, with a model spectral flux \hat{F}_λ , obtained from sets of simple stellar populations $S_\lambda(t, Z)$, with various star formation rates $\psi(t)$.

$$\chi^2 = \frac{\sum_\lambda (F_\lambda - \hat{F}_\lambda)^2}{\sigma_\lambda^2}$$

$$\hat{F}_\lambda(t_0) = \int_0^{t_0} f_{dust}(\tau_\lambda, t) \psi(t) S_\lambda(t, Z) dt,$$

With a two component dust model of Charlot & Fall (2000).

VESPA has been tested on synthetic spectra, and retrieves good agreement for high signal-to-noise galaxies. *Recovering galaxy hist*

Tojeiro et al 2009

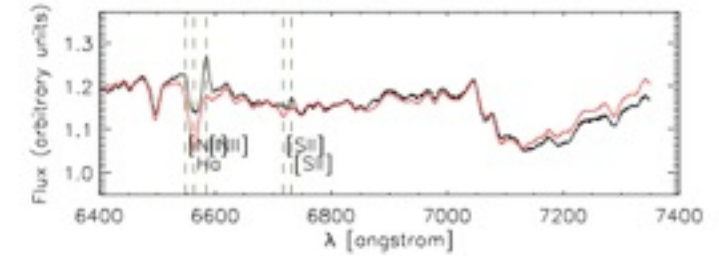
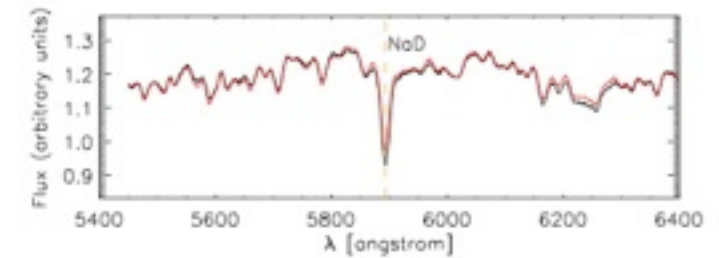
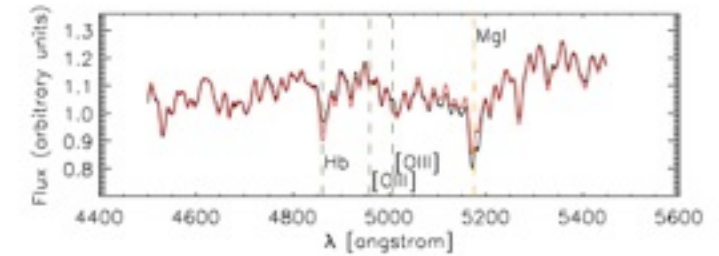
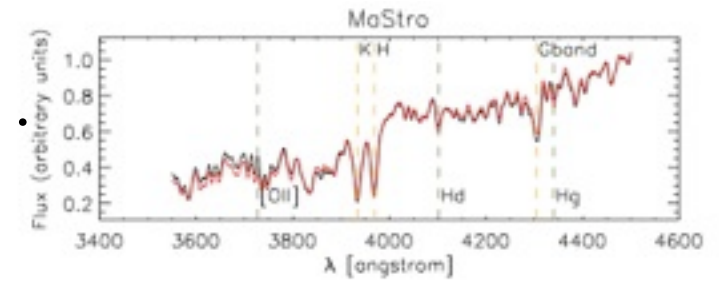
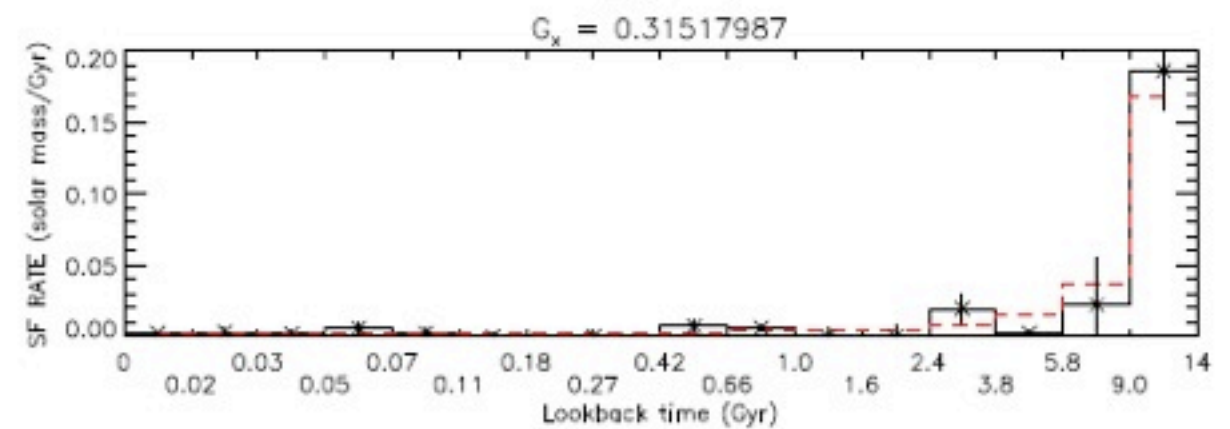
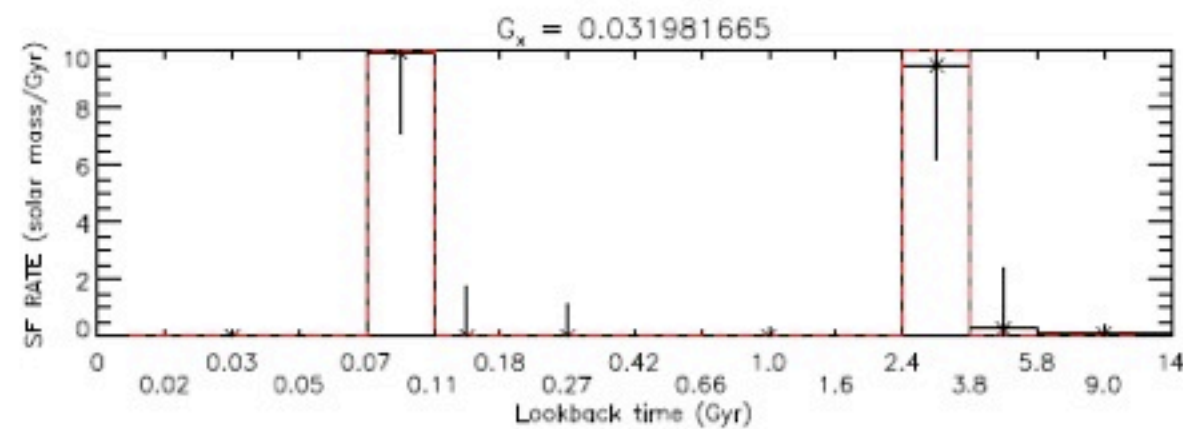
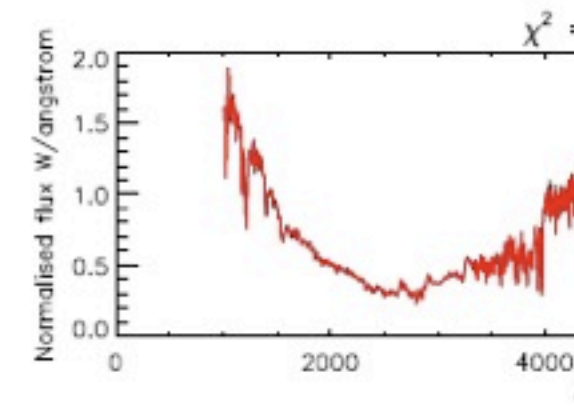
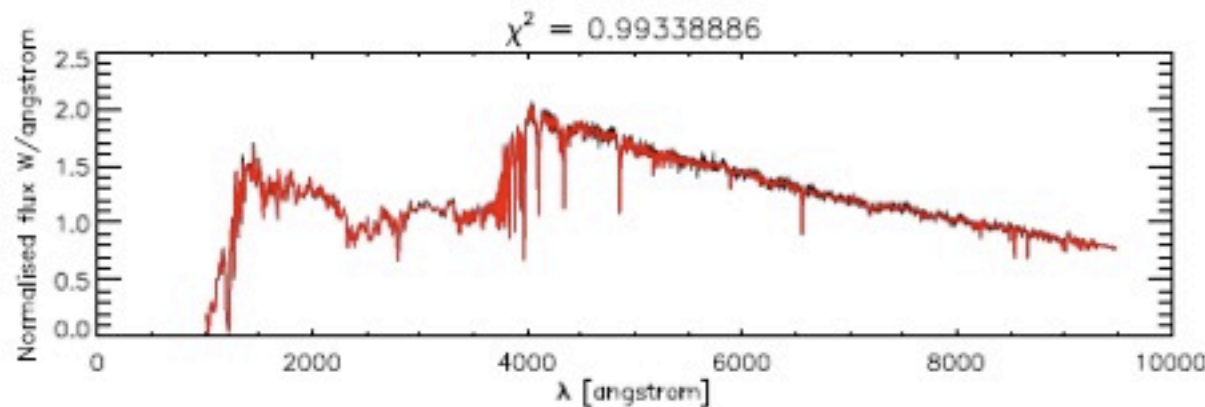
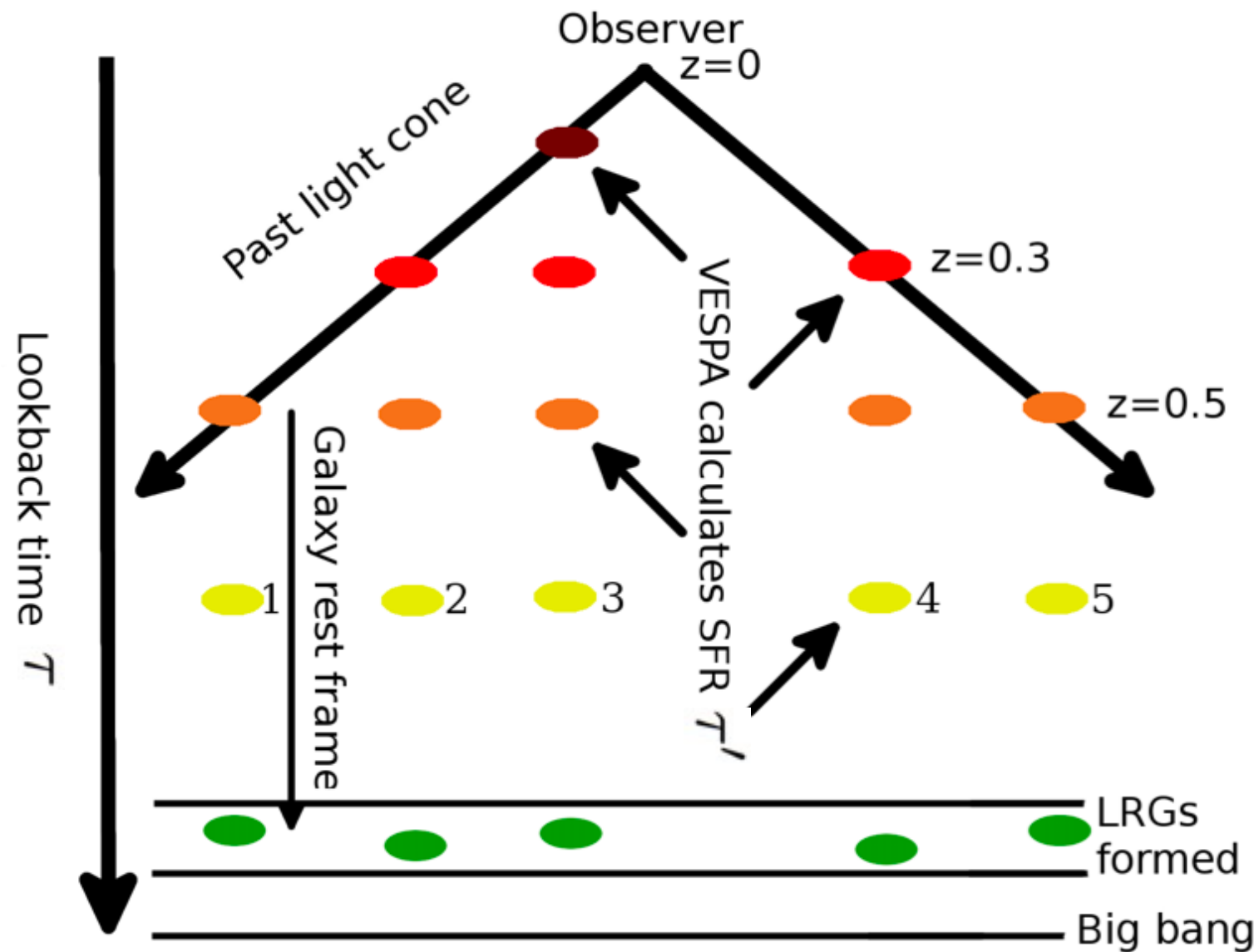
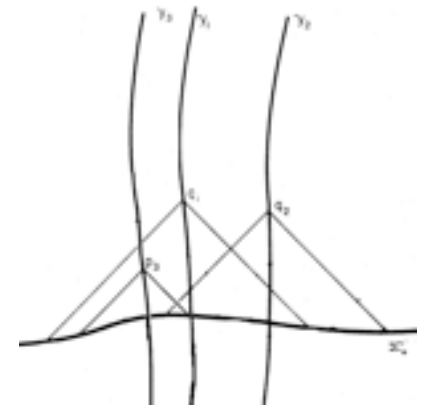


Figure A1. A typical fit, using the M10 models. The black line



VESPA and homogeneity

A cartoon of the VESPA process as applied to SDSS LRGs. We assume that LRGs form at approximately the same epoch, and have similar evolution histories. These assumptions form the basis of the homogeneity test.



We use VESPA to determine the rest-frame Star Formation Rates (SFR) as a function of time. We compare the SFR histories of galaxies at different redshifts ($z=0, 0.3, 0.4$) and positions on the sky, at some set higher redshift denoted by 1, 2, 3, 4, 5.

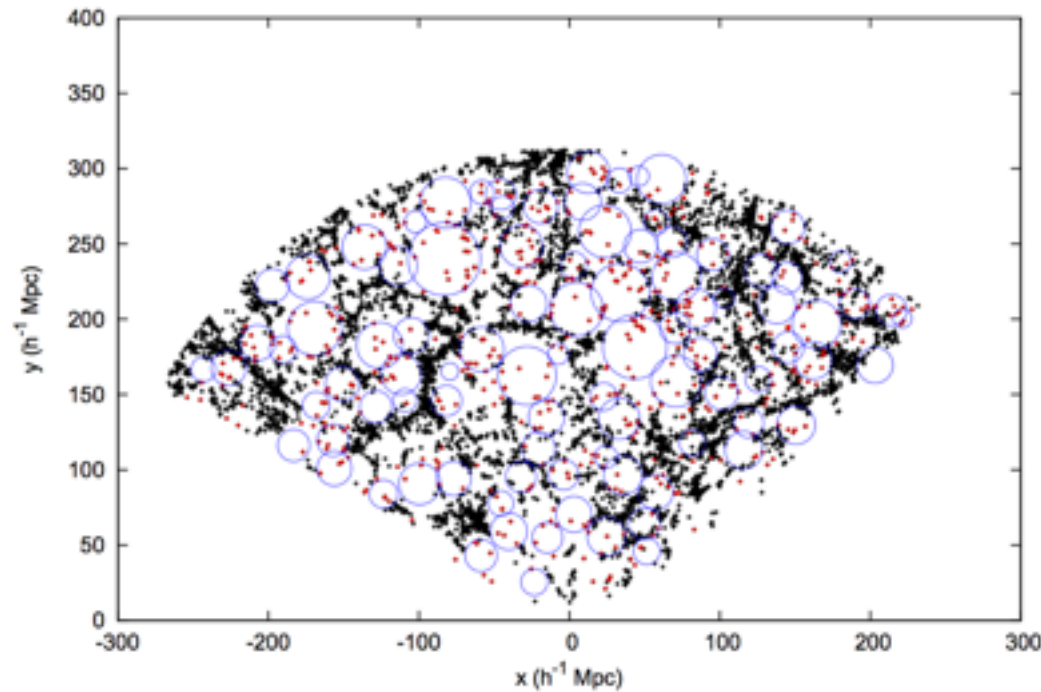
Voids with VESPA I

Sanity test: Can we use VESPA to quantify differences in stellar populations for galaxy samples already identified to be different in the literature?

Voids with VESPA I

Sanity test: Can we use VESPA to quantify differences in stellar populations for galaxy samples already identified to be different in the literature?

Fiona Hoyle et al (2012)



Data: SDSS main sample galaxies.

Galaxy void catalogue presented in Pan et al (2011) using the 'voidfinder' algorithm.

Small scale SDSS voids ~ 10 Mpc/h

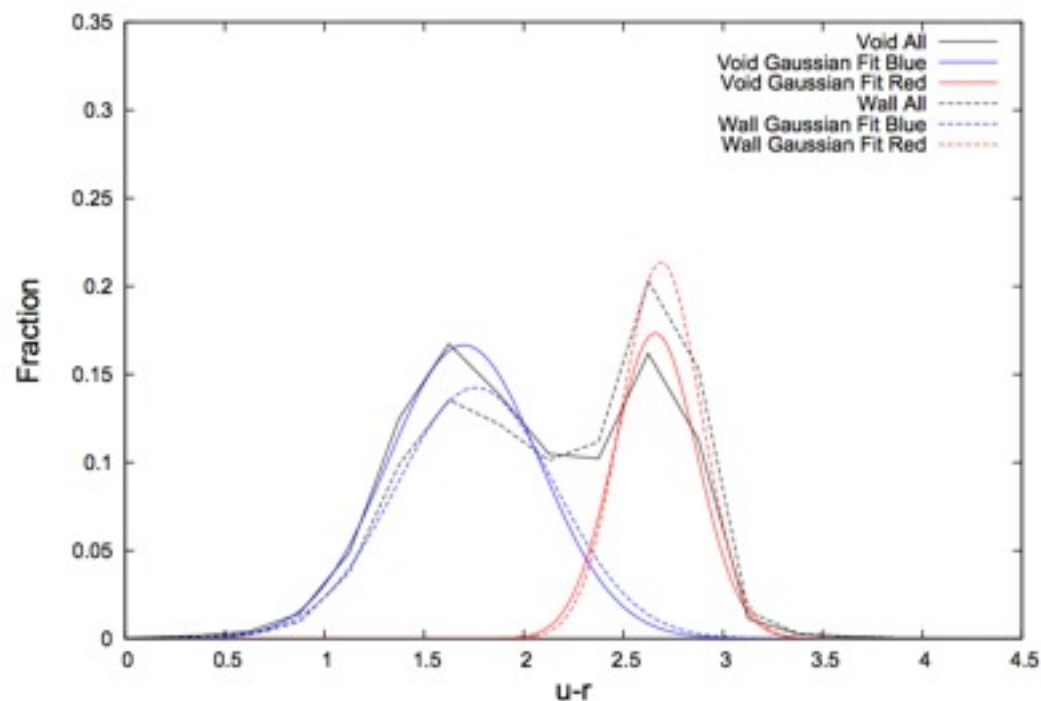
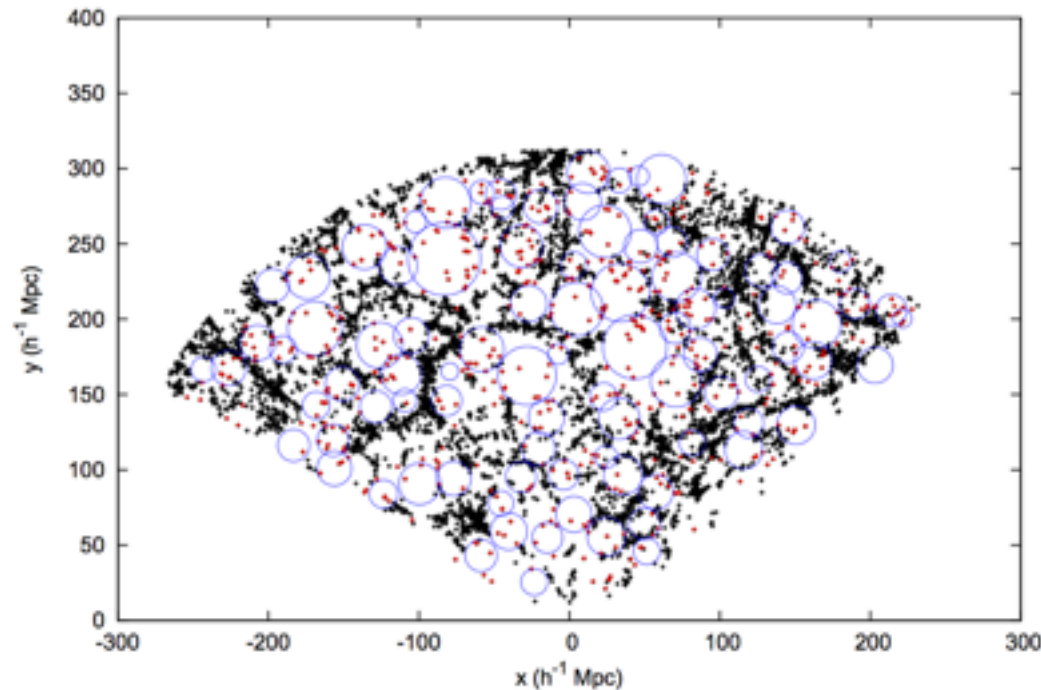
Smaller than the regions we will be examining (~ 350 Mpc/h)

Method: Compare the colour distribution of void galaxies and wall galaxies.

Voids with VESPA I

Sanity test: Can we use VESPA to quantify differences in stellar populations for galaxy samples already identified to be different in the literature?

Fiona Hoyle et al (2012)



Data: SDSS main sample galaxies.

Galaxy void catalogue presented in Pan et al (2011) using the 'voidfinder' algorithm.

Small scale SDSS voids ~ 10 Mpc/h

Smaller than the regions we will be examining (~ 350 Mpc/h)

Method: Compare the colour distribution of void galaxies and wall galaxies.

Sample	$u - r$ void	sd void	$u - r$ wall	sd wall
All	2.043	0.002	2.162	0.002
Bright	2.324	0.003	2.422	0.003

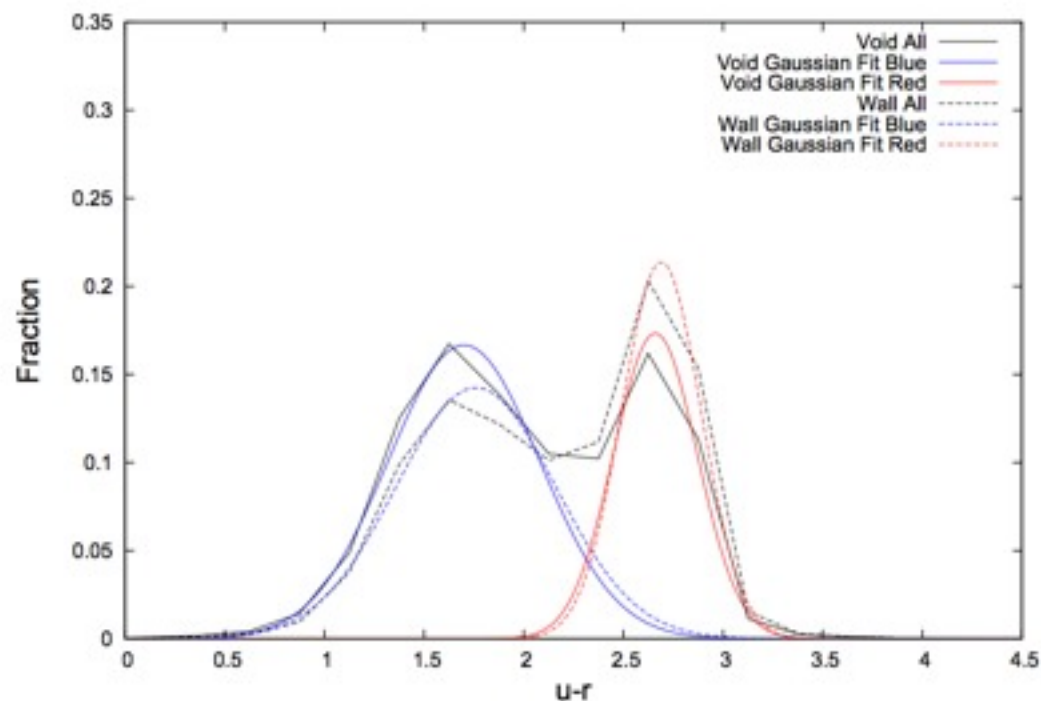
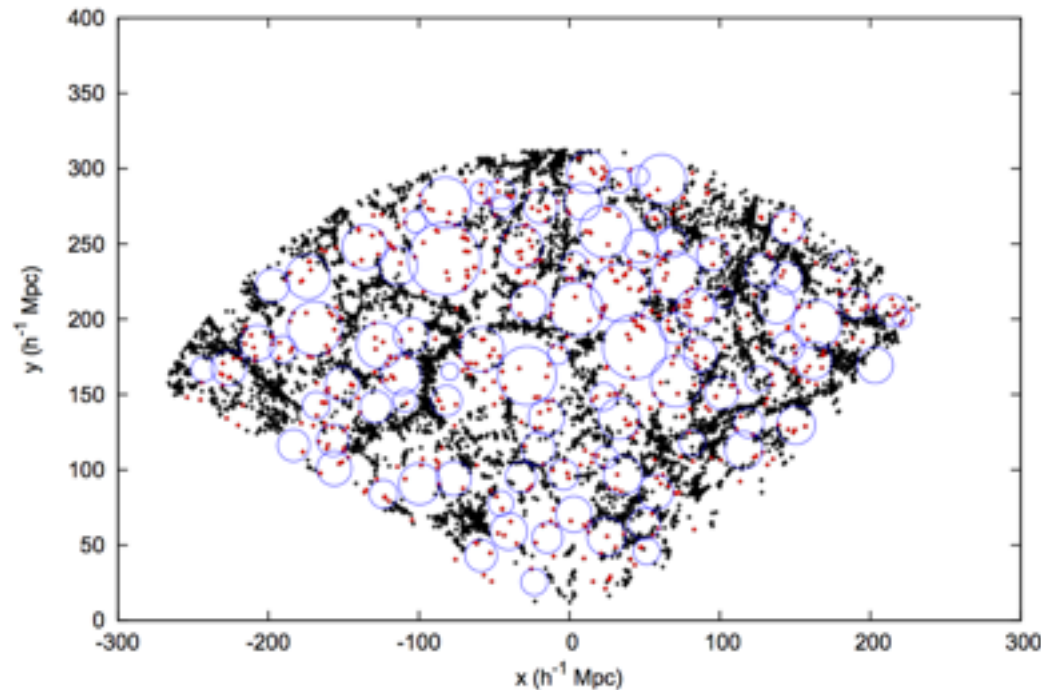
Results: The colour distributions are broad, the peaks are statistically different.

Void galaxies are bluer than wall galaxies.

Voids with VESPA I

Sanity test: Can we use VESPA to quantify differences in stellar populations for galaxy samples already identified to be different in the literature?

Fiona Hoyle et al (2012)



Data: SDSS main sample galaxies.

Galaxy void catalogue presented in Pan et al (2011) using the 'voidfinder' algorithm.

Small scale SDSS voids ~ 10 Mpc/h

Smaller than the regions we will be examining (~ 350 Mpc/h)

Method: Compare the colour distribution of void galaxies and wall galaxies.

Sample	$u-r$ void	sd void	$u-r$ wall	sd wall
All	2.043	0.002	2.162	0.002
Bright	2.324	0.003	2.422	0.003

Results: The colour distributions are broad, the peaks are statistically different.

Void galaxies are bluer than wall galaxies.

We can use VESPA to quantify how such a shift in colour would modify recovered values of SFR(time) or Mass(time)?

Voids with VESPA II

Data: Select SDSS galaxies from the VESPA database <http://www-wfau.roe.ac.uk/vespa/> which can be made to include SFRH, galaxy colours, redshifts.

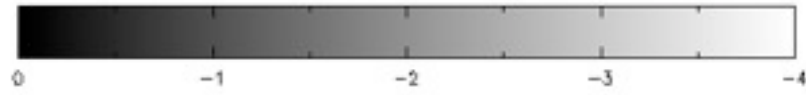
Method: Compare the average SFRH (full disclosure, normalised mass histories) of the galaxies, binned in colour u-r. Examine the difference between neighbouring colour bins.

Voids with VESPA II

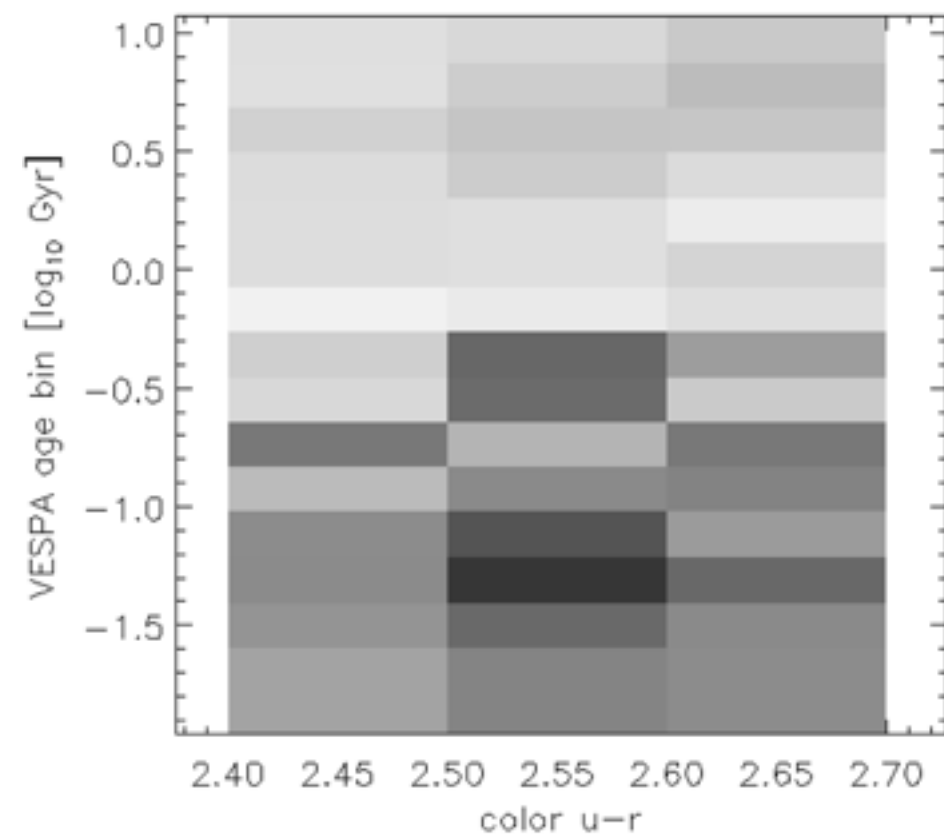
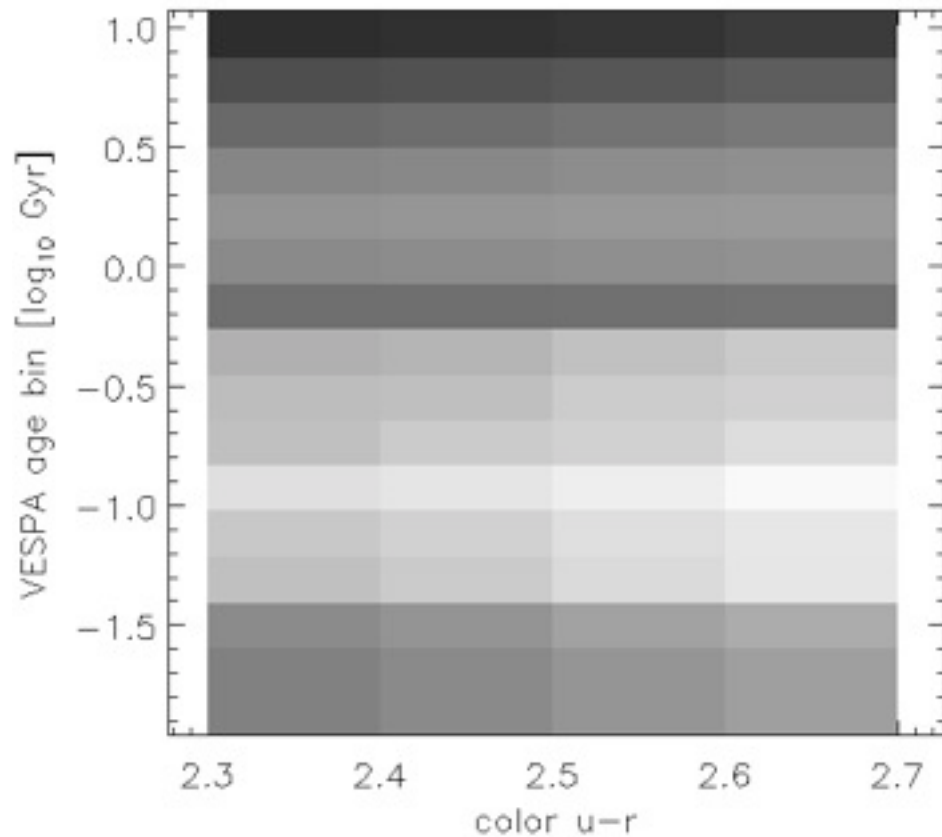
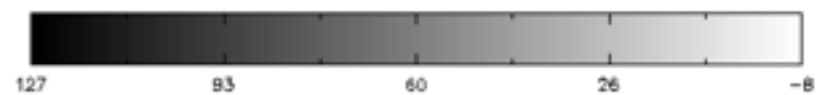
Data: Select SDSS galaxies from the VESPA database <http://www-wfau.roe.ac.uk/vespa/> which can be made to include SFRH, galaxy colours, redshifts.

Method: Compare the average SFRH (full disclosure, normalised mass histories) of the galaxies, binned in colour $u-r$. Examine the difference between neighbouring colour bins.

$$SFR_{(u-r)}$$



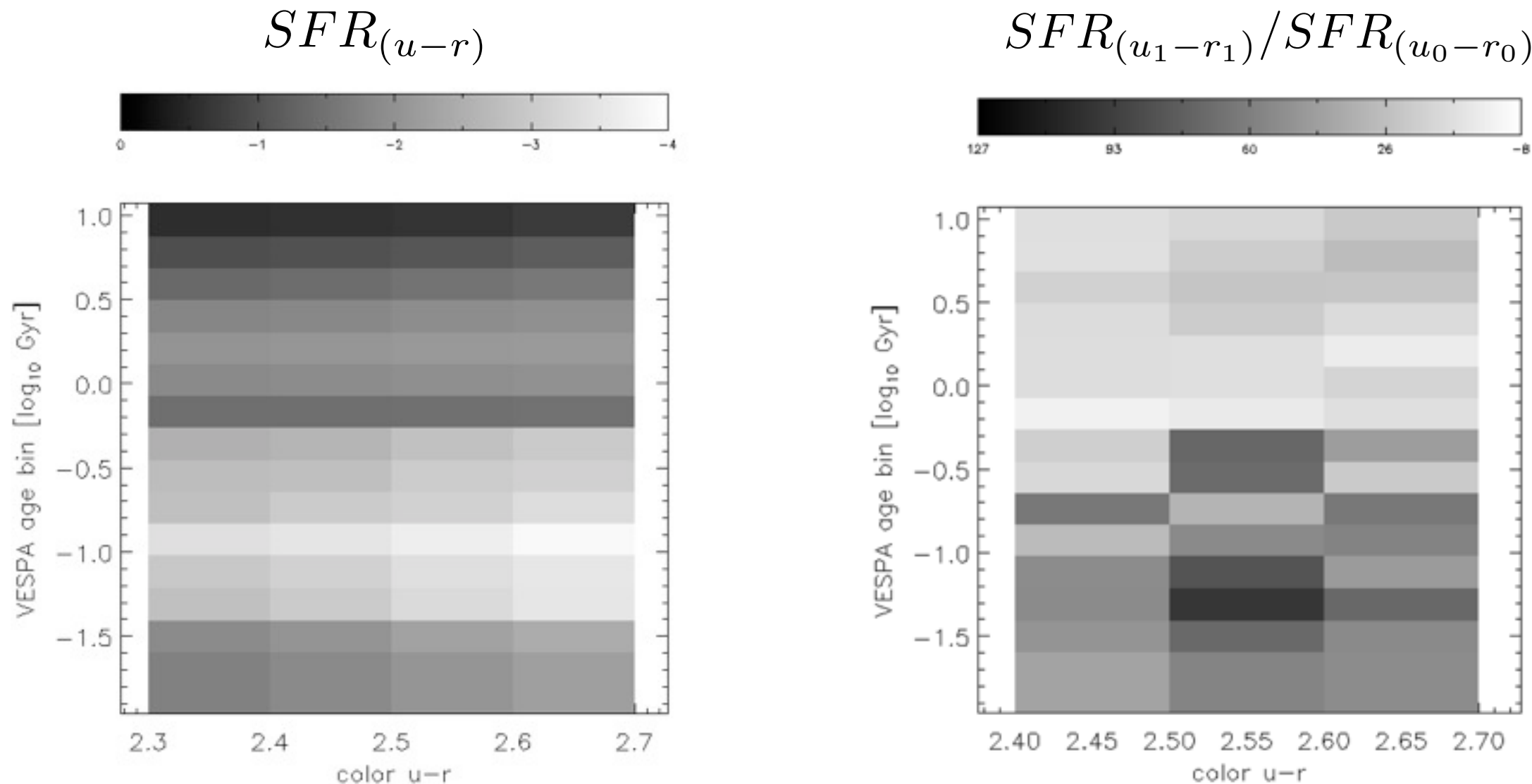
$$SFR_{(u_1-r_1)} / SFR_{(u_0-r_0)}$$



Voids with VESPA II

Data: Select SDSS galaxies from the VESPA database <http://www-wfau.roe.ac.uk/vespa/> which can be made to include SFRH, galaxy colours, redshifts.

Method: Compare the average SFRH (full disclosure, normalised mass histories) of the galaxies, binned in colour $u-r$. Examine the difference between neighbouring colour bins.



Results: The peaks of the SFRH are statistically different from each other. $\langle s.e. \rangle = 615 \pm 446$

Conclusions: VESPA could be used to examine the difference between galaxies in voids, and in walls.

Optimal stacking with VESPA

VESPA can recover SFRH with more time solutions, and higher accuracy, for increasingly higher signal-to-noise galaxy spectra.

SDSS LRG spectra (especially at higher redshift) can have low s-n.

To maximise the recovered solutions available to VESPA we follow Tojeiro et al (2011), who show that stacking sets of 200 (LRG) spectra produces the optimal s-n.

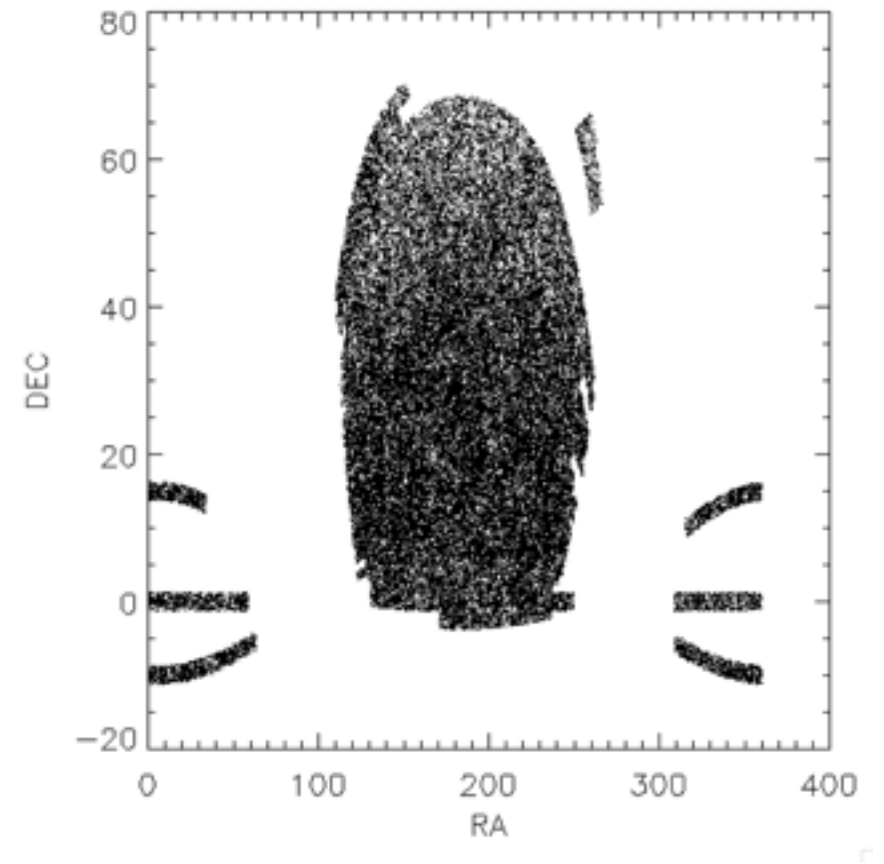
Further stacking more spectra, continues to improve the s-n, but the errors in the recovered solutions are dominated by the uncertainties in the stellar population models.

We choose to construct stacks with ~ 200 LRGs.

Stacking SDSS LRGs

We obtain all LRGs from the VESPA database.

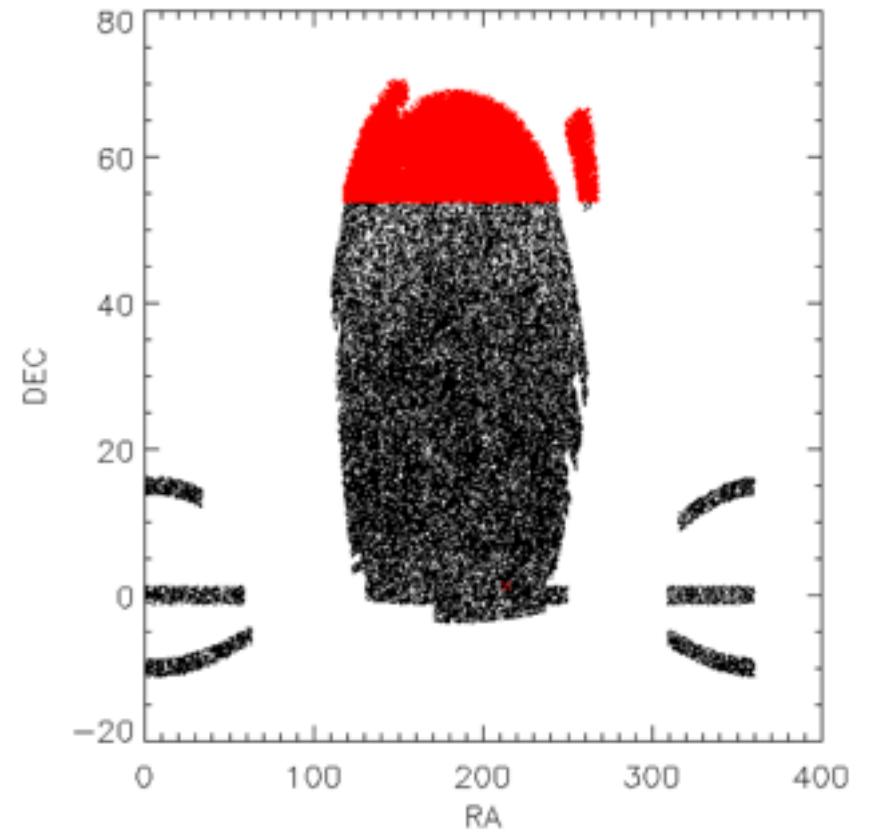
We divide the LRGs into 12 equal area sky patches



Stacking SDSS LRGs

We obtain all LRGs from the VESPA database.

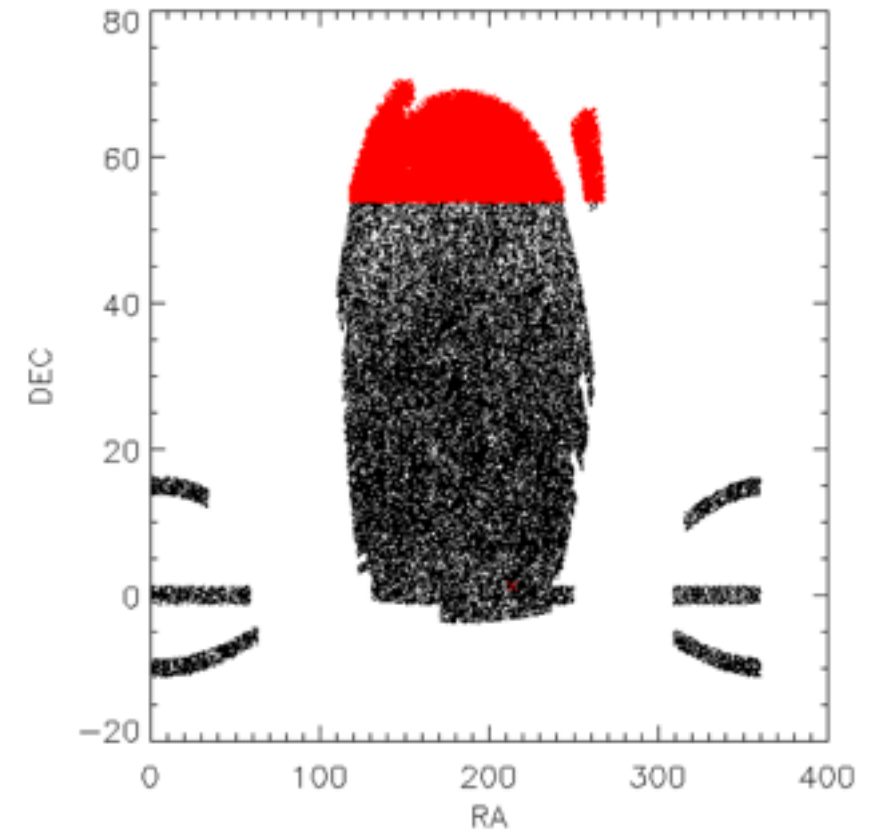
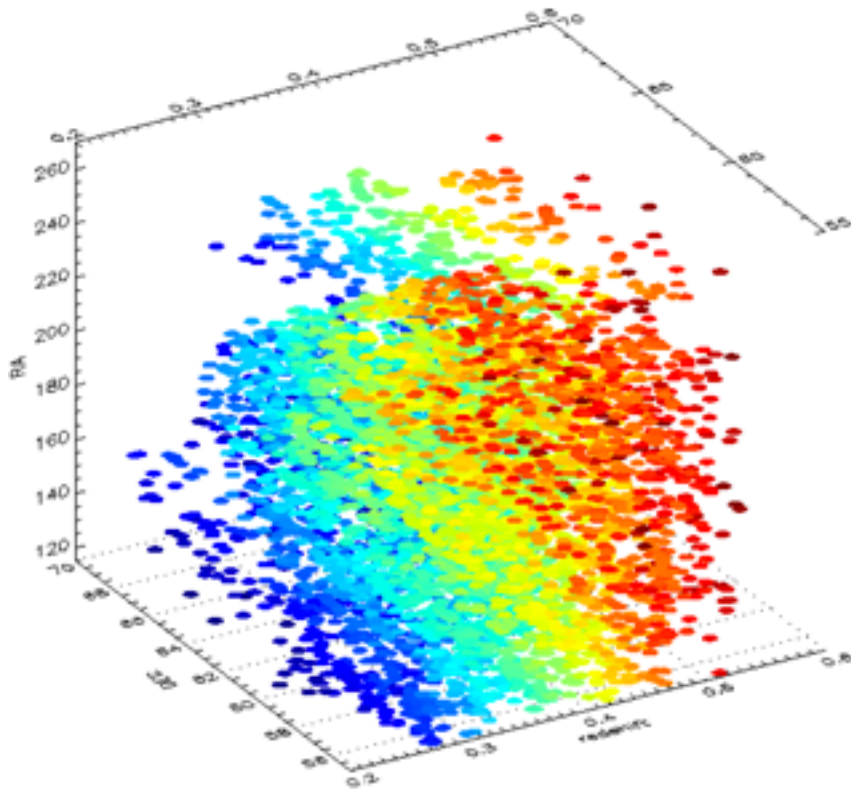
We divide the LRGs into 12 equal area sky patches



Stacking SDSS LRGs

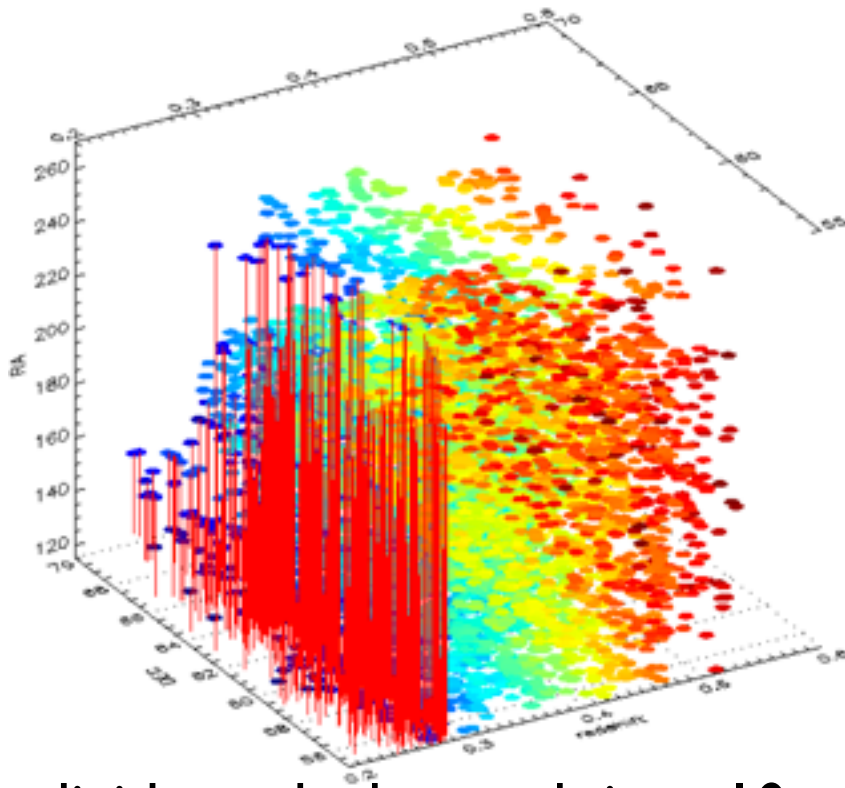
We obtain all LRGs from the VESPA database.

We divide the LRGs into 12 equal area sky patches

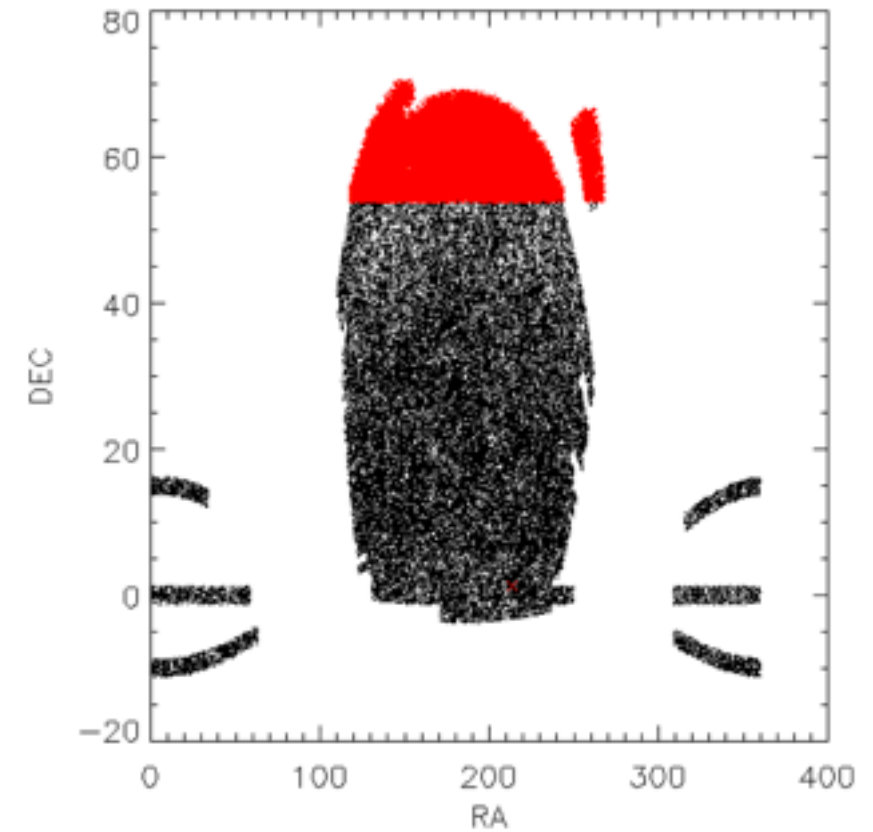


Stacking SDSS LRGs

We obtain all LRGs from the VESPA database.
 We divide the LRGs into 12 equal area sky patches



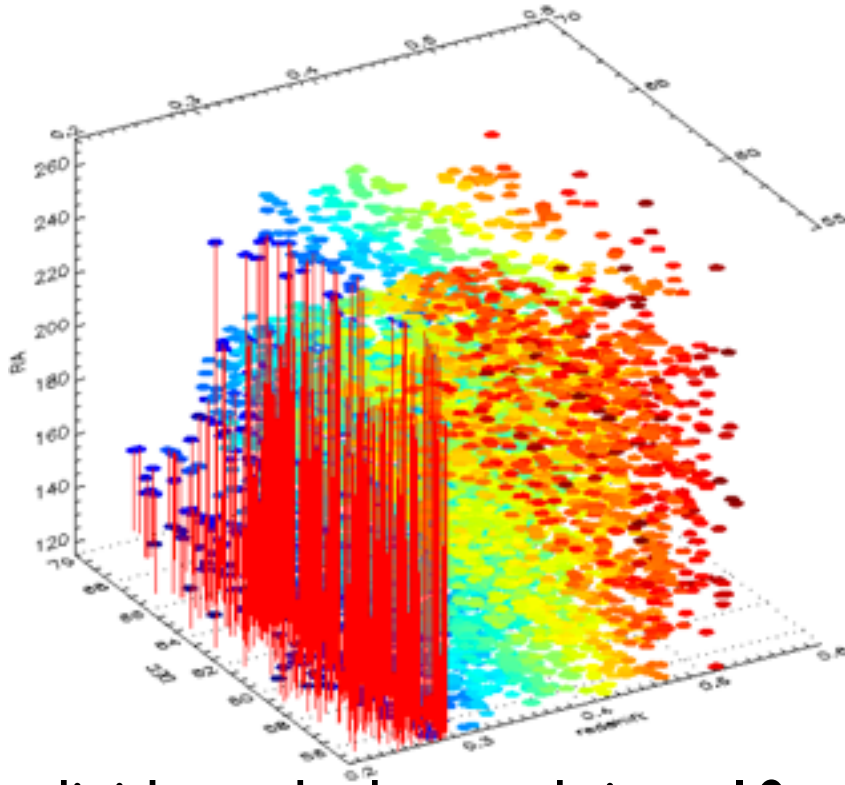
We divide each sky patch into 10 redshift bins
 A block B, refers to a redshift slice of a sky patch



Redshift ID	Range	Ngals	Vol Gpc ³
1	$0.200 < z < 0.279$	7874	0.90
2	$0.280 < z < 0.308$	9352	0.46
3	$0.309 < z < 0.327$	8532	0.34
4	$0.328 < z < 0.342$	8594	0.29
5	$0.343 < z < 0.359$	9181	0.36
6	$0.360 < z < 0.376$	8202	0.39
7	$0.377 < z < 0.398$	8754	0.55
8	$0.399 < z < 0.424$	8277	0.71
9	$0.425 < z < 0.457$	8272	1.00
10	$0.458 < z < 0.537$	8065	2.91

Stacking SDSS LRGs

We obtain all LRGs from the VESPA database.
 We divide the LRGs into 12 equal area sky patches



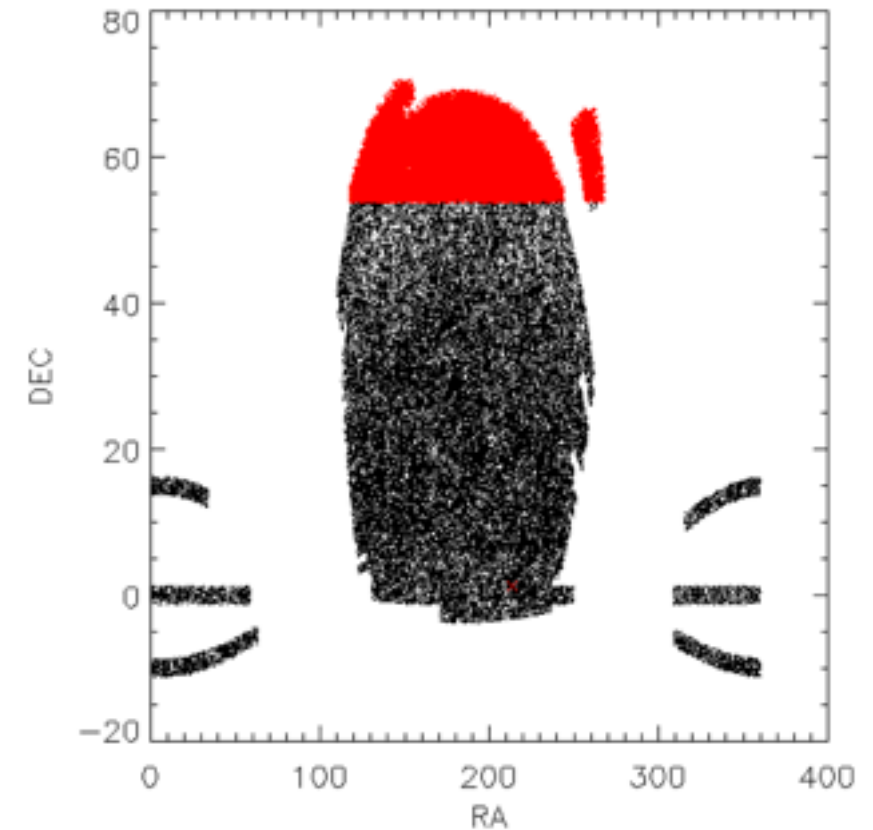
We divide each sky patch into 10 redshift bins
 A block B, refers to a redshift slice of a sky patch

$$B = 12 \times 10 = 120$$

$$R_B \approx 350 Mpc/h$$

$$N_s = 3 \quad \#LRGs /stack \sim 200$$

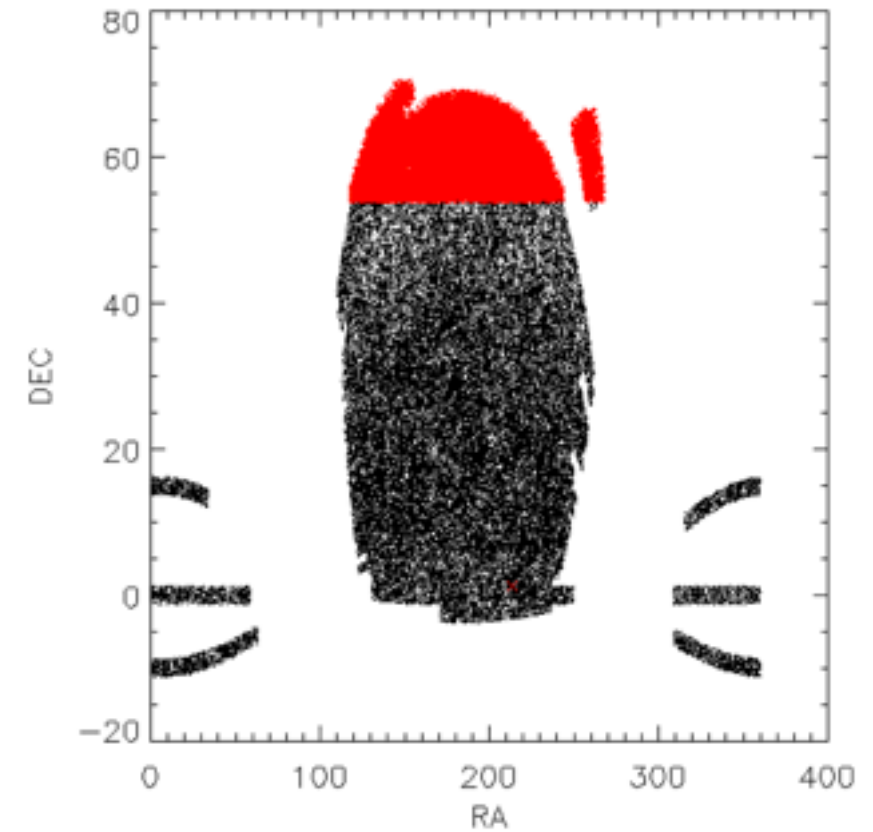
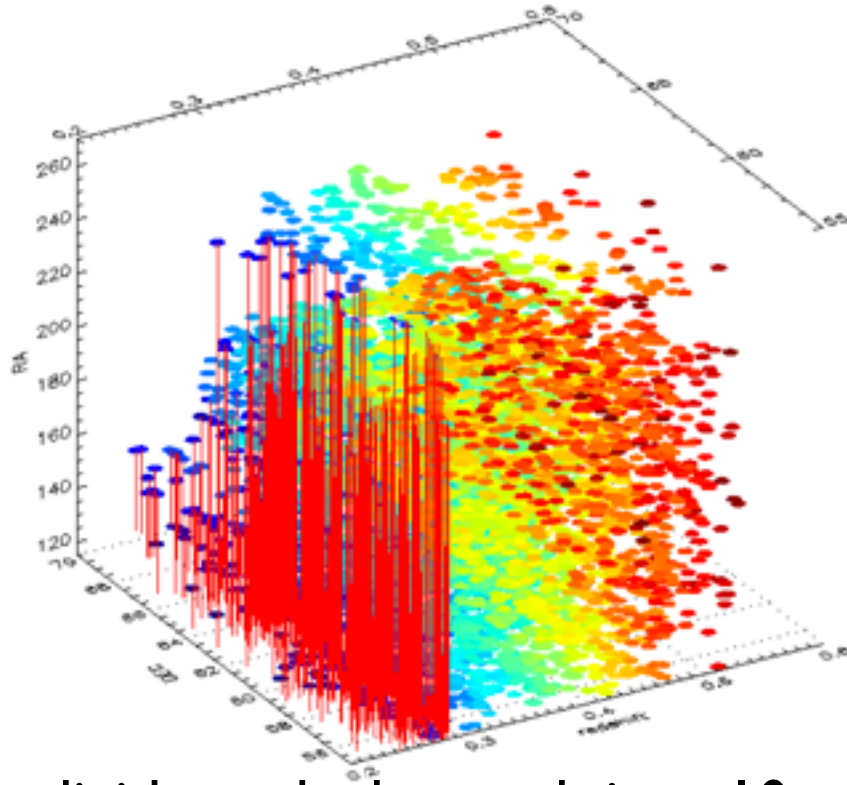
We are looking for consistency of
 the SRFH between these 120
 blocks.



Redshift ID	Range	Ngals	Vol Gpc ³
1	0.200 < z < 0.279	7874	0.90
2	0.280 < z < 0.308	9352	0.46
3	0.309 < z < 0.327	8532	0.34
4	0.328 < z < 0.342	8594	0.29
5	0.343 < z < 0.359	9181	0.36
6	0.360 < z < 0.376	8202	0.39
7	0.377 < z < 0.398	8754	0.55
8	0.399 < z < 0.424	8277	0.71
9	0.425 < z < 0.457	8272	1.00
10	0.458 < z < 0.537	8065	2.91

Stacking SDSS LRGs

We obtain all LRGs from the VESPA database.
 We divide the LRGs into 12 equal area sky patches



We divide each sky patch into 10 redshift bins
 A block B, refers to a redshift slice of a sky patch

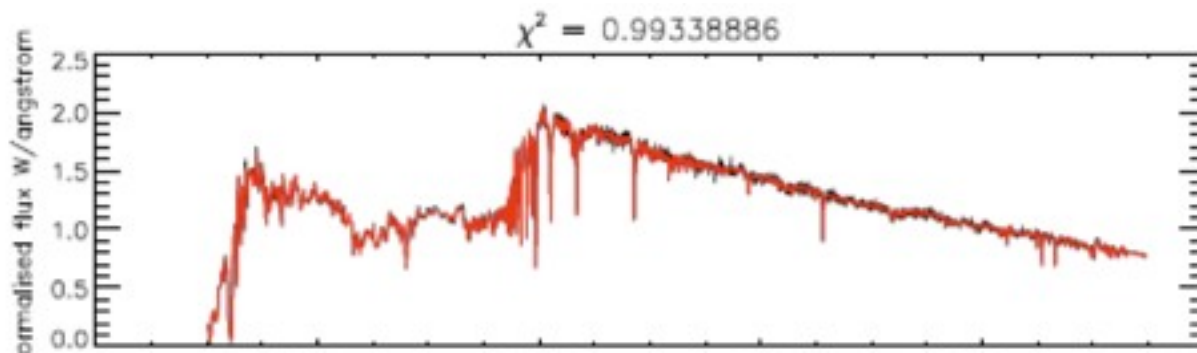
$$B = 12 \times 10 = 120$$

$$R_B \approx 350 Mpc/h$$

$$N_s = 3 \quad \#LRGs /stack \sim 200$$

Redshift ID	Range	Ngals	Vol Gpc ³
1	0.200 < z < 0.279	7874	0.90
2	0.280 < z < 0.308	9352	0.46
3	0.309 < z < 0.327	8532	0.34
4	0.328 < z < 0.342	8594	0.29
5	0.343 < z < 0.359	9181	0.36
6	0.360 < z < 0.376	8202	0.39
7	0.377 < z < 0.398	8754	0.55
8	0.399 < z < 0.424	8277	0.71
9	0.425 < z < 0.457	8272	1.00
10	0.458 < z < 0.537		

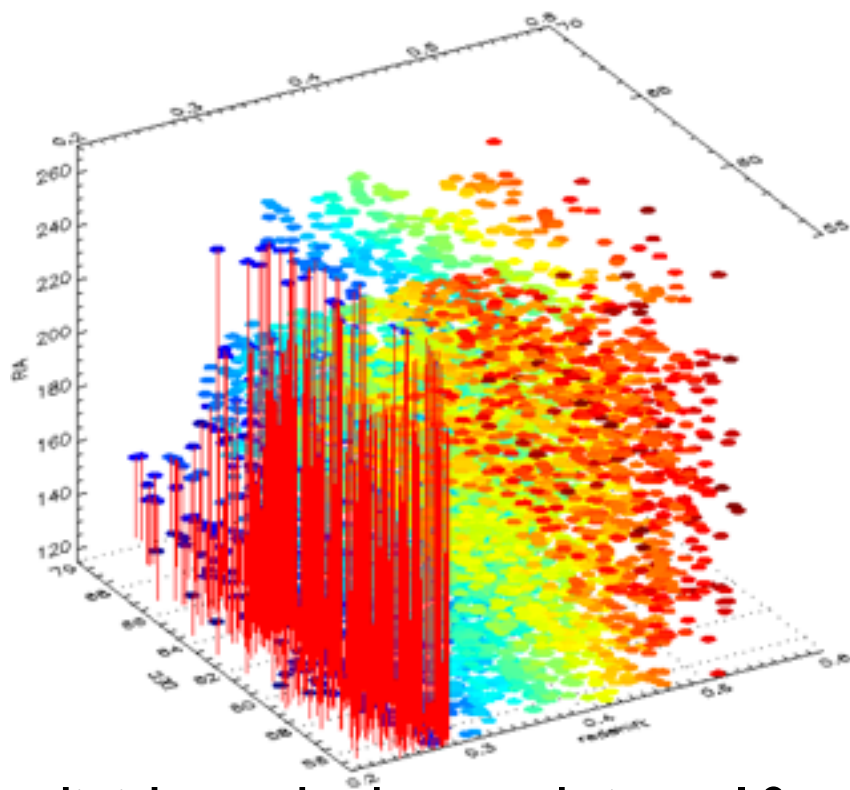
BinID	T _{B+} Bin Start [Gyrs]	T _{B+} Bin End [Gyrs]
0	0.002	0.074
1	0.074	0.177
2	0.177	0.275
3	0.275	0.425
4	0.425	0.657
5	0.657	1.020
6	1.020	1.570
7	1.570	2.440
8	2.440	3.780
9	3.780	5.840
10	5.840	7.440
11	7.440	8.239
12	8.239	9.040
13	9.040	10.28
14	10.28	11.52
15	11.52	13.50



High s-n allows us to reconstruct SFRH for each stack.

Stacking SDSS LRGs

We obtain all LRGs from the VESPA database.
 We divide the LRGs into 12 equal area sky patches

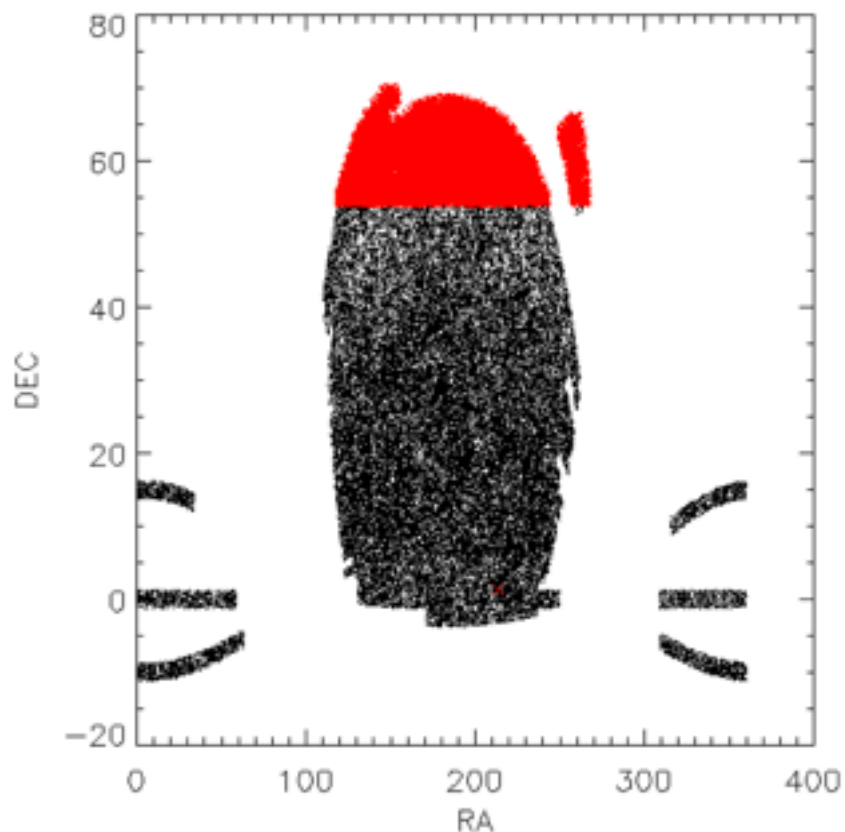


We divide each sky patch into 10 redshift bins
 A block B, refers to a redshift slice of a sky patch

$$B = 12 \times 10 = 120$$

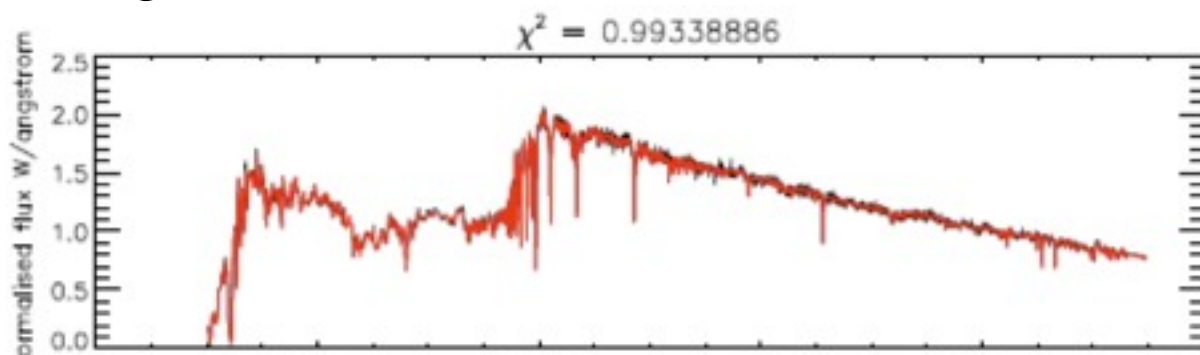
$$R_B \approx 350 Mpc/h$$

$$N_s = 3 \quad \#LRGs /stack \sim 200$$



Redshift ID	Range	Ngals	Vol Gpc ³
1	0.200 < z < 0.279	7874	0.90
2	0.280 < z < 0.308	9352	0.46
3	0.309 < z < 0.327	8532	0.34
4	0.328 < z < 0.342	8594	0.29
5	0.343 < z < 0.359	9181	0.36
6	0.360 < z < 0.376	8202	0.39
7	0.377 < z < 0.398	8754	0.55
8	0.399 < z < 0.424	8277	0.71
9	0.425 < z < 0.457	8272	1.00
10	0.458 < z < 0.537		

BinID	T _{B+} Bin Start [Gyrs]	T _{B+} Bin End [Gyrs]
0	0.002	0.074
1	0.074	0.177
2	0.177	0.275
3	0.275	0.425
4	0.425	0.657
5	0.657	1.020
6	1.020	1.570
7	1.570	2.440
8	2.440	3.780
9	3.780	5.840
10	5.840	7.440
11	7.440	8.239
12	8.239	9.040
13	9.040	10.28
14	10.28	11.52
15	11.52	13.50



High s-n allows us to reconstruct SFRH for each stack.

VESPA reconstr./derived quantities

Explicitly, we determine the following quantities from the VESPA output, to use in our statistical tests

For each stack N_s

$SFH(T_B, \tau')$ -- The recovered Star Formation Rate Histories, in the rest frame τ' , of the galaxy (stack) block.

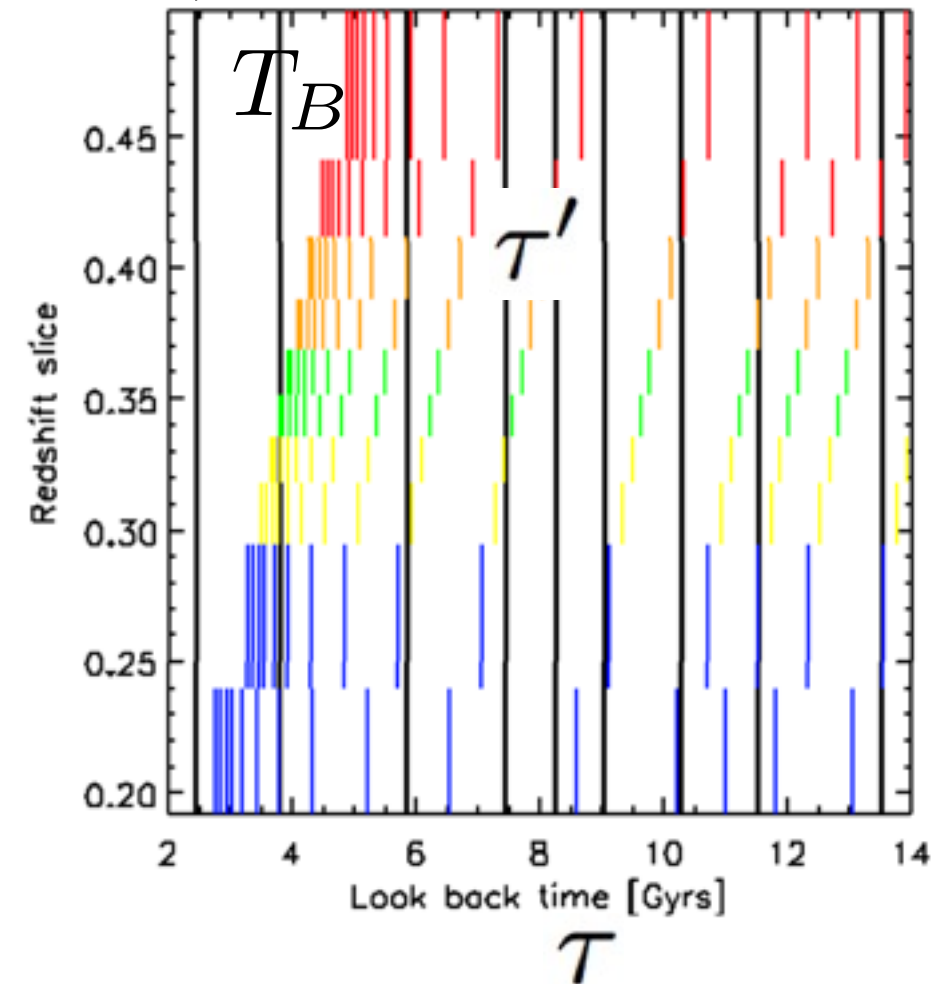
VESPA reconstr./derived quantities

Explicitly, we determine the following quantities from the VESPA output, to use in our statistical tests

For each stack N_s

$SFH(T_B, \tau')$ -- The recovered Star Formation Rate Histories, in the rest frame τ' , of the galaxy (stack) block.

$SFH(0, \tau)$ -- The recovered Star Formation Rate Histories, in the common frame τ .



VESPA reconstr./derived quantities

Explicitly, we determine the following quantities from the VESPA output, to use in our statistical tests

For each stack N_s

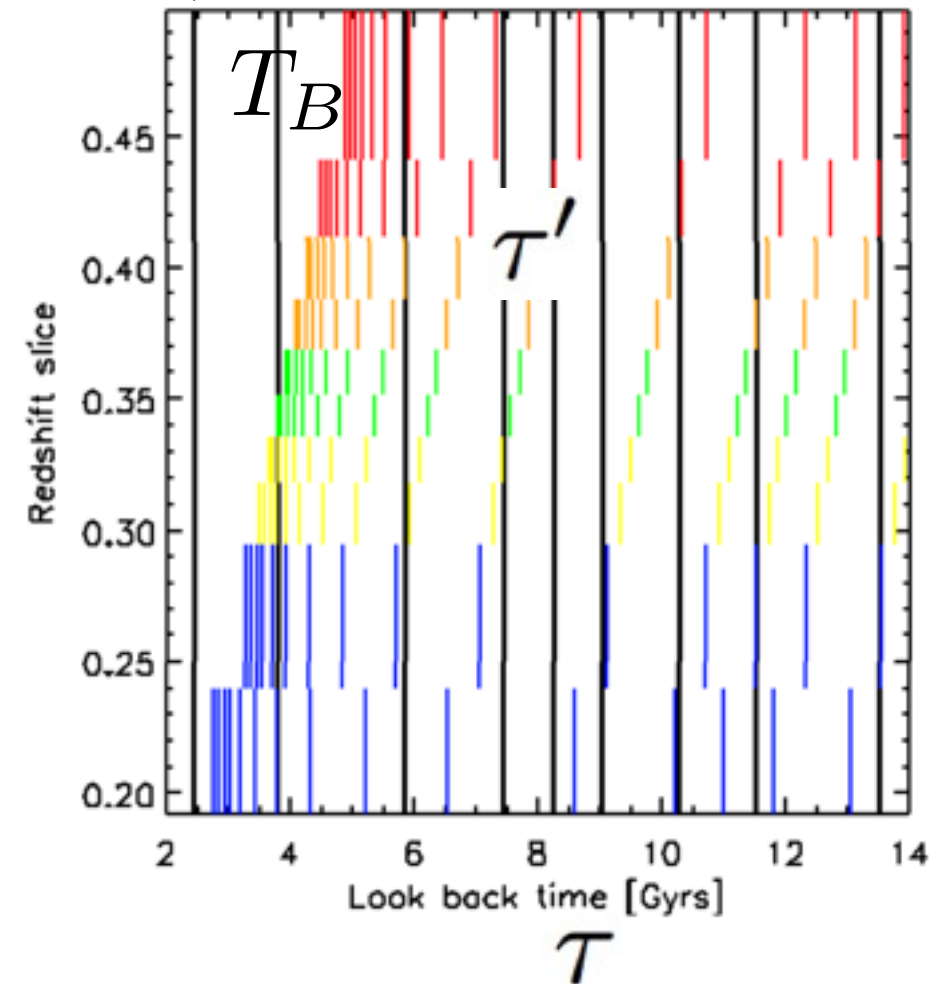
$SFH(T_B, \tau')$ -- The recovered Star Formation Rate Histories, in the rest frame τ' , of the galaxy (stack) block.

$SFH(0, \tau)$ -- The recovered Star Formation Rate Histories, in the common frame τ .

For each block B

$$A_B = 1/N_s \sum_{N_s} SFH(0, \tau = 15)$$

$$\sigma_B = \sigma(SFH(0, \tau = 15)) / \sqrt{(N_s)}$$



VESPA reconstr./derived quantities

Explicitly, we determine the following quantities from the VESPA output, to use in our statistical tests

For each stack N_s

$SFH(T_B, \tau')$ -- The recovered Star Formation Rate Histories, in the rest frame τ' , of the galaxy (stack) block.

$SFH(0, \tau)$ -- The recovered Star Formation Rate Histories, in the common frame τ .

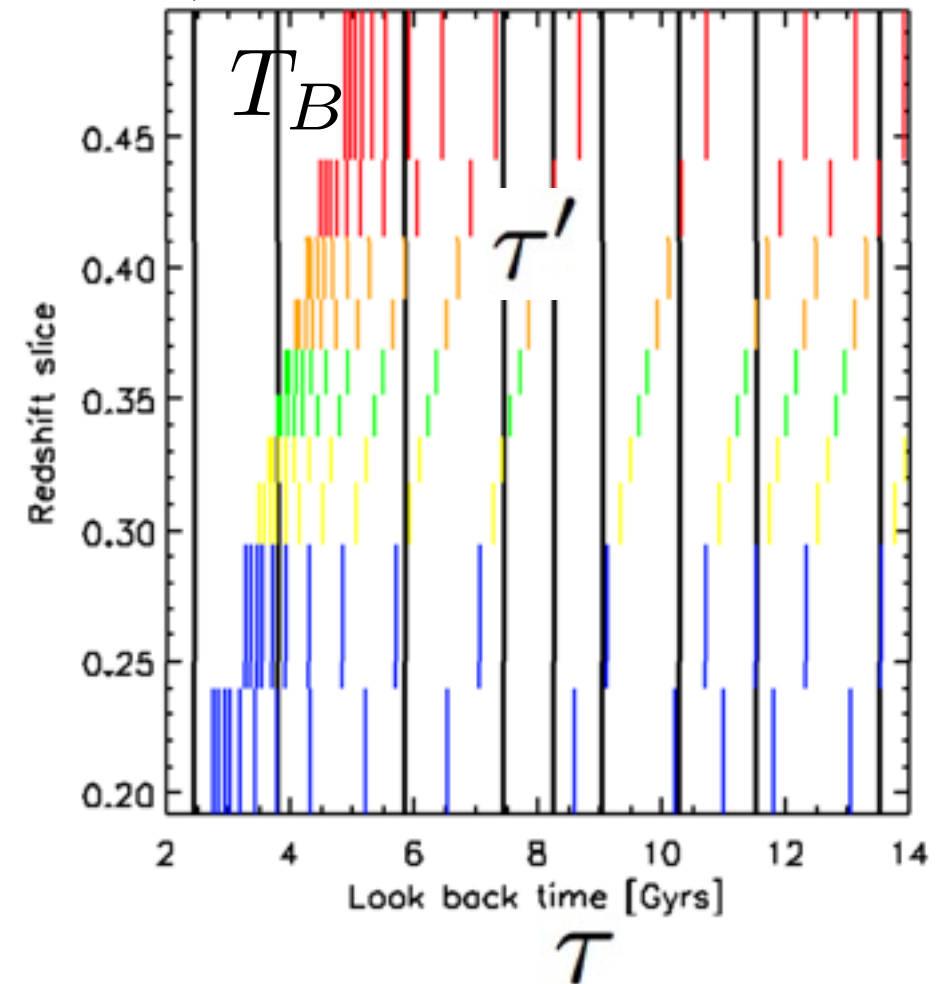
For each block B

$$A_B = 1/N_s \sum_{N_s} SFH(0, \tau = 15)$$

$$\sigma_B = \sigma(SFH(0, \tau = 15)) / \sqrt{(N_s)}$$

For each redshift slice z

$$A_z = \sum_B A_B(z) / 12 \quad \text{-- The mean value of } A_B \text{ at each redshift}$$



VESPA reconstr./derived quantities

Explicitly, we determine the following quantities from the VESPA output, to use in our statistical tests

For each stack N_s

$SFH(T_B, \tau')$ -- The recovered Star Formation Rate Histories, in the rest frame τ' , of the galaxy (stack) block.

$SFH(0, \tau)$ -- The recovered Star Formation Rate Histories, in the common frame τ .

For each block B

$$A_B = 1/N_s \sum_{N_s} SFH(0, \tau = 15)$$

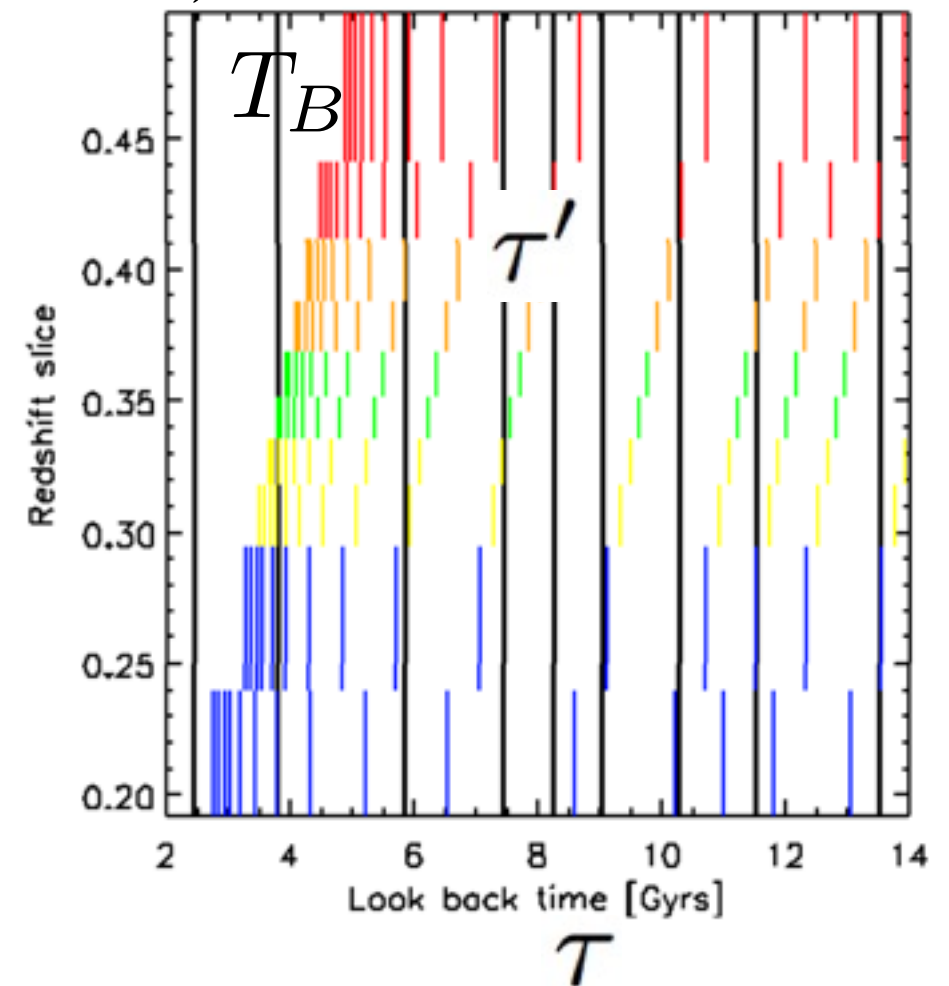
$$\sigma_B = \sigma(SFH(0, \tau = 15)) / \sqrt{(N_s)}$$

For each redshift slice z

$$A_z = \sum_B A_B(z) / 12 \quad \text{-- The mean value of } A_B \text{ at each redshift}$$

For the entire sample: (120) blocks $\mu = \langle A_B \rangle$ -- The mean value of A_B over all blocks

$\sigma_z = \sigma(A_z)$ -- The dispersion describing re-binning from the rest- to common- frame.



Simulated data

We create simulated data, to test our routines, and to determine expected levels of dispersion (which could mimic inhomogeneity) from sims created assuming homogeneity.

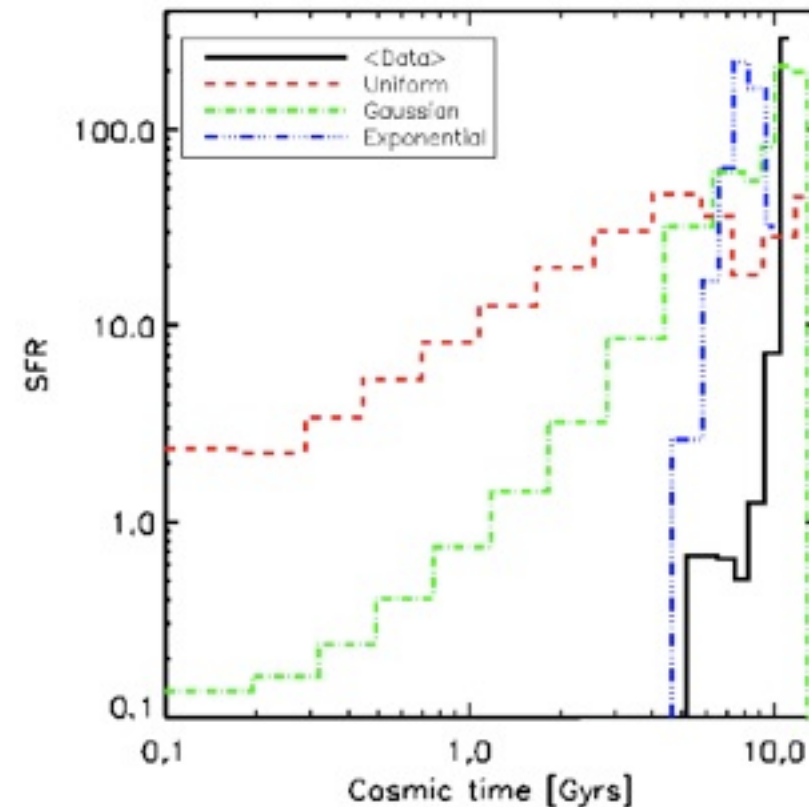
Simulated data

We create simulated data, to test our routines, and to determine expected levels of dispersion (which could mimic inhomogeneity) from sims created assuming homogeneity.

The simulations are created at the level of the rest-frame SFRH for various input cosmic (common frame) star formation rates.

We do not create mock spectra, and analyse them with VESPA here (too expensive), although this has been done before.

Sim. data id	SFR distr.	Remarks
1	Uniform	
2	Gaussian($\mu = 10, \sigma = \sqrt{2}$)	10 Gyrs
3	Exponential (1/2)	11 Gyrs cut off
4	From Data	Averaged SFRH(0, τ)



Simulated data

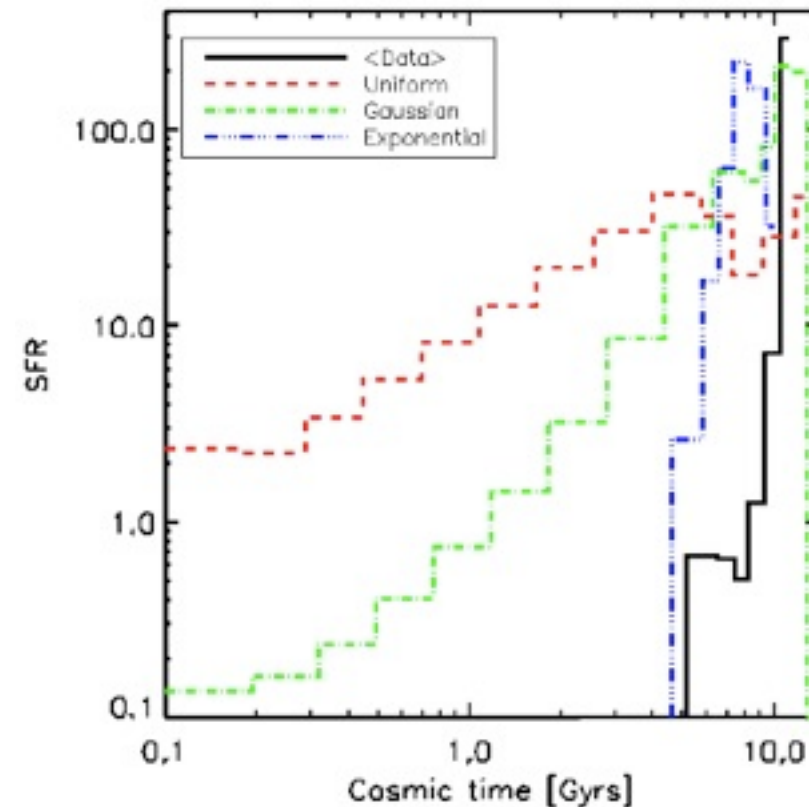
We create simulated data, to test our routines, and to determine expected levels of dispersion (which could mimic inhomogeneity) from sims created assuming homogeneity.

The simulations are created at the level of the rest-frame SFRH for various input cosmic (common frame) star formation rates.

We do not create mock spectra, and analyse them with VESPA here (too expensive), although this has been done before.

We concentrate on time bin 15, because the majority of star formation occurred in this epoch for LRGs. SFR is dependent on many variables, and the central limit theorem implies the resulting distribution can be treated as a Gaussian.

Sim. data id	SFR distr.	Remarks
1	Uniform	
2	Gaussian($\mu = 10, \sigma = \sqrt{2}$)	10 Gyrs
3	Exponential (1/2)	11 Gyrs cut off
4	From Data	Averaged SFRH(0, τ)



BinID	$T_B +$ Bin Start [Gyrs]	$T_B +$ Bin End [Gyrs]
0	0.002	0.074
1	0.074	0.177
2	0.177	0.275
3	0.275	0.425
4	0.425	0.657
5	0.657	1.020
6	1.020	1.570
7	1.570	2.440
8	2.440	3.780
9	3.780	5.840
10	5.840	7.440
11	7.440	8.239
12	8.239	9.040
13	9.040	10.28
14	10.28	11.52
15	11.52	13.50

Simulated data

We create simulated data, to test our routines, and to determine expected levels of dispersion (which could mimic inhomogeneity) from sims created assuming homogeneity.

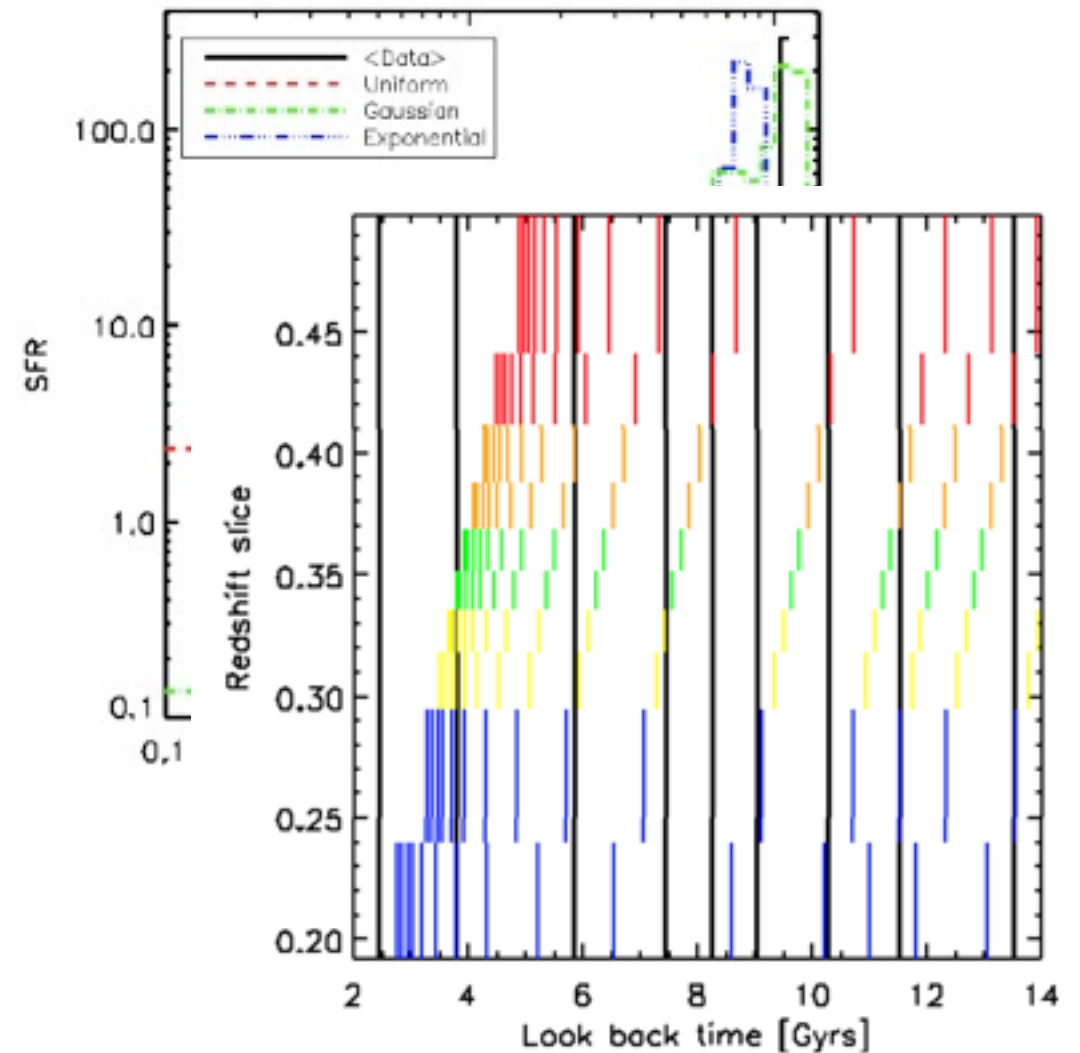
The simulations are created at the level of the rest-frame SFRH for various input cosmic (common frame) star formation rates.

We do not create mock spectra, and analyse them with VESPA here (too expensive), although this has been done before.

We map the input SFR to the rest-frame time-bins of each block. We add Gaussian noise to the SFR solution for each stack, with magnitude drawn directly from the data (for block B).

$$SFR^s(T_B, \tau') = SFR^s(T_B, \tau') \times (1 + G(\sigma_B(\tau') * \sqrt{(Ns)/A_B(\tau')}))$$

Sim. data id	SFR distr.	Remarks
1	Uniform	
2	Gaussian($\mu = 10, \sigma = \sqrt{2}$)	10 Gyrs
3	Exponential (1/2)	11 Gyrs cut off
4	From Data	Averaged SFRH(0, τ)



Simulated data

We create simulated data, to test our routines, and to determine expected levels of dispersion (which could mimic inhomogeneity) from sims created assuming homogeneity.

The simulations are created at the level of the rest-frame SFRH for various input cosmic (common frame) star formation rates.

We do not create mock spectra, and analyse them with VESPA here (too expensive), although this has been done before.

We map the input SFR to the rest-frame time-bins of each block. We add Gaussian noise to the SFR solution for each stack, with magnitude drawn directly from the data (for block B).

$$SFR^s(T_B, \tau') = SFR^s(T_B, \tau') \times (1 + G(\sigma_B(\tau') * \sqrt{(Ns)/A_B(\tau')}))$$

We re-bin back to the common frame and determine all of the quantities as before.

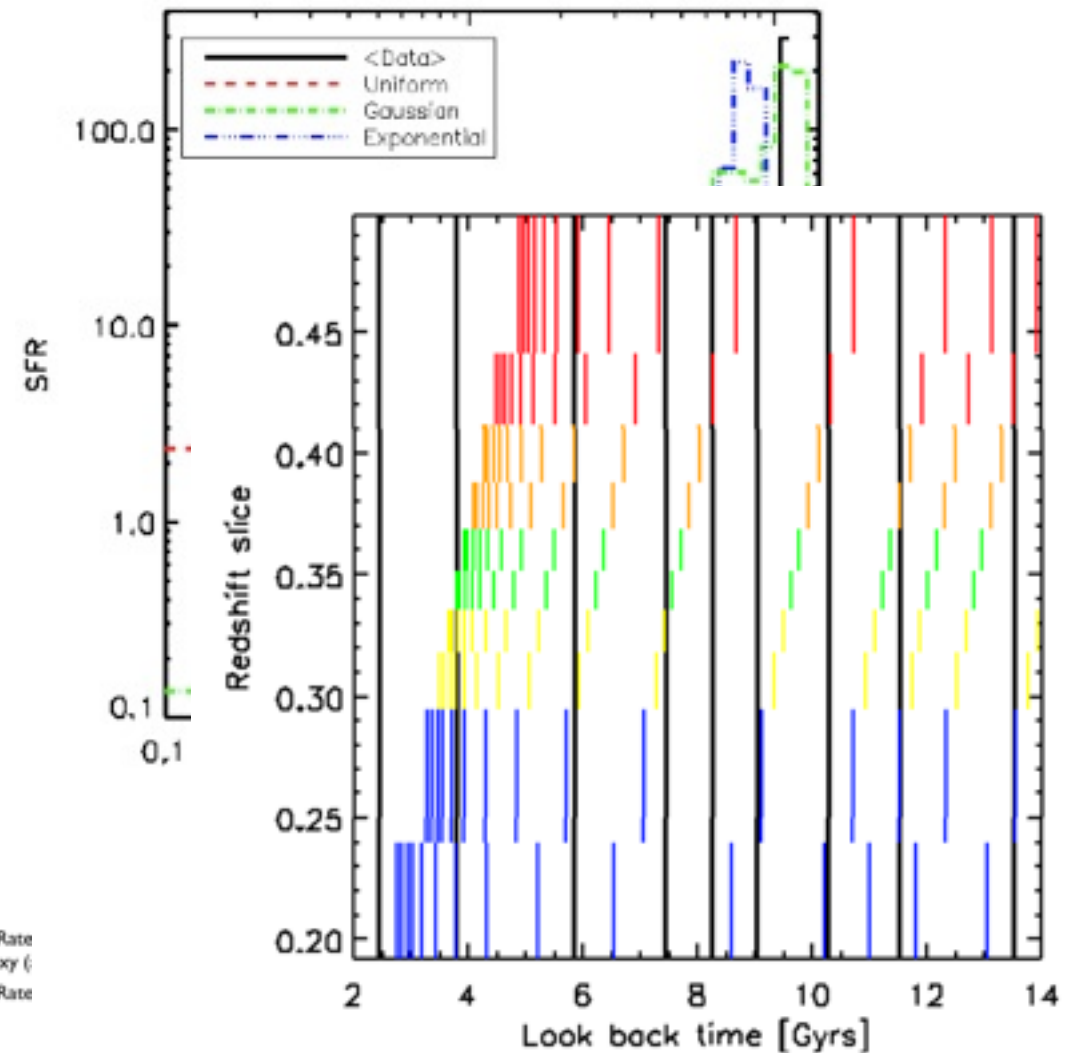
For each stack N_s
 $SFH(T_B, \tau')$ -- The recovered Star Formation Rate in the rest frame τ' , of the galaxy
 $SFH(0, \tau)$ -- The recovered Star Formation Rate in the common frame τ .

For each block B
 $A_B = 1/N_s \sum_{N_s} SFH(0, \tau = 15)$
 $\sigma_B = \sigma(SFH(0, \tau = 15)) / \sqrt{(N_s)}$

For each redshift slice z
 $A_z = \sum_B A_B(z) / 12$ -- The mean value of A_B at each redshift
 $\sigma_z = \sigma(A_z)$ -- The dispersion describing re-binned

For the entire sample: (120) blocks $\mu = \langle A_B \rangle$

Sim. data id	SFR distr.	Remarks
1	Uniform	
2	Gaussian($\mu = 10, \sigma = \sqrt{2}$)	10 Gyrs
3	Exponential (1/2)	11 Gyrs cut off
4	From Data	Averaged SFRH(0, τ)



Student t-distribution I

We examine the distribution of measured values of Star Formation around the mean, and see if it is consistent with the error we have associated to them. This is the usual Student t-test.

An inhomogeneity could appear as an outlier, or a set of outliers in this distribution.

$$t_s = \frac{A_B - \mu}{\sqrt{\sigma_B^2 + \sigma_z^2}},$$

$$f(t) = \frac{1}{\sqrt{\eta} B(1/2, \eta/2)} \left(1 + \frac{t^2}{\eta}\right)^{-(\eta+1)/2}$$

Student t-distribution I

We examine the distribution of measured values of Star Formation around the mean, and see if it is consistent with the error we have associated to them. This is the usual Student t-test.

An inhomogeneity could appear as an outlier, or a set of outliers in this distribution.

$$t_s = \frac{A_B - \mu}{\sqrt{\sigma_B^2 + \sigma_z^2}},$$

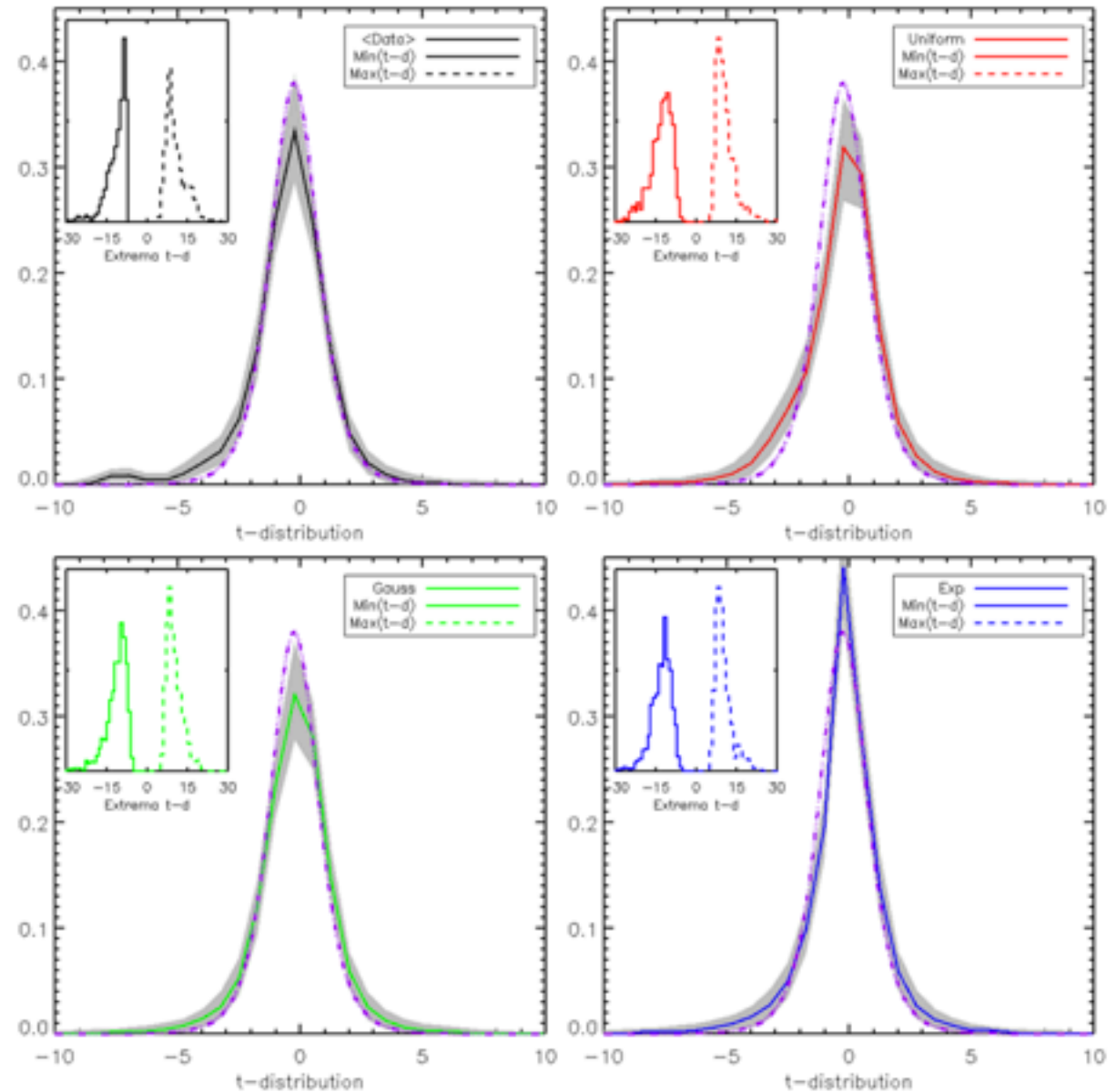
$$f(t) = \frac{1}{\sqrt{\eta} B(1/2, \eta/2)} \left(1 + \frac{t^2}{\eta}\right)^{-(\eta+1)/2}$$

We perform 1000 sets of simulations for each input SFR.

The grey regions are the 95% dispersion.

$$0.99 < \chi^2 / (120 - 2) < 1.1$$

The added dispersion from re-binning correctly accounts for the dispersion in the data



Student t-distribution I

We examine the distribution of measured values of Star Formation around the mean, and see if it is consistent with the error we have associated to them. This is the usual Student t-test.

An inhomogeneity could appear as an outlier, or a set of outliers in this distribution.

$$t_s = \frac{A_B - \mu}{\sqrt{\sigma_B^2 + \sigma_z^2}},$$
$$f(t) = \frac{1}{\sqrt{\eta} B(1/2, \eta/2)} \left(1 + \frac{t^2}{\eta}\right)^{-(\eta+1)/2}$$

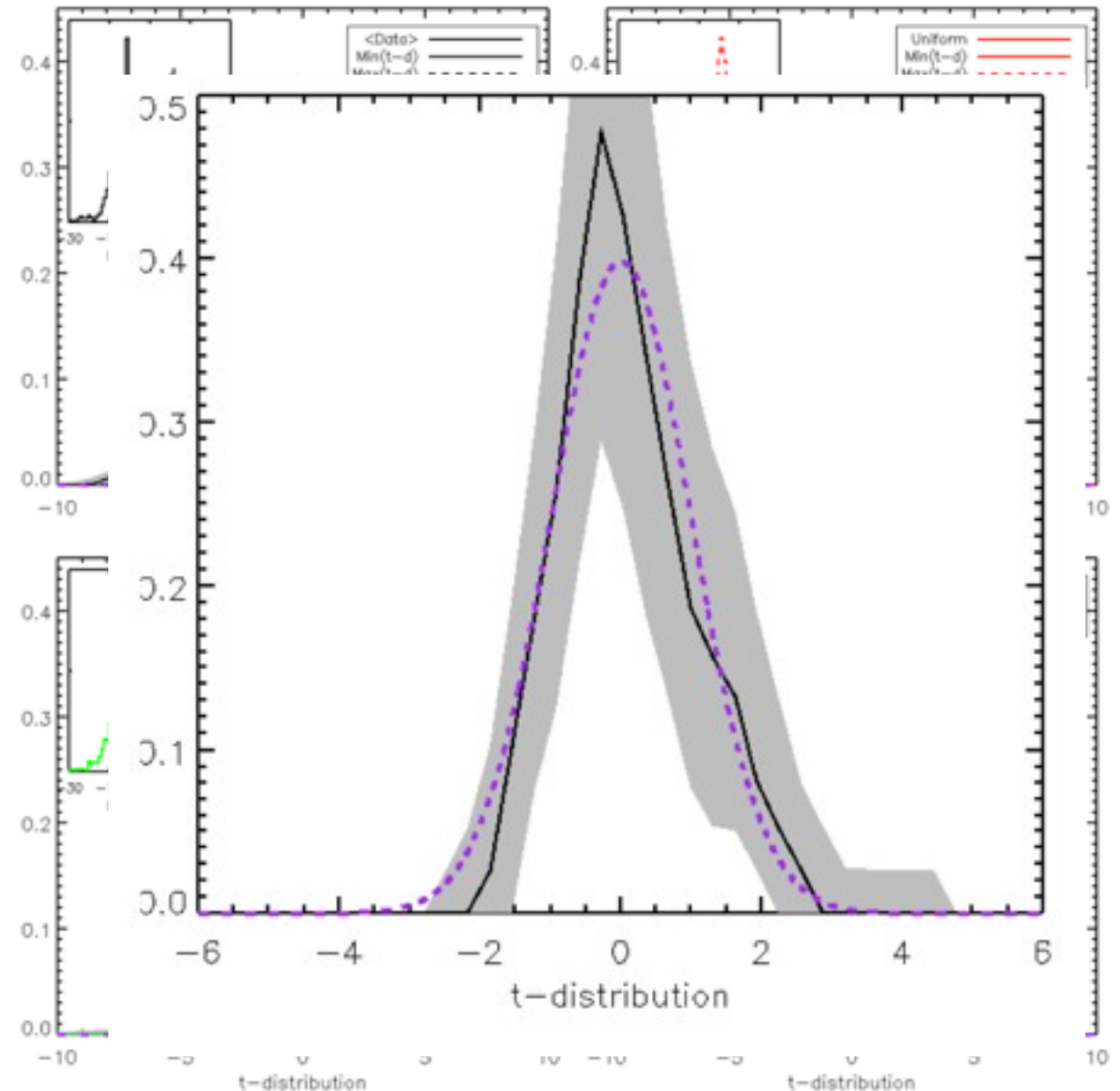
We perform 1000 sets of simulations for each input SFR.

The grey regions are the 95% dispersion.

$$0.99 < \chi^2 / (120 - 2) < 1.1$$

The added dispersion from re-binning correctly accounts for the dispersion in the data

The data distribution is consistent with the theoretical t-distribution $\chi^2 \sim 1.0$



Full probability distribution I

We can formally compute the full probability that all blocks are consistent with being drawn from a Gaussian distribution. By definition a homogeneous distribution is described well by its error components. If additional error components are favored by the data, then the distribution is no longer homogeneous.

Full probability distribution I

We can formally compute the full probability that all blocks are consistent with being drawn from a Gaussian distribution. By definition a homogeneous distribution is described well by its error components. If additional error components are favored by the data, then the distribution is no longer homogeneous.

$$P_B(V) = \frac{1}{\sqrt{2\pi}\sigma_V} \exp \left[- (A_B - \mu)^2 / 2\sigma_V^2 \right]$$

$$\sigma_V^2 = \sigma_B^2 + \sigma_z^2 + V\mu^2 .$$

We introduce a free parameter V , scaled to the mean, which we use as the test of homogeneity.

Any V which is favored, implies an additional error component should be added to the data to describe it as an (homogeneous) Gaussian distribution. Allowed values of V are the constraint on homogeneity.

$$P(V) = \Pi_B P_B(V)$$

Full probability distribution I

We can formally compute the full probability that all blocks are consistent with being drawn from a Gaussian distribution. By definition a homogeneous distribution is described well by its error components. If additional error components are favored by the data, then the distribution is no longer homogeneous.

$$P_B(V) = \frac{1}{\sqrt{2\pi}\sigma_V} \exp \left[- (A_B - \mu)^2 / 2\sigma_V^2 \right]$$
$$\sigma_V^2 = \sigma_B^2 + \sigma_z^2 + V\mu^2 .$$

We introduce a free parameter V , scaled to the mean, which we use as the test of homogeneity.

Any V which is favored, implies an additional error component should be added to the data to describe it as an (homogeneous) Gaussian distribution. Allowed values of V are the constraint on homogeneity.

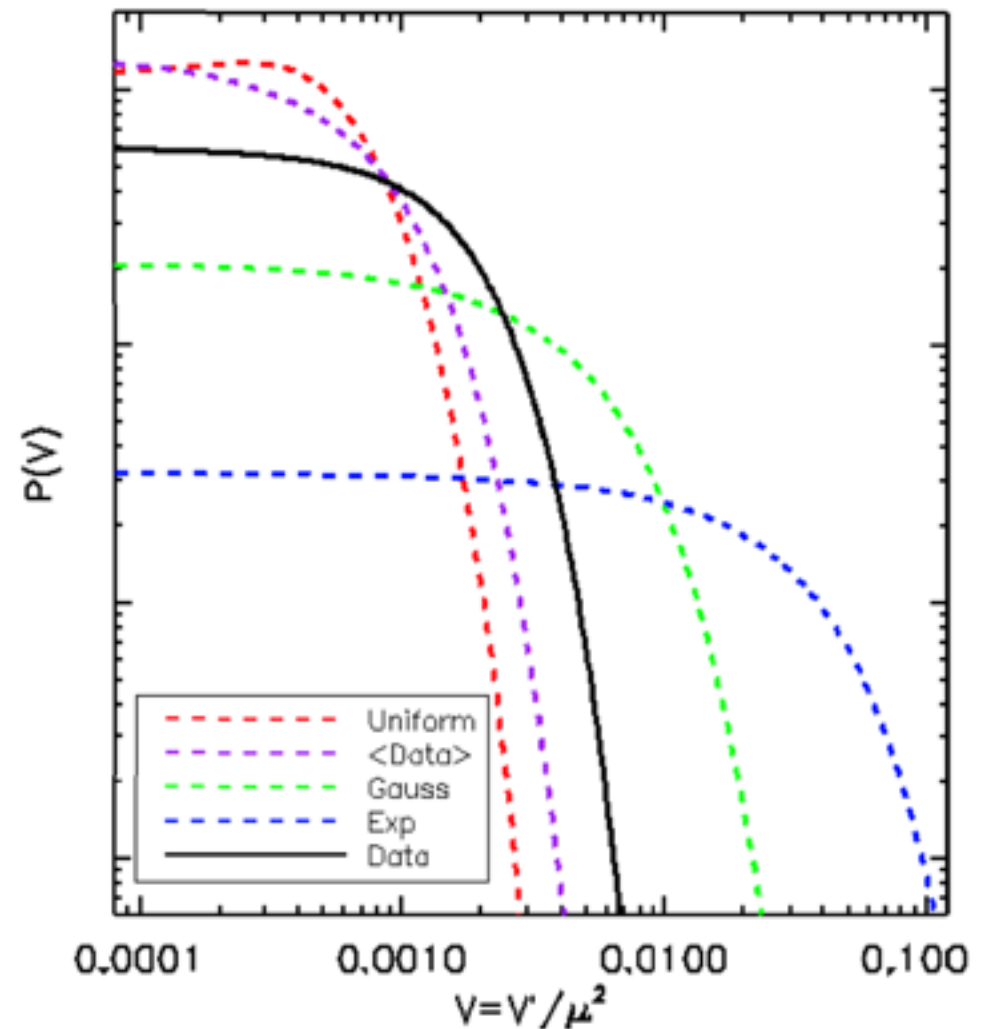
$$P(V) = \prod_B P_B(V)$$

The peak of the pdf $P(V)$ is at $V=0$.

The data does not require an additional error component to describe it as a Gaussian distribution.

We can integrate along the pdf until we enclose 95% and determine the value of V allowed at this confidence level:

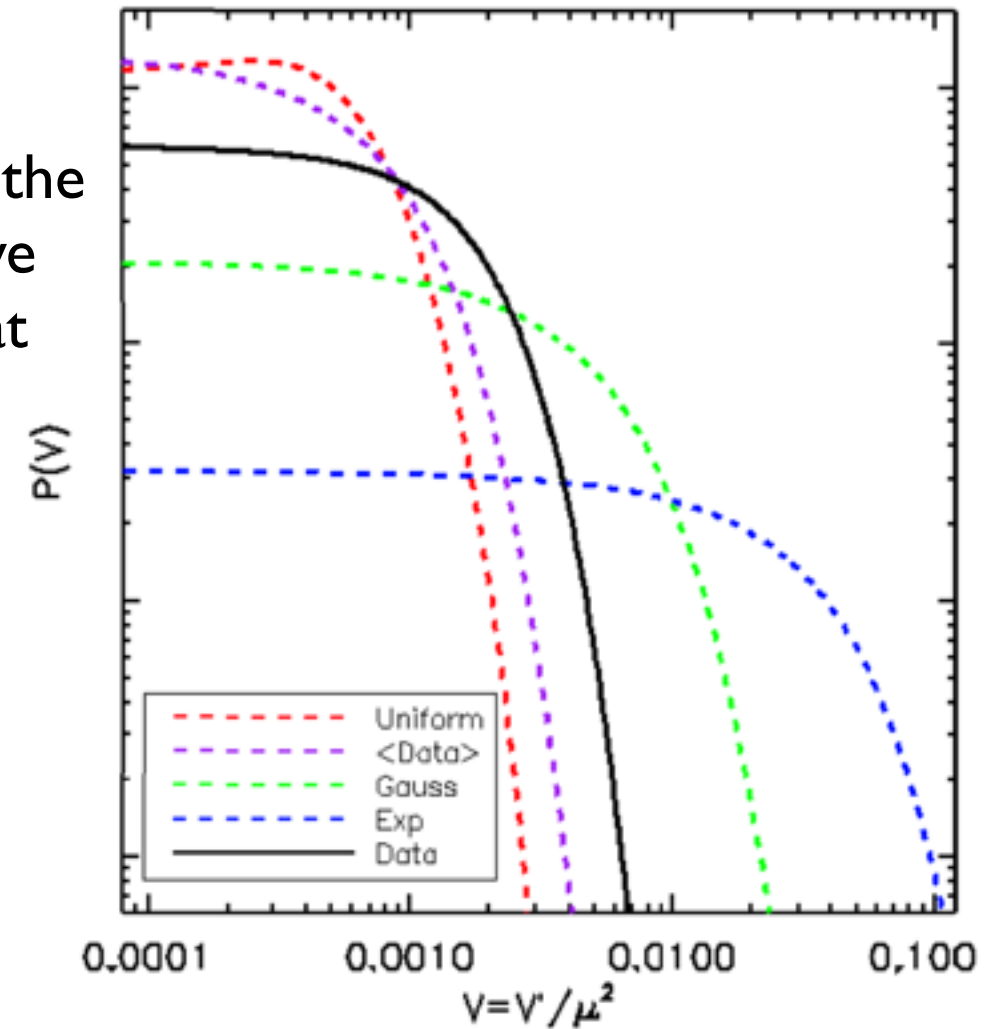
$$V < 0.0032$$



$$\sqrt{V} = 5.6\%$$

Full probability distribution II

If we use the Star Formation Rate as a proxy for homogeneity, and compare regions smoothed on scales of $\sim 350\text{Mpc}$, in the volume described by $0.2 < z < 0.5$ of $\sim 10,000$ square degrees of the Northern sky, between the look-back times of 11-13.5 Gyrs, we find that everywhere looks the same (homogeneity) to 5.6% (at 95% confidence)



$$\sqrt{V} = 5.6\%$$

at the 95% confidence level.

Full probability distribution II

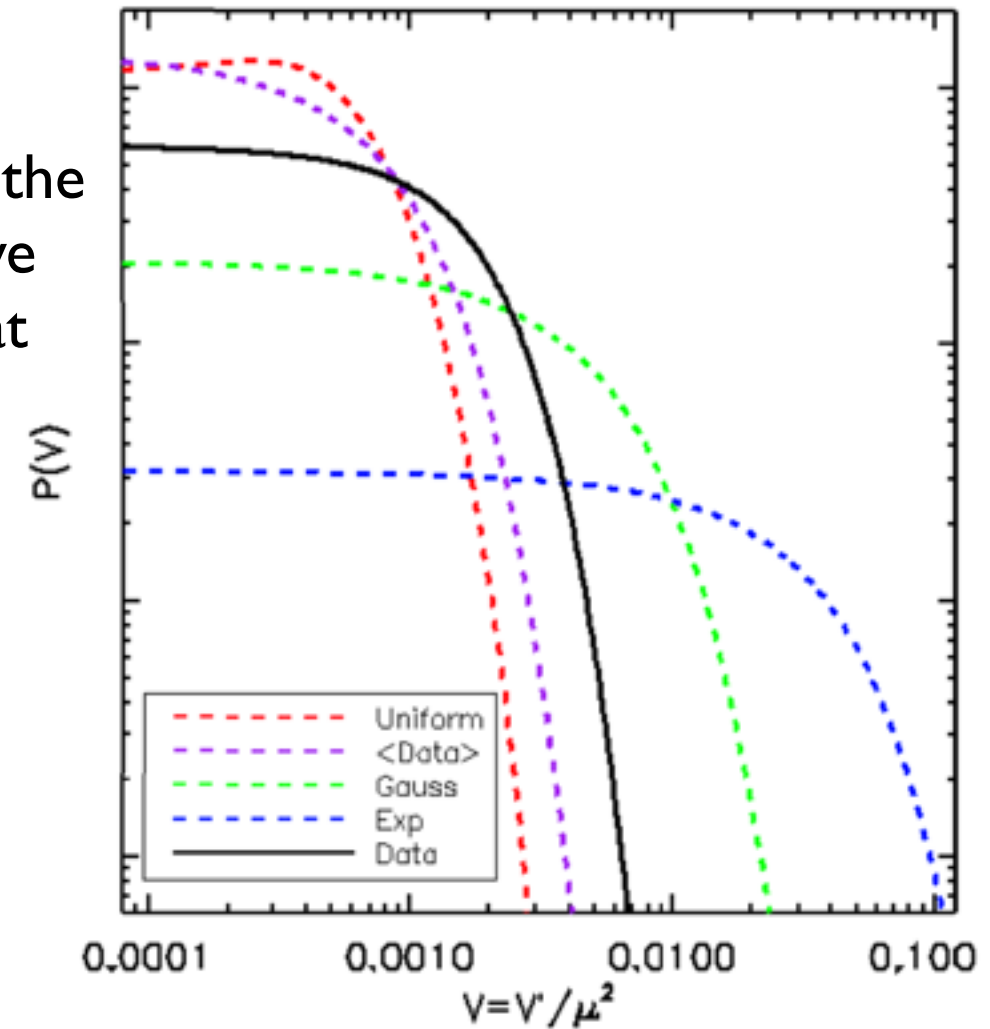
If we use the Star Formation Rate as a proxy for homogeneity, and compare regions smoothed on scales of $\sim 350\text{Mpc}$, in the volume described by $0.2 < z < 0.5$ of $\sim 10,000$ square degrees of the Northern sky, between the look-back times of 11-13.5 Gyrs, we find that everywhere looks the same (homogeneity) to 5.6% (at 95% confidence)

This general test of consistency with homogeneity is sensitive to;

Non Universal Bang-Times leading to LRGs forming at different times.

A redshift-time relation differing from concordance cosmology.

Different levels of star formation (irrespective of the cause, e.g., different environments or physics).



$$\sqrt{V} = 5.6\%$$

at the 95% confidence level.

Full probability distribution II

If we use the Star Formation Rate as a proxy for homogeneity, and compare regions smoothed on scales of $\sim 350\text{Mpc}$, in the volume described by $0.2 < z < 0.5$ of $\sim 10,000$ square degrees of the Northern sky, between the look-back times of 11-13.5 Gyrs, we find that everywhere looks the same (homogeneity) to 5.6% (at 95% confidence)

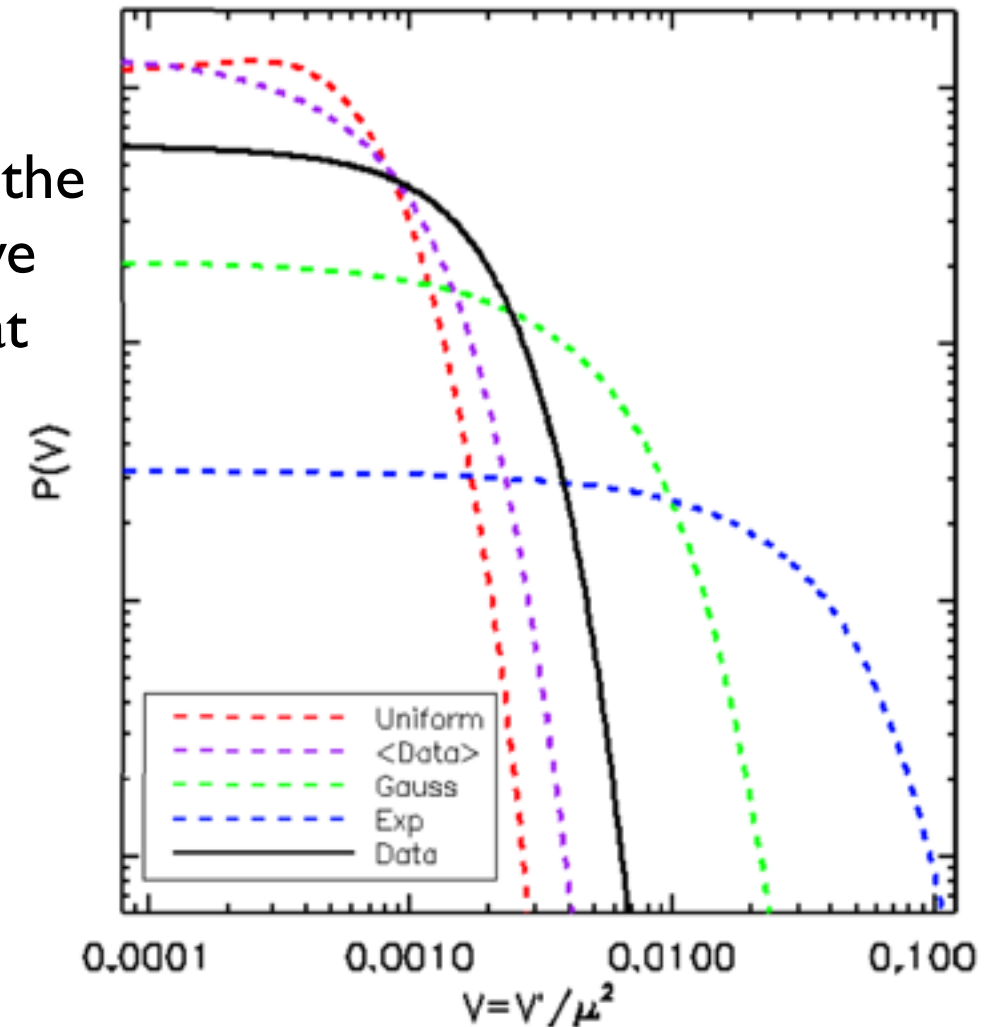
This general test of consistency with homogeneity is sensitive to;

Non Universal Bang-Times leading to LRGs forming at different times.

A redshift-time relation differing from concordance cosmology.

Different levels of star formation (irrespective of the cause, e.g., different environments or physics).

Note, this is still a test of ‘consistency’ with homogeneity, because we haven’t yet ruled out that some weird combination of the above could mimic homogeneity.

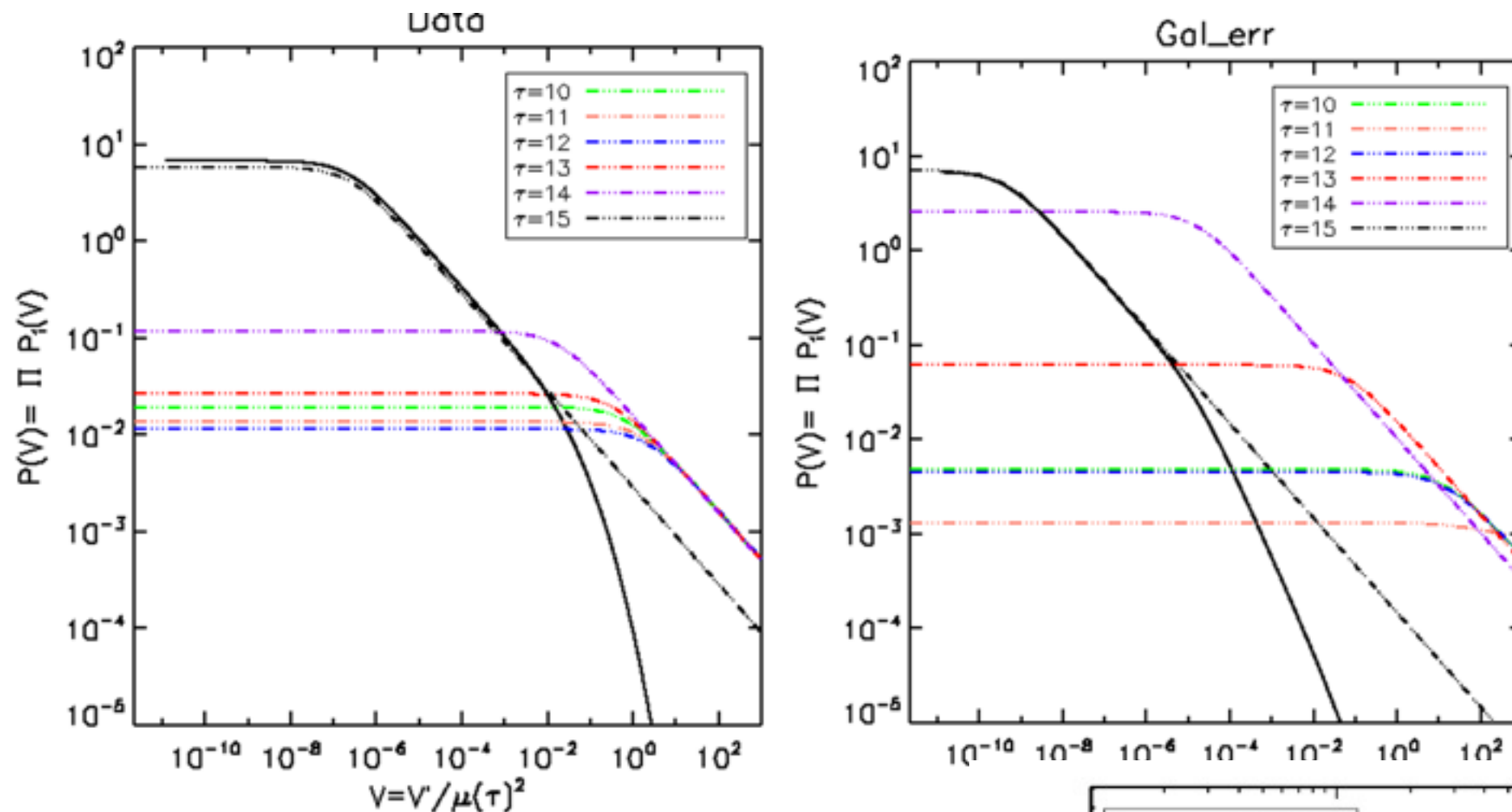


$$\sqrt{V} = 5.6\%$$

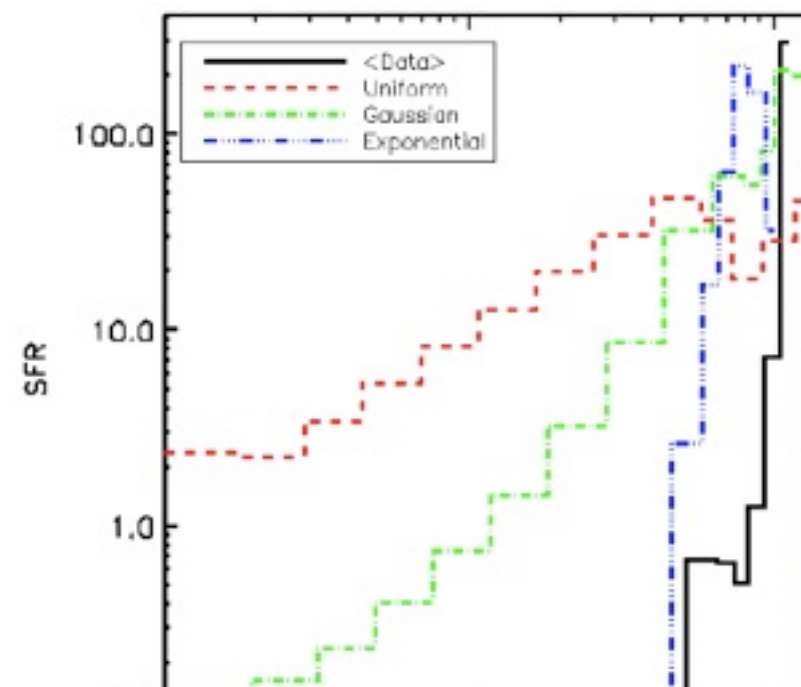
at the 95% confidence level.

Combining all time bins

<Preliminary work> We can tentatively explore the other time bins, which also contain information, but they are harder to extract constraints from.



Recall that we only expect low amounts of star formation in younger time bins for LRGs. Furthermore, we never allow -ve SFR values, so the distributions become log normal.



Conclusions

- Homogeneity can be used to replace dark energy, but not consistently with observations.
- Described a new test of homogeneity, using the distribution of Star Formation Rate Histories (SFH) as a proxy for homogeneity.
- Shown how VESPA can extract SFH from SDSS LRG stacked spectra.
- Sketched what the effect of voids (~ 10 Mpc/h) would have on the distributions of VESPA recovered SFR.
- Accounted for systematics from redshift re-binning.
- Used the t-distribution as a sanity check.
- Computed the full probability distribution, that the SFH is consistent with a Gaussian (homogeneous) distribution.
- Quantified an addition of a some possible systematic error 'V' which allows the data to departure from a homogeneous (Gaussian) distribution.
- We find that $V=0$ is the most likely value, and that $V < 6\%$ at the 95% level.

Using SFRH as a proxy, the Universe looks homogeneous, between 11.5-13.5 Gys ago, over the full SDSS footprint, for galaxy blocks between $0.2 < z < 0.5$.

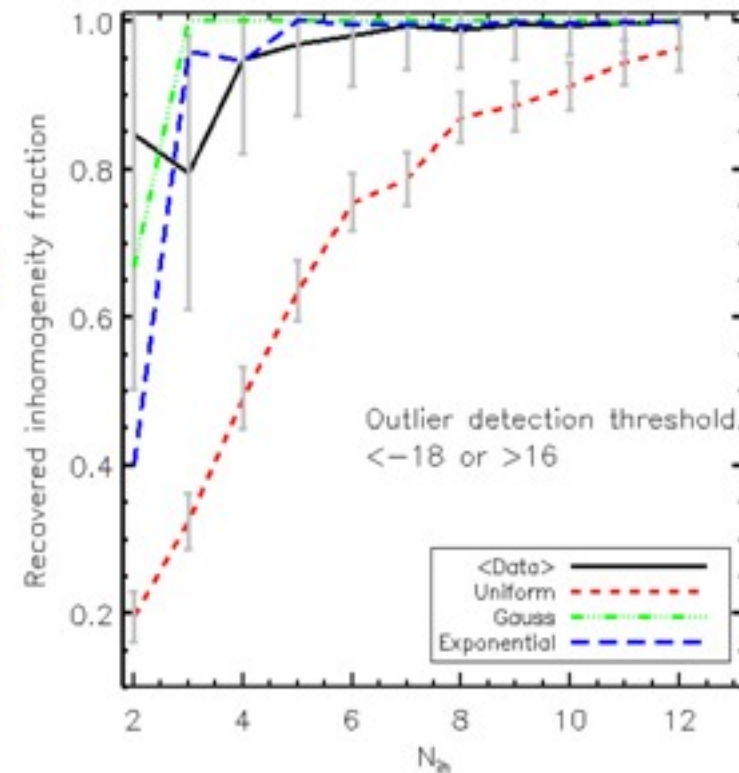
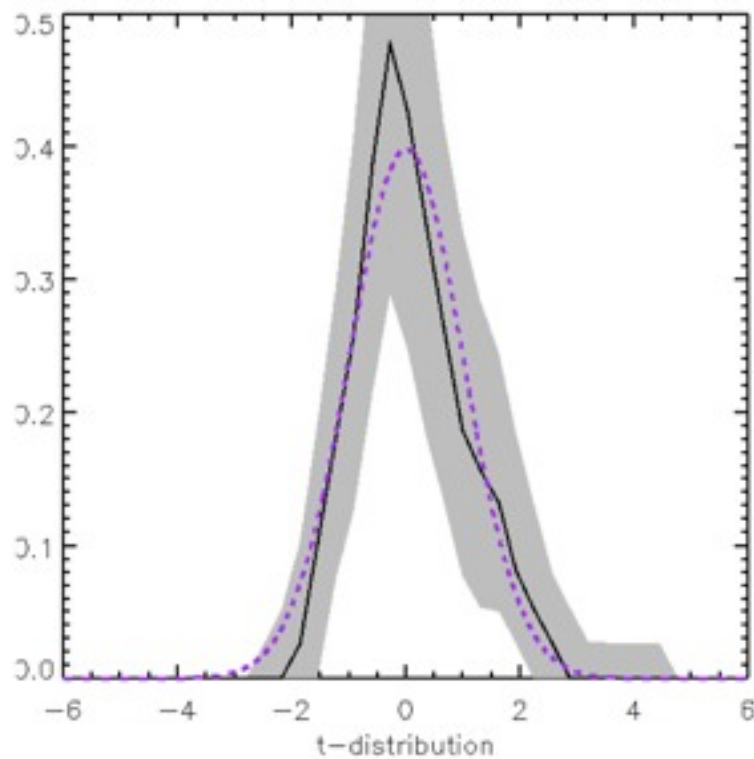
- This is still a consistency check with homogeneity, because we haven't yet ruled out some strange combination of processes.
- We note that there is more info in each of the time distributions, but difficult to extract and compare with a model.

Student t-distribution II

We can also use the student t-test, calibrated to the simulations as a 0th order test of inhomogeneity, by examining the distribution of outliers

$$t_s = \frac{A_B - \mu}{\sqrt{\sigma_B^2 + \sigma_z^2}},$$

$$\text{SFRH}_{B_r,i}(0, \tau_r) \rightarrow \text{SFRH}_{B_r,i}(0, \tau_r) - \langle \text{SFRH}_{B_r}(0, \tau_r) \rangle + N_{\text{ih}} \times \sigma(\text{SFRH}_B(0, \tau_r))$$



Student t-distribution II

We can also use the student t-test, calibrated to the simulations as a 0th order test of inhomogeneity, by examining the distribution of outliers

$$t_s = \frac{A_B - \mu}{\sqrt{\sigma_B^2 + \sigma_z^2}},$$

$$\text{SFRH}_{B_r,i}(0, \tau_r) \rightarrow \text{SFRH}_{B_r,i}(0, \tau_r) - \langle \text{SFRH}_{B_r}(0, \tau_r) \rangle + N_{\text{ih}} \times \sigma(\text{SFRH}_B(0, \tau_r))$$

